



HELSINKI UNIVERSITY OF TECHNOLOGY  
Department of Automation and Systems Technology  
Control Engineering Laboratory

**Antti Pohjoranta**

**Microvia fill electroplating:  
a model for process monitoring development**

Master's Thesis for the degree of Master of Science in Technology submitted for inspection, Espoo, August 28th, 2006.

Espoo, August 28th, 2006

Supervisor: Professor Heikki Koivo, Ph.D.  
Instructor: Robert Tenno, TkT.

# Preface

This Master's thesis was done within a project titled *Model Based Estimation Methods for Analysis of Electronics Manufacturing* (MESTA), carried out during 2005 and 2006. **Aspocomp**, the Finnish Funding Agency for Technology and Innovation (**TEKES**) and the Helsinki University **Control Engineering Laboratory** took part in the project and I owe gratitude to all parties.

Personally I want to thank my instructor **Robert Tenno** whose inspiring attitude and never ending energy helped me to go on. Also **Timo Närhi** at Aspocomp deserves a special thanks for his time and effort. Professor **Heikki Koivo** and Mrs. **Tarja Rapala-Virtanen** at Aspocomp I thank for giving me an opportunity in the project. (The Finnish tax payers I thank for the opportunity to study in general.) Working at the Control Engineering lab is fun, which is thanks to the great folk there. Also I want to thank **dad** for once showing me chemistry, the king of sciences.

It feels good writing a preface to something you've worked on for a half-a-year or so. Still, I can't help thinking that in the meantime, people die of stupid fighting going on in Lebanon, Israel, Iraq. In China and Russia journalists and human rights activists are arrested for their thoughts. In New Orleans people still live in mobile homes, though it's already a year since Hurricane Katrina. Famine and violence fell people, mostly children, in Darfur and Kongo. At the rate deforestation is going on in the Amazon, the whole rainforest will be gone by the time I turn 70, if nothing's done. The Baltic Sea is so polluted that the EU is regulating how much herring it's healthy to eat. The global climate is changing for a fact and all people still do is complain that gasoline is too expensive. The list feels endless. One might ask why do we need better circuit boards..?

Matters can still be helped. Lets all remember to do our share.

Espoo, 28th August 2006

Antti Pohjoranta

|  |   |
|--|---|
| <b>Author:</b>   | Antti Pohjoranta  |
| <b>Name of the Thesis:</b>   | Microvia fill electroplating:<br>a model for process monitoring development |
| <b>Date:</b>   | August 28, 2006   |
| <b>Number of pages:</b>  | 76 + 7  |
| <b>Department:</b>   | Department of Automation and Systems Technology                             |
| <b>Professorship:</b>  | AS-74, Systems Engineering  |
| <b>Supervisor:</b>   | Professor Heikki Koivo  |
| <b>Instructor:</b>   | Robert Tenno, D.Sc.   |
| <p>A microvia is a hole going through one substrate layer on a multilayered printed circuit board (PCB). By filling this hole with copper, an interconnect between two electric circuits running on different layers is created. Applying microvia filling in combination with modern circuit design enables shrinking PCBs and the apparatus built around them.</p> <p>The via holes are filled by electrodeposition from an acid-copper solution. In the microvia filling process, the via hole is filled completely with copper, leaving a smooth copper surface for the next PCB layer to be built on. In a successful microvia fill process, copper is reduced more where there is a cavity on the surface and less there where the surface is level or protrusive. The phenomenon is achieved by mixing special additive chemicals in the electrolysis bath.</p> <p>The degree of fill in microvias cannot be measured during plating. A simulation model comprising the relevant physical and chemical phenomena is the only rational way to approximate the process state. This thesis presents a model of the microvia filling process that sets the basis for development of model based control for the via filling process. The thesis describes the fundamental phenomena related to microvia filling, namely diffusion and migration inflicted mass transfer, the current-potential dependency in an electrochemical system and the effects of via surface shape change during plating. The literature review presents the various additive chemicals and surface chemical phenomena caused by them.</p> <p>The thesis model is implemented using the finite element method. The model includes all basic physical and chemical phenomena related to the process and takes into account the modelling domain shape change effects. Additive chemicals' effects are also included in the model. With operating conditions given, the model can predict the required plating time with decent accuracy.</p> <p>Taking into account the complexity as well as the proprietary nature of microvia filling processes, the thesis work result can be regarded useful. The implemented model can be used as such and during the work the total scope of related problems was determined which is elementary in order to systematically proceed in the modelling work. Finally, objects for further study as well as designs for required experiments are presented.</p> |   |
| <p><b>Keywords:</b> microvia filling, copper electroplating, PCB manufacturing</p>   |   |

|  |  |
|--|--|
| <b>Tekijä:</b>   | Antti Pohjoranta   |
| <b>Työn nimi:</b>  | Mikrovian elektrolyyttisen täyttöpinnointus:<br>malli prosessimonitoroinnin kehitystä varten |
| <b>Päivämäärä:</b>   | 28.8.2006 <b>Sivuja:</b> 76 + 7  |
| <b>Osasto:</b>   | Automaatio- ja systeemitekniikan osasto  |
| <b>Professori:</b>   | AS-74, Systeemitekniikka   |
| <b>Työn valvoja:</b>   | Professori Heikki Koivo  |
| <b>Työn ohjaaja:</b>   | TkT Robert Tenno   |
| <p>Mikrovia on monikerrospiirilevyn yhden levyn läpi kulkeva reikä. Täyttämällä tämä reikä kuparilla muodostetaan yhteys kahdessa eri piirilevykerroksessa kulkevien johdinsiirien välille. Mikroviateknologia yhdistettynä moderniin piirisuunnitteluun mahdollistaa piirilevyjen johdintiheyden kasvattamisen ja näin ollen piirilevyjen sekä niille rakentuvien laitteiden pienentämisen.</p> <p>Viareiat täytetään elektrolyyttisesti rikkihappo-kuparisulfaatti-liuoksesta. Täyttöpinnointusprosessissa mikrovia täyttyy täydellisesti kuparimetallilla ja reiän kohdalle jää peilikirkas kuparipinta valmiiksi seuraavan piirilevykerroksen ladontaa varten. Prosessin onnistuminen edellyttää kuparin pinnoittumista elektrolyyttiliuoksesta piirilevyille hallitun epätasaisesti siten, että kuparia pelkistyy eniten sinne, missä pinnassa on syvin reikä ja vähemmän sinne, missä pinta on tasainen tai siinä on kohouma. Ilmiö saadaan aikaan erityisten pinnoituslisäaineiden avulla.</p> <p>Mikroviojen pinnoitusastetta ei voida pinnoituksen aikana mitenkään mitata ja prosessin lunnonilmiöt huomioon ottava malli on ainoa rationaalinen tapa arvioida pinnoituksen etenemistä. Tässä diplomityössä on kehitetty täyttöpinnointusprosessin malli, joka luo perustan prosessin mallipohjaiselle ohjaukselle. Työssä esitellään pinnoitusprosessiin liittyvät perusilmiöt: diffuusion ja migraation aiheuttama massansiirto, sähkökemiallisen reaktion jännite-virta-tasapaino sekä läpivientireiän muuttumisen vaikutukset. Kirjallisuusosassa käydään läpi monipuolisesti eri pinnoituslisäaineet sekä prosessissa esiintyvät pintakemialliset ilmiöt.</p> <p>Työssä kehitetty malli on toteutettu elementtimenetelmää käyttäen. Malli ottaa huomioon kaikki pinnoitusprosessin oleelliset fysikaaliset ja kemialliset ilmiöt sekä mallituskohteen muodonmuutokset. Myös pinnoituslisäaineiden vaikutus sisältyy malliin. Malli ennustaa pinnoitusprosessin vaatiman pinnoitusajan annetuissa prosessiolosuhteissa kohtalaisesti.</p> <p>Täyttöpinnointusprosessin monimutkaisuuden sekä prosessiin liittyvien liikesalaisuuksien takia työn tulosta voidaan pitää hyödyllisenä. Kehitetty malli on sinällään käyttövalmis ja työn myötä täyttöpinnointusprosessien ongelmakenttä on kartoitettu ja sen systemaattinen ratkaisu voi jatkua. Työn lopuksi kerrotaan tärkeimmät jatkotutkimuksen kohteet sekä niihin liittyvät koe- ja tutkimussuunnitelmat.</p> |  |
| Avainsanat: täyttöpinnointus, kuparielektrolyysi, piirilevyjen valmistus   |  |

# Contents

|  |           |
|--|-----------|
| <b>Preface</b>   | <b>2</b>  |
| <b>Table of Contents</b>                                   | <b>5</b>  |
| <b>Abbreviations and symbols</b>                           | <b>7</b>  |
| <b>1 Introduction and background</b>                       | <b>10</b> |
| 1.1 The thesis project                                     | 11        |
| 1.1.1 Research problem and purpose of work                 | 11        |
| 1.2 Copper electroplating                                  | 12        |
| 1.2.1 The copper reduction reaction                        | 12        |
| 1.2.2 Superconformal electroplating                        | 14        |
| 1.2.3 Current flow   | 14        |
| 1.2.4 Copper electroplating summarized                     | 15        |
| 1.3 Multilayered PCB manufacturing                         | 16        |
| 1.3.1 Creating interconnects parallel to the board surface | 17        |
| 1.3.2 Creating interstitial interconnects                  | 19        |
| 1.4 The microvia fill process                              | 19        |
| 1.4.1 Motives for microvia fill by electroplating          | 19        |
| 1.4.2 Problems related to microvia fill by electroplating  | 19        |
| 1.4.3 Measuring via fill performance                       | 21        |
| 1.4.4 Microvia fill electroplating control basics          | 22        |
| 1.4.5 Multilayered PCBs and microvia filling summarized    | 23        |
| 1.5 Chemistry  | 23        |
| 1.5.1 Main electrolyte components                          | 24        |
| 1.5.2 Electrolyte additives                                | 25        |
| 1.5.3 Surface adsorption                                   | 30        |
| 1.5.4 Essential chemical interactions summarized           | 31        |
| 1.6 Mass transfer and conductivity                         | 32        |
| 1.6.1 Diffusion - migration down a concentration gradient  | 33        |

|          |  |           |
|----------|--|-----------|
| 1.6.2    | Migration along an electric potential gradient . . . . .           | 35        |
| 1.6.3    | The Nernst-Planck equation . . . . .                               | 36        |
| 1.6.4    | Electrical conductivity of electrolyte . . . . .                   | 36        |
| 1.6.5    | Mass transfer related issues summarized . . . . .                  | 37        |
| 1.7      | Electrode processes . . . . .                                      | 38        |
| 1.7.1    | Deposition growth and current . . . . .                            | 38        |
| 1.7.2    | Current in an electrochemical system . . . . .                     | 38        |
| 1.7.3    | Summary of the relevant electrode process principles . . . . .     | 41        |
| 1.8      | Previously done modelling work and existing models . . . . .       | 42        |
| 1.8.1    | The diffusion limited mass transfer of additives model . . . . .   | 42        |
| 1.8.2    | The curvature enhanced accumulation of accelerator model . . . . . | 43        |
| 1.8.3    | Status quo . . . . .   | 43        |
| 1.8.4    | Implementation techniques . . . . .                                | 44        |
| <b>2</b> | <b>Modelling microvia filling</b>                                  | <b>46</b> |
| 2.1      | The microvia filling process model . . . . .                       | 46        |
| 2.1.1    | Assumptions, exclusions and simplifications – scope of the model   | 46        |
| 2.1.2    | The finite element method . . . . .                                | 48        |
| 2.1.3    | Implementation of the model . . . . .                              | 48        |
| 2.1.4    | Modelling principles summarized . . . . .                          | 62        |
| <b>3</b> | <b>Experimental verification and discussion</b>                    | <b>64</b> |
| 3.1      | Via filling experiments . . . . .                                  | 64        |
| 3.1.1    | Comparing via fill measurements to modelling results . . . . .     | 68        |
| 3.2      | Voltammetric measurements . . . . .                                | 71        |
| 3.3      | Conductivity measurements . . . . .                                | 73        |
| 3.4      | Copper electrode equilibrium potential measurements . . . . .      | 74        |
| 3.5      | Discussion and future work . . . . .                               | 75        |
| 3.5.1    | What the model does . . . . .                                      | 75        |
| 3.5.2    | What the model does not and why . . . . .                          | 75        |
| 3.5.3    | Improving the model - outline of experiments required . . . . .    | 76        |
| 3.6      | Conclusion . . . . .   | 79        |
| <b>A</b> | <b>Via fill test sample images</b>                                 | <b>85</b> |
| <b>B</b> | <b>Via fill model screen-captured images</b>                       | <b>91</b> |

# Abbreviations and symbols

|            |  |
|------------|--|
| ABT        | 2-aminobenzothiazole   |
| ALE        | Arbitrary Lagrange-Eulerian                                    |
| BTA        | Benzotriazole  |
| CEAC       | Curvature enhanced accelerator accumulation                    |
| DC         | Direct current   |
| EMF        | Electromotive force  |
| FEM        | Finite element method  |
| FR         | Fill ratio   |
| JGB        | Janus Green B  |
| M          | mol/l  |
| MCP        | Midway-to-corner point   |
| MLB        | Multilayered printed circuit board                             |
| MPS, MPSA  | 3-mercaptopropane-1-sulfonic acid                              |
| PCB        | Printed circuit board  |
| PDE        | Partial differential equation                                  |
| PEG        | Polyethylene glycol  |
| PWB        | Printed wiring board   |
| SEM        | Scanning electron microscope                                   |
| SPS        | bis-(sodiumsulphopropyl) disulfide                             |
| $A_i$      | Total area of electrode $i$ , $m^2$                            |
| $A$        | Local area on cathode surface, $m^2$                           |
| $a_i$      | Activity of species $i$ or activity of copper on electrode $i$ |
| $\alpha_i$ | Transfer coefficient of process $i$                            |

|                      |  |
|----------------------|--|
| $\beta_i$            | Coefficient accounting for standard free energy and activity coefficient of species $i$                |
| $c_i$                | Concentration of species $i$ , mol/m <sup>2</sup>  |
| $c_{i,b}$            | Concentration of species $i$ in the solution bulk, mol/m <sup>2</sup>                                  |
| $D_i$                | Diffusion coefficient of species $i$ , m <sup>2</sup> /s   |
| $d$                  | Distance, m  |
| $\delta$             | Thickness of diffusion boundary, m   |
| $E$                  | Potential difference (electromotive force) over a system, V  |
| $\eta$               | Overpotential, V   |
| $\eta_i$             | Overpotential on electrode $i$ , V   |
| $F$                  | Faraday's constant, 96485 As/mol   |
| $\phi$               | Potential, V   |
| $\delta\phi$         | Potential difference over a boundary, V  |
| $\delta\phi_{eq}$    | Potential difference over a boundary in chemical equilibrium, V  |
| $\delta\phi_{eq}^0$  | Potential difference over a boundary in chemical equilibrium measured against a reference electrode, V |
| $\varphi$            | Association parameter between solute and solvent   |
| $\Gamma_i$           | Surface concentration of species $i$ , mol/m <sup>2</sup>  |
| $\Gamma_{s,i}$       | Surface saturation concentration of species $i$ , mol/m <sup>2</sup>                                   |
| $I$                  | Current, A   |
| $i_i$                | Current density on electrode $i$ , A/m <sup>2</sup>  |
| $i_l$                | Limiting current density, A/m <sup>2</sup>   |
| $i_0$                | Total exchange current density, A/m <sup>2</sup>   |
| $i_{i,0}$            | Exchange current density on electrode $i$ , A/m <sup>2</sup>   |
| <b>J</b>             | Current density (vector), A/m <sup>2</sup>   |
| $k, k_i$             | Constant scaling coefficient   |
| $l$                  | 2D-mesh boundary element length, m   |
| $l_0$                | 2D-mesh boundary element length initially, m   |
| $\Lambda_i$          | Molar conductivity of $i$ , Sm <sup>2</sup> /mol   |
| $M_i$                | Molecular weight of species $i$ , g/mol  |
| $\mu$                | Solvent viscosity, Pas or Total chemical term  |
| $\mu_i$              | Chemical term related to species $i$   |
| <b>N<sub>i</sub></b> | Material flux of species $i$ (vector), mol/m <sup>2</sup> /s   |
| <b>n</b>             | The mesh boundary normal vector  |

|              |   |
|--------------|---|
| $\psi$       | Boundary movement velocity (vector), m/s                            |
| $\psi_i$     | Boundary movement velocity in direction of element vector $i$ , m/s |
| $Q$          | Total charge, C   |
| $R$          | Ideal gas coefficient, 8.314 J/mol/K                                |
| $R_i$        | Electric resistance, $\Omega$                                       |
| $\rho_i$     | Density of $i$ , kg/m <sup>3</sup>                                  |
| $\sigma$     | Conductivity (of electrolyte), S/m                                  |
| $T$          | Temperature, K or C°  |
| $t$          | Time, s   |
| $\theta_i$   | Proportional surface coverage of species $i$                        |
| $U_i$        | Voltage drop over a system $i$ , V                                  |
| $V$          | Volume, m <sup>3</sup>  |
| $V_m$        | Molar volume of solute, m <sup>3</sup> /mol                         |
| $n$          | Amount of moles, mol  |
| $u_i$        | Mobility of $i$ , mols/kg   |
| $\mathbf{v}$ | Velocity (vector) m/s   |
| $X$          | The horizontal coordinate in the fixed coordinate system            |
| $x$          | The horizontal coordinate in the moving coordinate system           |
| $Y$          | The vertical coordinate in the fixed coordinate system              |
| $y$          | The vertical coordinate in the moving coordinate system             |
| $z_i$        | Electron number of species $i$                                      |

# Chapter 1

## Introduction and background

Electronics manufacturing is a motivating research subject. The world electronics market is worth an estimated 1 000 billion euros annually<sup>1</sup> and in Finland the electronics industry comprises nearly a fifth of all domestic industry product<sup>2</sup>.

Electronics is everywhere and there is a printed circuit board in virtually every modern electronic appliance. This makes PCB manufacturing a core sector inside the electronics industry.

On one side of one layer of a typical multilayered printed circuit board (PCB), there are approximately 20 000 via holes to be filled with copper during the electrochemical via fill process. There can be up to 16 layers on the whole board and all the via holes must be perfectly filled in order for every single interconnect on the PCB to conduct current.

Though at first the meaning of a tiny copper plug inside a piece of plastic might feel insignificant, going through this train of thoughts helps putting the issue into perspective.

The microvia filling process is an electrochemical process aiming to completely but not excessively fill the holes on a multilayer PCB where interconnects between two circuit layers are made. Exact control over this process is elementary for successful production of up-to-date electronic devices. In-depth knowledge and accurate modelling of the process is required to further develop the complete manufacturing process as end-users continuously demand smaller and less power consuming products.

This thesis goes through the aspects related to the microvia fill process using electroplating and presents a model of the process created for monitoring and development purposes.

---

<sup>1</sup>Finnvera, 2003, <http://www.finnvera.fi/vuosikertomus2004/?s=0&p=2213>

<sup>2</sup>Tilastokeskus, 2004, [http://www.stat.fi/til/atoi/2004/atoi\\_2004\\_2006-02-23\\_tau\\_006.html](http://www.stat.fi/til/atoi/2004/atoi_2004_2006-02-23_tau_006.html)

## 1.1 The thesis project

This thesis is a part of a co-operation project between the National Technology Agency of Finland (TEKES), Aspocomp Oy and the Control Engineering Laboratory at Helsinki University of Technology (TKK). The project is entitled *Model based estimation methods in analysis of electronics manufacturing* (MESTA) and aims to improve competitiveness of the Finnish electronics industry by developing sophisticated control applications for the branch.

All experiments and most of the measurements related to the thesis were conducted at the Aspocomp plant in Salo. Scanning electron microscopy was carried out at the Control Engineering Laboratory. Voltammetric measurements were conducted at the Laboratory of Physical Chemistry and Electrochemistry, TKK, Espoo.

### 1.1.1 Research problem and purpose of work

Aspocomp has years of experience in operating electroplating processes in general, but the microvia filling process in question here was taken into production use at the Salo plant only recently. Therefore rather little knowledge of the process chemistry and affecting mechanisms exists at the plant currently.

The via fill process is complex, including problems related to mass-transfer, electrochemistry and surface chemistry as well as the modelling domain geometry. Even small changes in process parameters can dramatically affect the output quality. Copper deposition growth cannot be measured at each individual via hole during the process and therefore a process model is the only way to reliably anticipate process output in case of changing process conditions.

The aims of this research work are to deepen the knowledge of copper electroplating in micro-scale features on PCBs and to model the microvia fill by electroplating process for monitoring and production design purposes. As is shown in the final discussion section (3.5), this thesis work and the model presented here only set the basis for further research to be performed within the subject.

The model is to be developed on sound theoretical principles, applying numerical data only in the parametrization and validation phase. In practice, the model aims to predict the fill ratio achieved at a certain plating time, or conversely, the time required for filling a microvia under some electroplating circumstances, near the regular operating conditions.

Modelling and control work is often done by people with little chemical or electronics manufacturing background. Therefore this thesis text is written as an all-a-round introductory text to microvia filling process modelling, explaining the basic phenomena and principles in a simple manner. The aim is to require as little previous knowledge of the reader as possible.

## 1.2 Copper electroplating

Copper electrodeposition and electrolysis in general is a well established technology. As electric interconnect material in home electronics appliances, copper has been the de-facto material for decades already. This is mainly due to copper's excellent electric and mechanical properties. Metal copper has high electrical conductivity and tolerates physical strain well.

Within microchip manufacturing the copper interconnect technology is, however, a newcomer. For example, IBM applied copper electroplating in high-volume chip manufacturing only in 1998 [1]. In the microchip industry, the transition from previously used aluminum to copper as interconnect material, was and is driven by the never-ending need for ever smaller and less power consuming applications. Due to its better conductivity, copper allows higher currents with less power consumption than aluminum. Copper is also more resistant to electromigration which enables the use of higher current densities without losing reliability. These properties of copper and the need for also PCBs to shrink in size, promote advanced copper interconnect technologies in PCB manufacturing as well.

The techniques for producing high-density copper interconnects are reasonably new and not thoroughly researched. Research data within the field is usually very case-specific and most of the studies are made from the viewpoint of microchip manufacturing, where the dimensions are generally three orders of magnitude smaller than those in PCB manufacturing.

This section will go through the general theoretical aspects of copper electroplating, especially from the perspective of printed circuit board manufacturing and the micro via fill process.

### 1.2.1 The copper reduction reaction

Electroplating or electrodeposition is reducing metal ions electrochemically from a solution, where metal ions are dissolved, onto a solid and electrically conductive surface. The copper reduction reaction (1.1) is the core of all copper electroplating. All external means applied via equipment or plating solution chemistry aim to alter the speed of copper reduction.



Reduction of copper is driven by an external electrical power source. The power source is connected to the positively and negatively charged conductors, the electrodes, which are immersed in the electrolysis bath. The bath solution is often called the electrolyte solution or just electrolyte. The electrodes are called the anode and the cathode, the cathode being the one always connected to the negative pole of the power source. In the case of PCB manufacturing the cathode is the pre-treated PCB substrate

where interconnects are made.

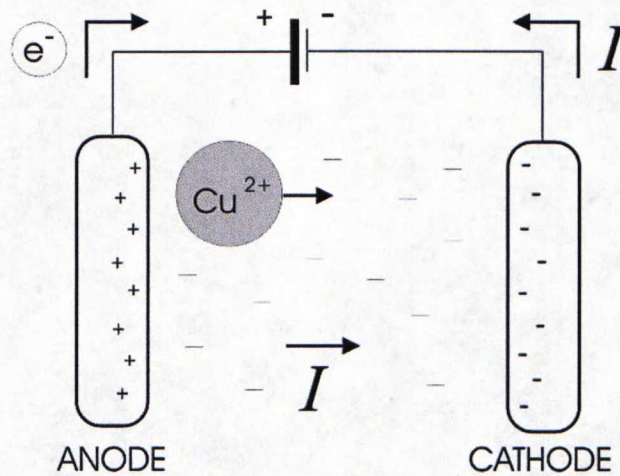


**Figure 1.1:** A schematic illustration of the electrolysis system.

The electrolyte is a solution where copper ions dissolve easily, and which has a relatively high electric conductivity. In the PCB industry, the electrolyte is most often composed of mainly copper sulphate ( $\text{CuSO}_4 \cdot 5\text{H}_2\text{O}$ ) and sulphuric acid ( $\text{H}_2\text{SO}_4$ ) dissolved in water [2]. For example, in the Aspocomp via fill process, the copper ion concentration is approximately 0.8 mol/l in an aqueous solution that also contains approximately 1 mol/l sulphuric acid.



**Figure 1.2:** One large and several small crystals of solid copper sulphate, alongside the amount of electrolyte solution where the crystals were crystallized from by evaporating the solvent.

Sulphuric acid is added to the electrolyte in order to improve electrolyte conductivity and decrease electrode polarization [3]. This has beneficial effects on deposit

characteristics, prevents precipitation of basic salts and enables use of higher current density [2].

Deposition of copper efficiently depletes the electrolyte of copper ions unless more copper is provided to the electrolyte continuously. Copper ions are commonly brought to the system either via solid copper metal anodes or by continuously replenishing the electrolyte with a solution containing readily dissolved copper ions.

Though the electrolyte is continuously agitated, a quiescent layer of fluid always remains near the solid surfaces that are in contact with the electrolyte. Within this layer, diffusion is the main means of species' mass transfer. This also applies to copper ions near the cathode, where they continuously are being extracted from the solution into the metal lattice. Thus, copper ion diffusivity becomes a limiting factor for electrodeposition speed.

### 1.2.2 Superconformal electroplating

What makes via fill by electroplating so special as a process, is that in a sense, it is defying laws of nature. Copper is being deposited faster on the bottom of the via than on the PCB surface!

The *natural* way for copper to deposit would be subconformally (Fig. 1.3, (b)), meaning that protrusive regions with strong potential gradients and good material flow would attract more copper ions and develop a thicker deposit than the hidden features. By increasing electrolyte agitation, copper ion concentration and electric conductivity of the electrolyte, conformal deposit growth is obtained (Fig. 1.3, (c)).

Though copper ion concentration is greatest outside the features, on the planar surface of the PCB billet, and though the potential field gradient is greatest at protrusive sites, like the via mouth, copper is still deposited faster on the bottom and inside the via than in those mentioned regions. This phenomenon, superconformal electroplating (Fig. 1.3, (a)), is achieved by using appropriate electrolyte chemistry.

### 1.2.3 Current flow

The copper electroplating system forms an electric circuit, where the main components are the bath (a resistance), the electrodes (conductors) and the electric power source (an electromotive force). Hence, the electrodes are externally connected by conductor wires via the electric power source, and on the other hand via the electrolysis bath by a current conducting solution.

The power source supplies the circuit with current, which in a PCB electroplating system is either pulsed current or direct current (DC). At the Aspocomp Salo plant, DC electroplating is used.

Reducing a cupric ( $\text{Cu}^{2+}$ ) ion from the electrolyte to make it a part of the solid copper metal lattice, requires two unit charges to be supplied to the reducing ion over the metal-electrolyte interphase. This results in a continuous flow of charged particles

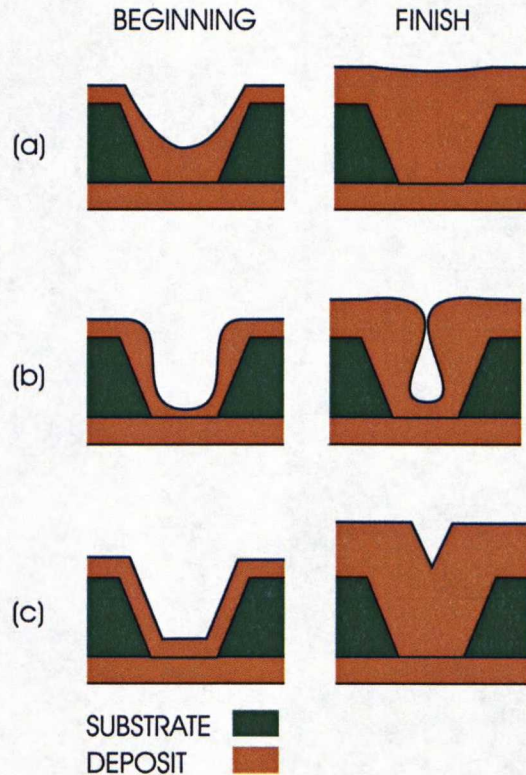


**Figure 1.3:** An illustration of typical deposit growth forms; a) superconformal, b) sub-conformal and c) conformal growth.

to the interphase. The flow of charges creates a current, which by definition is, motion of charge.

The direction of current is defined as the movement direction of the positive charge. When considering the copper electrolyte bath, the positive charges that move from anode to cathode are exactly the copper ions. On the other hand, current also flows in the wires connecting the electrodes externally to the electric power source. In the wires current is carried by electrons, which are negatively charged particles, meaning current flows opposite to their movement direction, and so the circuit is closed.

Since the electric power source actually creates a potential difference ( $E$  in Figure 1.4) between its poles, i.e. the electrodes, an electric field is developed over the whole electrolyte. The electric field induces an electric force on the charged particles in the electrolyte, causing them to migrate along or against the potential gradient, depending on their charge.

#### 1.2.4 Copper electroplating summarized

Copper electroplating is a system where copper ions are electrochemically extracted from a solution onto a solid surface, to form metallic copper. The metallic copper deposit forms the interconnects on PCBs.

The process requires the current to flow through the system and for electrochemical reactions to take place at the anode and cathode. The system can be observed as both,

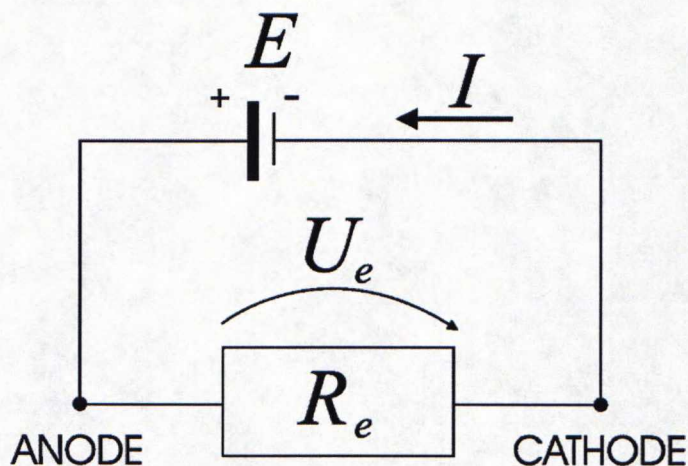


**Figure 1.4:** A simplified illustration of the electrolysis' electrical circuit.  $R_e$  denotes the electrical resistance formed by the electrolyte.

an electric circuit and an electrochemical reaction system.

Mass transfer by convection in the bulk electrolyte, and by diffusion as well as migration in the very vicinity of the electrodes, plays a key role in the system.

### 1.3 Multilayered PCB manufacturing

The printed circuit board (PCB) or printed wiring board (PWB) is the chassis for all components in an electronics device. Earlier a single two-sided PCB might have been sufficient to supply enough mounting space as well as the required interconnects for all components necessary. As appliances became more sophisticated and space requirements tightened, increasing the planar PCB area became impossible and stacking several single-layered PCBs on top of each other became a standard solution. The created PCB stack is called a multilayered PCB or multilayered board (MLB).

In multilayered PCBs not only the board surface area in the  $xy$ -plane (see Fig. 1.5) but also the total board thickness matters. Nowadays, an MLB can contain up to 16 interconnect layers. A part of the interconnects run through the board, in the  $z$ -axis' direction (Fig. 1.5), so to say. Compared to single-layered PCBs, revised circuit design methods as well as advanced manufacturing technologies are required for MLB production and microvia fill is one such technology.

The reason for rather discussing PCBs, printed *circuit* boards, than PWBs, printed *wiring* boards, is increasingly that modern PCBs actually contain whole circuits instead of only wiring. Embedded component technologies have enabled including electronic components inside and on the surfaces of multilayered PCBs.

Manufacturing a multilayered printed circuit board is a series of several chemical and electrochemical subprocesses. In the very core is the copper interconnect plating processes. This is where the current conducting interconnects are made on the board.

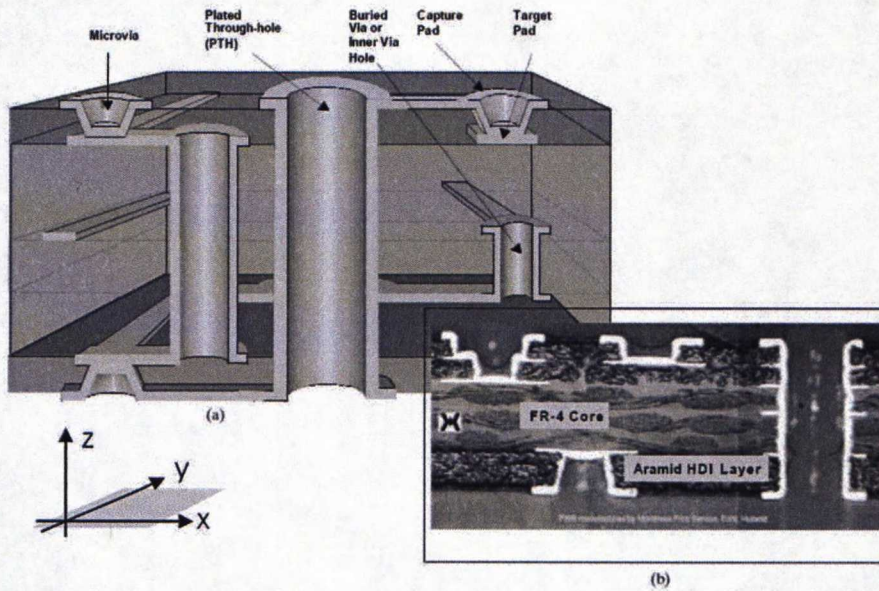


**Figure 1.5:** An illustration of a multilayered printed wiring board (a) and a cross-section image of a real PWB. The axes depict the dimensions and their directions in a PCB. Picture courtesy of [4].

### 1.3.1 Creating interconnects parallel to the board surface

The interconnects running in the board surface direction are basically made in the same fashion as in any PCB manufacturing process so far, using photolithography. The raw material for each layer in a multilayered PCB, is a thin epoxy resin board, coated with copper. The board can also be glass fiber reinforced to increase mechanical durability.

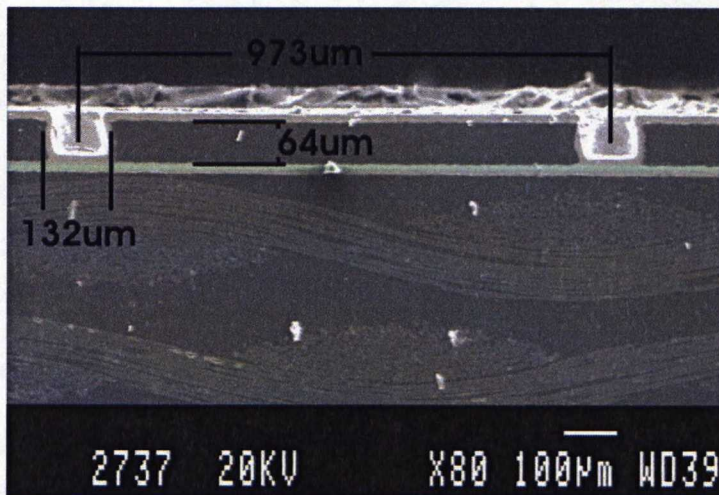


**Figure 1.6:** Two partially filled microvias on a PCB with the layout dimensions added. The fibers on the board can be seen in the figure.

The metal interconnects are created on the PCBs in a photolithographic process known as *print-and-etch* (Fig. 1.7). The copper-coated board is first coated with a photoresistant substance. A mask of the desired circuitry layout is placed on the

photoresist-coated board and the masked board is exposed to UV-light. The UV-light activates the photoresist and the mask determines where the light hits the photoresist and where not.

There are two types of photoresist materials. The *positive* type photoresist is activated by UV-radiation and forms the protective resist layer only after exposition. The *negative* type resist material, on the other hand, is already protective when applied on the copper surface and is retrospectively deactivated by UV-light. The exposition mask is designed depending on photoresist type.

Next the UV-exposed board is dipped into an etch bath where the protective photoresist shields the copper there, where the interconnects are desired. Elsewhere, where no interconnect is needed, the etch erodes the copper away. This procedure is done on each layer of the multilayered PCB individually.

What is left on the board after cleaning, is the copper circuitry ready for further processing.

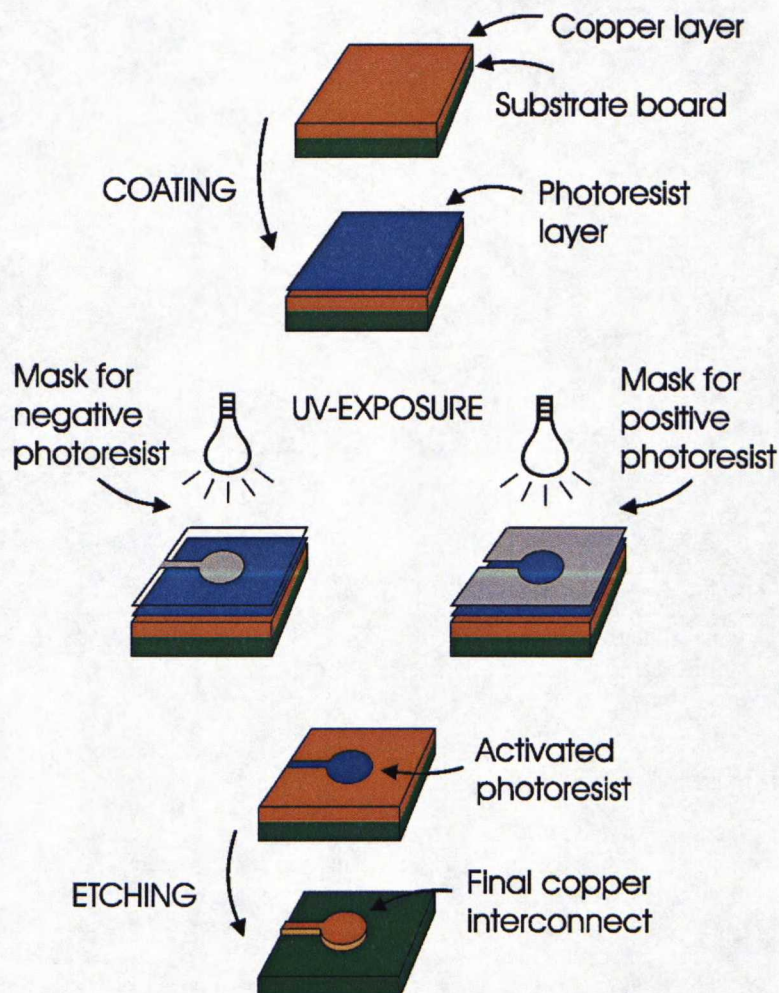


**Figure 1.7:** A schematic illustration of the photolithographic "print-and-etch" process where metal interconnects are created on a PCB layer. The process is completed individually for each layer of a multilayered PCB.

### 1.3.2 Creating interstitial interconnects

There are various ways for creating the interconnects going through the multilayered PCBs (in the z-axis direction). The microvia fill by electroplating technology is one, but also conductive paste is used to fill drilled microvias. Further, the Neo Manhattan bump interconnection (NMBI) process or buried bump interconnection technology (B<sup>2</sup>it) are techniques converse to the via fill process. In these techniques, no hole on the dielectric layer is filled but instead a bump is created on the conductive material to form the interconnect, before the layers are stacked together [4, 5].

In microvia filling, the holes required for creating interstitial interconnections are made on individual board layers by laser ablation. Holes are made so that they reach through the whole dielectric layer and the outer (upper) copper layer. A hole on the outer copper layer is created by either piercing it with the laser or etching a hole on it before laser drilling. The inner (bottom) copper layer reflects the beam back so that the hole does not become deeper than necessary.

After the holes are made, their walls need to be made electrically conductive in order for electroplating to work. For instance, at the Aspocomp Salo plant, first a thin layer of copper is deposited chemically in an electroless copper bath. Then on top of this layer a layer of approximately 5-10µm of copper is deposited as so called *flash* copper. Next, the board is pretreated by microetching the copper surface before entering the via fill electroplating bath [5].

## 1.4 The microvia fill process

### 1.4.1 Motives for microvia fill by electroplating

The microvia fill by electroplating technology brings three distinct benefits compared to other interstitial interconnect technologies.

Firstly, the via is filled with solid copper whose electric conductivity and resistance to electromigration are superior to those of e.g. a conductive paste. Further, the material in the via is the same as in any other interconnect, reducing problems related to impedance and reliability design [5].

Second, copper has excellent thermal conductivity, which is good considering cooling of circuit boards.

Thirdly, the via can be filled without applying any mechanical strain on the board, in a standard acid-copper bath, as a part of the overall electrochemical production line. A solid, electroplated copper plug is also mechanically very durable.

### 1.4.2 Problems related to microvia fill by electroplating

A successfully electroplated microvia is completely but not excessively full, leaving a smooth surface for the next MLB layer to be built on (Fig. 1.4.2).

The problems of via filling by electroplating are commonly related to electrolyte

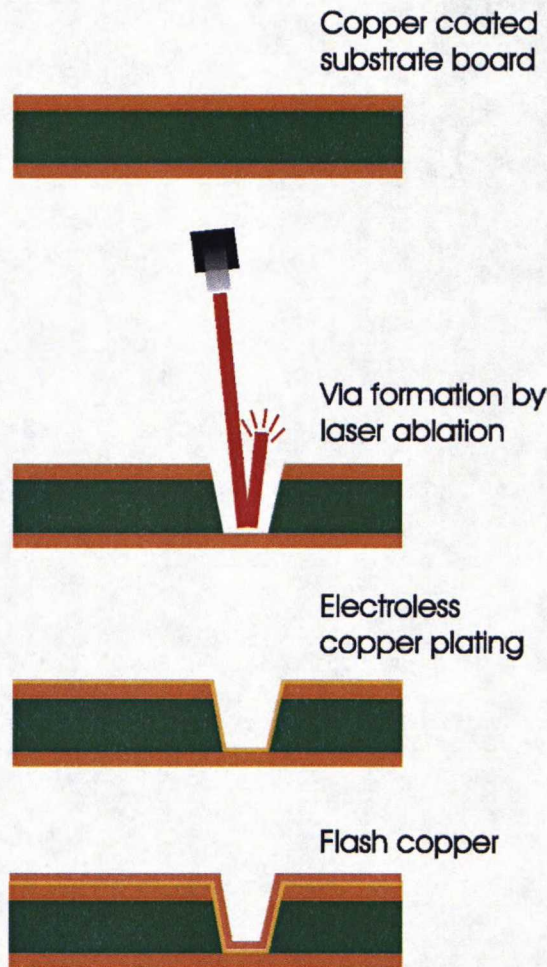


**Figure 1.8:** An illustration of PCB preprocessing before via fill by electroplating.

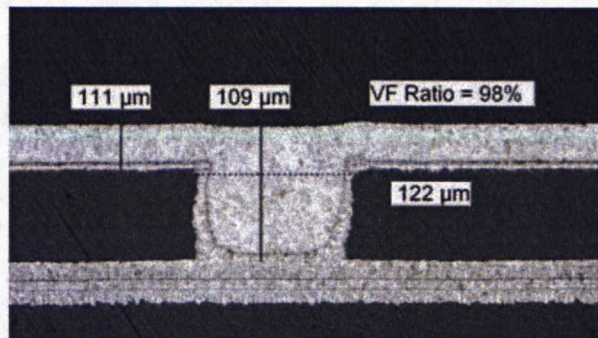


**Figure 1.9:** A cross-section SEM image of a successfully filled microvia. The fill ratio is close to 1 (100%). Picture courtesy of Aspocomp [5].

chemistry. The process is complex and difficult to control and even minor deviations in the electrolyte composition can lead to a drastically worsened output quality. Further, the electrolyte recipe is without exception proprietary information of the equipment or chemistry provider, which there are plenty of. For example, Atotech, Enthone and Rohm&Haas are mentioned among others in [5].

The main functions of an interconnect is to conduct current. Conductivity of filled microvia interconnects can be hampered by poor contacts to the surrounding layers and an incomplete fill (Fig. 1.10). The smoother the filled via surface is, the better is the contact with the covering layer. Only partially filled vias create a *bottleneck* for current, which increases local current density causing reliability problems due to increased electromigration and resistive heating. Empty vias, caused by e.g. gas entrapment, interrupt the circuit completely.

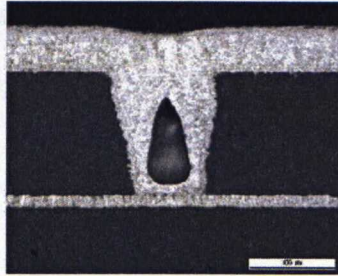


**Figure 1.10:** A void inside a microvia. Picture courtesy of Aspocomp [5].

Overfilled as well as underfilled vias (Fig. 1.4.2, 1.4.2) pose a problem in the following manufacturing processes. When laser ablation of the dielectric layer is done exactly on top of an unevenly filler via, the laser beam scatters from the uneven copper surface and the hole for the next microvia becomes deformed. Unsatisfactory fill of the next layer via becomes then very probable [5].



**Figure 1.11:** A SEM image of the cross-section of an overfilled via. The upper layer via has deformed due to the bump on top of the bottom layer via. The created interconnection is unreliable. Picture courtesy of Aspocomp [5].

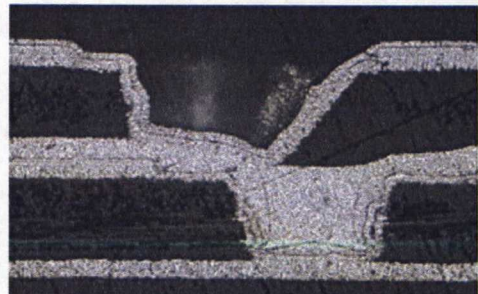


**Figure 1.12:** An incompletely filled buried microvia has caused the laser beam to deflect asymmetrically from its uneven top surface. As a result, the drilled outer layer via hole is malformed. Picture courtesy of Aspocomp [5].

### 1.4.3 Measuring via fill performance

Besides qualitative measures for fill performance, described above, also clear quantitative measures exist. One simple measure is the formed dimple depth (Fig. 1.13). The dimple depth can easily be measured without harming the measured object, by using

e.g. a laser interferometer. The problem with this measurement method is however, that no knowledge of the plated copper layer thickness is obtained.

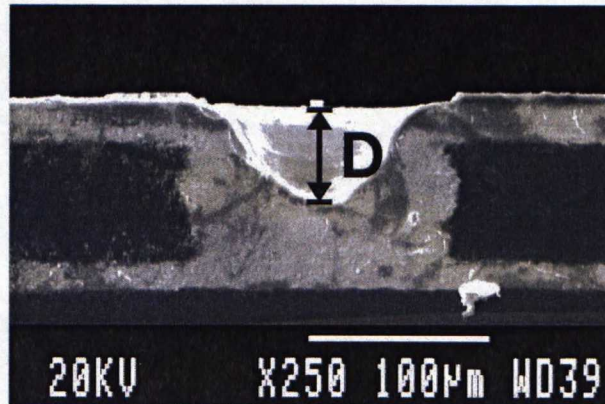


**Figure 1.13:** *D* (black arrow) denotes the dimple depth measure of the via in question.

A better picture of the whole process is obtained by creating a cross-sectional picture of the via (like all the pictures shown here) by microsectioning and photographing a filled test piece. The measured object is naturally destroyed completely but valuable information of e.g. the via fill ratio (Fig. 1.14) is obtained this way. The fill ratio is a good measure for the process levelling capability. Also other properties, such as absolute deposit thickness at various sites around the via as well as via dimensions can be measured from a cross-sectional picture.

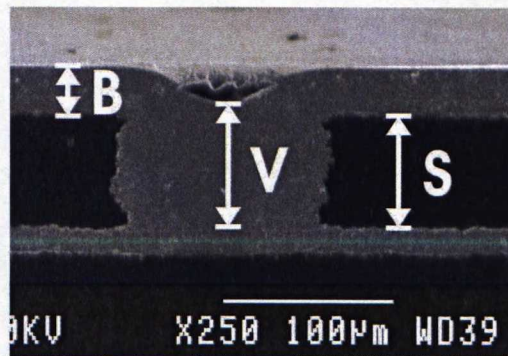


**Figure 1.14:** *B* (white arrow) denotes growth of the copper deposit on the PCB surface and *V* (white arrow) is growth on top of the center of via. *S* denotes the substrate layer thickness. Via fill ratio, *FR*, is calculated as  $FR = (B + S)/V$ .

#### 1.4.4 Microvia fill electroplating control basics

Due to the proprietary nature of the process, an operator can control the microvia fill electroplating process mainly by plating current density and plating time. As the plating chemistry stays constant, via size has the main influence on required plating time. Plating current density determines the rate of copper reduction and must thus be optimized in order to keep lead-time as short as possible. Too high a plating current

however, causes copper depletion to occur within the plated features, which in turn leads to faulty vias.

Copper deposit thickness in every via on the plated board cannot be measured during deposition. Only an estimate of the total amount of deposited copper can be obtained based on electrolysis power consumption. A good process model, however, can estimate and predict the outcome of the fill process and enable control actions to be taken on-line, before fault inspection, in order to prevent loss and to achieve the desired fill result. In this case, the process model forms the basis of a sophisticated process control method.

#### 1.4.5 Multilayered PCBs and microvia filling summarized

Multilayered printed circuit boards have metallic interconnections running, not only in the board's planar direction but also through the board, in the z-axis' direction. Several methods exist for creating these interstitial interconnections on multilayered PCBs and microvia filling by electroplating is one such method.

An electroplated microvia is solid metallic copper and has good electric, thermal as well as mechanical properties, which is why the microvia filling technology is favored. Problems related to microvia filling often stem from the rather complex process chemistry.

The performance of a microvia filling process is measured based on for example the dimple depth left by a fill process (the smaller the better) or the fill ratio achieved at a certain process (the closer to 100% the better).

### 1.5 Chemistry

The in-depth chemistry of copper electroplating is complex and includes several concurrently proceeding reactions, which form series of reactions possibly observed as a difference in copper reduction speed or surface shape evolution. The foundation of all copper electroplating is, however, the copper redox<sup>3</sup> reaction system.



The total forward to the right reaction shown above – copper reduction – happens in two steps:



Of these the first step is the rate determining step. The reaction rate of the second

---

<sup>3</sup>reducing and oxidizing

step may be up to three orders of magnitude greater than that of the first step.

Despite the speed of the second reaction step, an equilibrium concentration of cuprous ( $\text{Cu}^+$ ) ions can be observed in examinations and the cuprous ions are believed to have a substantial role in the copper electroplating additive chemistry [6].

Additives can change the total rate of copper reduction by either aiding or hindering formation of  $\text{Cu}^+$  ions.

What is essential about this reaction in respect to via fill modelling is that always when one cupric ion reduces into copper metal, two unit charges are transferred over the metal-solution interphase. This will need to be accounted for when calculating the relationship between plating current (density) and deposit growth.

### 1.5.1 Main electrolyte components

The copper electroplating bath is essentially an aqueous solution of copper sulphate and sulphuric acid. The concentrations of these main constituents can vary greatly. Table 1.1 lists typical electrolyte component concentrations used in microvia filling.

| Electrolyte component   | Concentration   |
|-------------------------|-----------------|
| $\text{CuSO}_4$         | 0.8 mol/l       |
| $\text{H}_2\text{SO}_4$ | 1.0 mol/l       |
| HCl                     | 1.0 mmol/l      |
| Organic additives       | 0.01–1.0 mmol/l |

**Table 1.1:** A typical microvia fill plating solution recipe (used in e.g. the experiments related to this thesis).

Copper sulphate is the initial source for copper ions during the electrodeposition process. Its concentration has the main influence on deposition rate and microvia fill success [7].

The concentration of sulphuric acid is generally markedly higher than that of copper sulphate. Higher acid concentration increases electrolyte conductivity and thus decreases local variations in potential [8].

The electrolyte conductivity is essentially determined by the copper salt and acid concentration. Other species are present in such minor concentrations that their contribution to solution conductivity can be ignored. Absolute conductivity of the electrolyte increases as ion concentration increases but the dependency is not linear, meaning that the molar conductivity of electrolyte components decreases as solution concentration increases [9].

Electrolyte conductivity is presented in more details in Section 1.6.4.

## 1.5.2 Electrolyte additives

The cornerstone of successful copper electrodeposition in high-density interconnect manufacturing is a good electrolyte additive chemistry. Generally, the additives are compounds, present in very minor concentrations, which by some chemical or physicochemical mechanism either inhibit the copper reduction reaction, accelerate copper reduction or inhibit other additives from inhibiting the reduction reaction (i.e. neutralize an inhibiting additive). In combination with local metal surface activity, local current density and differences in concentration, a variation in local copper deposition rate can be achieved with the use of additives. As mentioned earlier, the additives can actually turn the whole process contrary to common sense, enabling fastest copper reduction where its concentration is smallest!

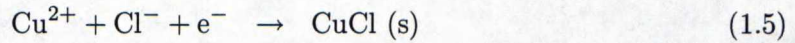
The additive chemistry and kinetics of (nano- and) micro-scale copper electroplating have recently been studied very much and a variety of publications related to the chemical compounds described below have been published since the late 90's. In this thesis, however, the emphasis is not on resolving the affecting mechanisms of additives in detail but instead, the focus is on finding out what is essential for modelling the phenomena and implementing these conclusions in the model. Still, an overview of the additive system chemistry is necessary in order to locate and understand the governing phenomena.

The exact chemistry applied in copper electroplating is rarely known to the process operator, which is also the case at Aspocomp's Salo factory. The lack of in-depth process knowledge even further emphasizes the meaning of being robustly able to on a general level characterize the governing phenomena and their mutual relations—rather than their individual magnitude. Tight requirements for exactly explaining the chemical mechanisms of all subprocesses can be somewhat relaxed.

Caution: the nomenclature of the electroplating additives is diverse and rather *colorful*. (Probably not least due to the business-related issues.) The terms used here are only one variant and selected in order to have an as self-explanatory terminology as possible.

### Chlorine

The basic additive in copper electroplating baths, known for already a long time, is chlorine. Chloride ions aid formation of smoother deposits in high current density areas and reduce anode polarization [3]. As a single additive present in an acid-copper plating bath, chloride ions accelerate copper reduction slightly [10, 11]. It is proposed in [11] that the chloride ion provides a second reaction mechanism for copper reduction in addition to the chloride free reduction (1.3, 1.4), and an increase of copper reduction results of reduction happening through two mechanisms in parallel.



As will be described later, chlorine also plays a significant role in plating chemistry as other additives are added to the solution.

Chlorine is provided as chloride by adding e.g. NaCl, or HCl to the solution. Typical chloride concentrations in commercial plating baths vary approximately between 1 mmol/l and 2.9 mmol/l (30-90 ppm) e.g. [12, 13, 14].

Too low or too high a chloride concentration will cause a coarse and dull deposit and a too high chloride concentration can polarize the anode severely enough for the deposition to stop [4]. In [15], however, successful deposition is carried out in a chloride concentration as high as 23 mmol/l (720 ppm) and the author claims chloride concentration alone is not as important as its ratio to other additives' concentrations. This will be discussed later.

Chlorine, when not part of a complex, is present in the plating electrolyte as a (hydrated) chloride ion ( $\text{Cl}^{-}$ ). Thus its mass transfer is governed by both migration and diffusion.

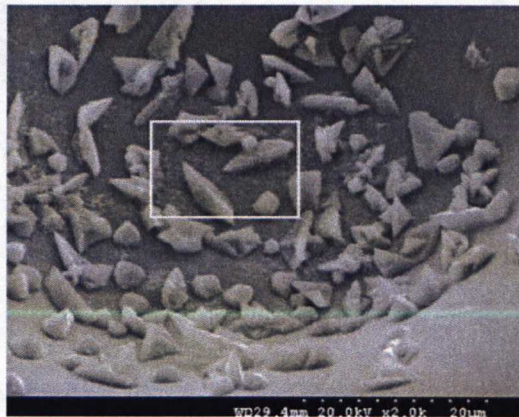


**Figure 1.15:** Copper chloride crystals accumulated on top of an electroplated microvia. SEM-image with 2000x magnification, 30° inclination [15].

### Reduction inhibiting additives – suppressors and levellers

The second type of additive universally present in copper electroplating baths (for electronics manufacturing) is a reduction inhibiting agent of some kind. These additives slow down the copper reduction reaction by some mechanism and can enable locally differing deposition speed.

Reduction inhibiting agents can be divided into two different types which have a distinctively different affecting mechanism. The first kind are denoted suppressor

additives and are typically large-sized polymers. The other type, denoted levellers, are cyclic or heterocyclic nitrogen-including compounds, significantly smaller in molecule size than the previous. Both are organic compounds.

A typical example of a polymer used as a suppressor agent is polyethylene glycol (PEG), with a molecular mass between 3 400 g/mol and 8 000 g/mol e.g. [16, 6]. Examples of leveller additives are Janus Green B (JGB, 475 g/mol), thiourea (77 g/mol) and benzotriazole (BTA, 119 g/mol), and 2-aminobenzothiazole (2-ABT, 150 g/mol) [17, 18, 19].

Concentration of suppressor additives in a typical copper electroplating bath can be e.g. from 10  $\mu\text{mol/l}$  [20] to 25  $\mu\text{mol/l}$  [13] to 100  $\mu\text{mol/l}$  [6] for PEG as suppressor. Concentration of the leveller additives is also in micromolar scale but depends strongly on the additive compound as well as electrolyte composition.

The inhibition effect of a suppressor additive is based on it forming a complex agent with a halide, which most often is chloride [21]. The suppressor polymer+ $\text{Cl}^-$  complex is proposed to create a blocking layer on the cathode, thus physically stopping access of the reducing species to the cathode surface [6, 13]. The blocking mechanism does not explicitly require that the polymer is consumed on the cathode [17]. Similar to the illustration in Figure 1.16 of the PEG+ $\text{Cl}^-$  suppressor complex in effect is presented in [16].

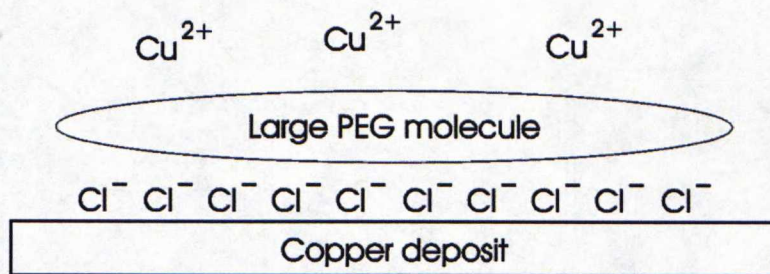


**Figure 1.16:** An illustration of how the large PEG polymer molecule in combination with chloride ions forms a blocking layer on the copper cathode surface.

A field-emission SEM micrograph in Figure 1.17 shows PEG molecules with a molecular weight of 7500 g/mol adsorbed on an electroplated copper surface. The adsorbed molecules are an estimated 30nm in diameter. Also chlorine was used as an additive in the plating solution. (Figure 1.17 is taken from [22], though originally published by the same author in [23].)

The above proposed mechanism gives rise to the importance of the chloride additive in the electrolyte. It effectively states, that if chloride ions are consumed on the cathode, this also reduces the effective concentration of the suppressing complex. Chloride ion consumption, as precipitation to  $\text{CuCl}$  crystals, was explained earlier in Section 1.5.2.

Polymers are electrically neutral molecules and therefore their mass transfer is determined by only diffusion. Being rather large in size, their diffusivity is minor compared to the diffusivity of smaller leveller additives. The leveller additives are also



**Figure 1.17:** A field-emission SEM picture of surface-adsorbed PEG molecules ( $M_w = 7500$  g/mol).

electrically neutral as molecules, but have a polar or ionic nature – their total charge is internally distributed unevenly over the molecule.

The exact chemical mechanism by which the described nitrogen-including compounds – the levellers – inhibit deposition cannot be considered known, but the basic principle assumed by researchers is that levellers interact with an accelerator additive (described next) present in the bath as to negate the accelerator's effect. Though the mechanism is not clear, clearly visible results have been reported in [18] and the principles for levelling mechanisms have been examined in e.g. [24].

Further, according to [25], the levelling agent has to be added to the electrolyte in order to prevent the accelerator from increasing deposition growth on the wafer surface and protrusive sites.

### Consumption of inhibiting additives

Consumption of the surface adsorbed species, whether a suppressor or a leveller, can happen either via incorporation into the copper deposit or a chemical reaction on the copper surface. Both lead essentially to the same result: a steady state mass flux and a concentration gradient of the inhibiting additive.

A concentration gradient of the inhibiting species means that inside, and especially at the bottom, of a via the additive's concentration is significantly smaller than at the outer edges of the via, and this results in locally different inhibition of the reduction reaction. Inhibition is greater on the via mouth than inside the via, leading to deposit growth being faster inside the via than on the level wafer surface.

Incorporation of leveller type additives has been reported in e.g. [19] and several models have been built upon the steady state mass flux of inhibiting agent assumption, e.g. [1, 26].

Yet, there are also reports claiming that the consumption of inhibiting agents during deposition is negligible [27].

In this thesis it is presumed that also the inhibition caused by possibly non-consumed additives, such as the polymer-type suppressors, is in any case dependent on some consumed species, specifically the chloride ion.

The main deficiency with models relying only on a reduction inhibition differential caused by diffusion limited mass transfer is, however, their incapability to produce deposition overgrowth (or "bump formation" [28]), which is regularly observed in real electroplating baths. This limitation can be addressed by taking accelerator species and deposited feature geometry changes into account, as described in the next section.

### **Accelerating – or suppressor neutralizing – additives**

The third type of additive species commonly present in a modern copper electroplating bath, is an agent that negates the effect of suppressing additives and thus effectively accelerates the deposition [4]. Therefore these additives are often referred to as accelerators.

Accelerator chemicals are organic compounds that contain sulphur. For example bis-(sodiumsulphopropyl) disulfide (SPS, 308 g/mol) or 3-mercaptopropane-1-sulfonic acid (MPSA, MPS, 155 g/mol) are used [29, 6].

Accelerator additives are usually present in the bath solution in micromolar concentrations, e.g. in the range of 0.1 to 10  $\mu\text{mol/l}$  [30]. It has been shown, however, that it is not so much the absolute concentration of the accelerator in question as it is the accelerator concentration relative to the chloride ion concentration in the electrolyte that matters [15, 31].

The molecular weight of accelerators is notably lower than that of suppressors, which enables them a better diffusivity compared to the large-sized suppressor-polymers. Studies show that accelerator species are consumed in deposition systems [14, 32]. However, other studies also argue that under certain conditions the accelerator additives have an ability to remain "floating" on the deposit surface during deposition [33].

According to recent researches regarding copper interconnect electroplating in micro-chip manufacturing, the local metal surface shape change (or area change) has a strong influence on local deposit growth velocity [34, 29, 35]. This coupling between micro-scale shape changes on the metal surface and the local increase or decrease of copper reduction rate is explained by the capability of the accelerator species to remain segregated on the copper surface and thus accumulate to those locations where surface shrinkage is greatest. Increased incorporation of accelerator into the copper deposit at areas where surface shrinkage is the greatest has also been reported [36].

Regardless of whether accelerators do get significantly incorporated into the deposit or not, they function by disrupting the copper-deposition inhibiting suppressor layer, e.g. [37, 38].

It is easy to imagine the sulfur-containing accelerator species (to first chemically adsorb on the copper surface and then) being incorporated into the rapidly growing copper deposit. On the other hand, the "bulldozing" effect that a shrinking, convex

copper surface would have on a segregated accelerator layer on top of the surface, is just as easy to imagine as the cause for the curvature enhanced deposition phenomenon mentioned. Thus, there is reason to believe that both phenomena take place on the cathode and the overall accelerator effect is determined by a balance between area change and accelerator consumption rate.

Though the common accelerator additives (SPS, MPSA) are often displayed in the literature as salts or ions, in this thesis they are considered as molecules without absolute electric charge. This relaxation is based on the fact that the accelerator species' concentration is small enough to have no significant meaning on electrolyte conductivity. As for mass transfer properties (Section 1.6), mass transfer of the accelerator additives is presumed to be diffusion limited due to their large molecule size. The electric field in the diffusion layer is weak, having an insignificant effect on the mass flux of accelerator additive species.

### 1.5.3 Surface adsorption

Only the very elementary concepts related to adsorption and adsorption theories' application in this thesis are presented here.

*Adsorption isotherms* are applied to describe the static relationships between additives' surface coverage on the cathode as well as the competitive nature of their adsorption. Kinetic models that derive surface coverage of additives based on the rates of their adsorption reactions can also be used to describe surface coverage in steady state. The formulae presented below are used to compute surface concentration and adsorption fluxes of additive chemicals in the via fill model of this thesis.

Adsorption of species in the electrolyte onto the metal surface can be considered as a chemical system, that always tends towards an equilibrium of electrochemical potentials of the species  $i$  in the electrolyte and the adsorbed species  $i$ . The electrochemical potential of species  $i$  in the liquid is determined by the species volumetric concentration<sup>4</sup> and on the metal surface by the species' surface concentration. Also the electrical state of the system as well as temperature affect the system behavior.

At equilibrium, the relationship of the properties mentioned for a certain species  $i$ , is given by the adsorption isotherm equations [39].

The most common kind of adsorption isotherm is the *Langmuir isotherm*. The Langmuir isotherm formulation assumes that (i) there are no interactions between the species adsorbed on the metal surface, (ii) that the free metal surface is equally good for adsorption everywhere and that (iii) the surface eventually saturates of the adsorbing species. Saturation is reached as soon as a uniform monolayer of the adsorbing species is adsorbed on the metal surface [39].

If the surface concentration ( $\text{mol}/\text{m}^2$ ) of a single species  $i$  present is denoted by  $\Gamma_i$  and the maximum (saturation) coverage by  $\Gamma_{s,i}$ , then the Langmuir isotherm of  $i$  can

---

<sup>4</sup>or more precisely, it's activity

be expressed by the following equation.

$$\Gamma_i = \frac{\beta_i c_i}{1 + \beta_i c_i} \Gamma_{s,i} \quad (1.8)$$

Here  $\beta_i$  accounts for the activity coefficient as well as standard free energy of adsorption of species  $i$  in the present conditions. Generally  $\beta_i$  describes the balance between adsorption and desorption (reaction rates) of  $i$ .  $c_i$  is the volumetric concentration of  $i$  in the electrolyte.

The equation elucidates the kinetic principles according to which, the rate of adsorption is only dependent on the concentration of species  $i$  in the solution  $c_i$  and the amount of free surface ( $\Gamma_{s,i} - \Gamma_i$ ) available for  $i$  to adsorb on. The rate of desorption again is assumed only dependent on the surface concentration of  $i$ .

Though, the amount of available adsorption sites on a metal surface (e.g. on a copper lattice) is always relatively equal, the saturation surface coverage  $\Gamma_{s,i}$  still varies for different species. This is simply due to e.g. different molecule size and orientation of adsorbed species; bigger molecules cover the surface faster, more tightly stacking molecules fit better on the same surface area.

Often the fractional surface coverage of species  $i$  is of more interest than its absolute surface concentration. The fractional surface coverage is simply  $\theta_i = \Gamma_i / \Gamma_{s,i}$ , and it naturally has no unit. Now the above given Langmuir isotherm of species  $i$  can be expressed as  $\theta_i = (1 - \theta_i) \beta_i c_i$ .

When several species are present in the electrolyte and adsorbing on the metal surface *competitively*, the Langmuir isotherm can be extended to cover this situation. Now all adsorbed species are considered when calculating the free surface area available for adsorption of each individual species  $i$  [39].

When  $N$  species are present, the equation for surface coverage of species  $i$ , expressing also its Langmuir isotherm, becomes as follows.

$$\Gamma_i = \frac{\beta_i c_i}{1 + \beta_i c_i} \left( \Gamma_{s,i} - \sum_{j \neq i}^N \Gamma_j \right) \quad (1.9)$$

For a two-component system ( $i = 1, 2$ ), assuming that each species adsorption and coverage is independent of each other, equation (1.9) can be simplified to a function of species' volumetric concentrations.

$$\Gamma_1 = \frac{\beta_1 c_1}{1 + \beta_1 c_1 + \beta_2 c_2} \Gamma_{s,1} \quad (1.10)$$

#### 1.5.4 Essential chemical interactions summarized

All the essential chemical interactions of the electroplating bath species take place on either one of the electrodes. The main concern here is on the cathode, where the surface chemistry of species adsorbed on the level board surface and in the vias, determine how the via fill process behaves. As shown, there are several different theories on how species

on the copper surface interact but the principles applied in this thesis are as follows.

- The copper ion concentration on the cathode surface is one main determining factor for the copper reduction reaction rate.
- Copper, in some form, interacts with chloride to form copper chloride ( $\text{CuCl}$ ) crystals. This interaction both aids the copper reduction reaction as well as consumes chloride ions on the cathode surface.
- The suppressing agent interacts with chloride ions to produce a large-sized complex agent, which essentially covers the cathode as an even layer, thus suppressing the copper reduction reaction. The suppressing effect of the suppressor is therefore dependent on both the suppressor additive concentration as well as the chloride ion concentration on the cathode surface.
- The accelerating agent adsorbs on the copper surface more strongly than the suppressing agent and practically remains stationary on the surface as the surface shape changes. This characteristic enables the accelerator to supersede the suppressing complex where present and thus undo the suppressor's suppressing effect. Further, due to its strong adsorption on the copper surface, the accelerator tends to accumulate where the surface area decreases and conversely, thin out where the surface area increases.
- The fractional effective surface coverage of each additive species determines their proportional impact on the copper reduction rate.

## 1.6 Mass transfer and conductivity

Mass transfer is an essential part of the copper electroplating problem. By optimizing agitation, bath temperature, electrolyte composition and other controllable macro-scale system parameters, one can improve process quality to some extent, but eventually the main phenomena take place in the micro-scale domain. Reduction of cupric ions happens on the metal surface, within the electric double layer, which on its behalf is covered by a quiescent diffusion layer where the main limiting mass transfer phenomena occur. Thus, diffusion evoked by concentration differences, migration caused by the electric field, and ion-ion interactions essentially determine how well matter is transferred to and from the electrodes (from and to the bulk solution). Figure 1.18 illustrates the effect that changes in the mass transfer conditions can have on deposit surface quality.

Since many of the thermodynamic properties of species as well as the physical process conditions can be somewhat altered by properly selecting process parameters and equipment, it is worthwhile to go through the factors that determine mass transfer in the electroplating bath. The equations presented here are also the ones used for modelling species' mass transfer with the finite element method (described in Chapter 2).



**Figure 1.18:** A SEM image elucidating the effect of mass transfer limitation on plated deposit surface smoothness. The mass transfer conditions are kept constant in every image but plating rate (i.e. deposition current density) is elevated from 5  $\mu\text{m}/\text{min}$  in (a) to 6  $\mu\text{m}/\text{min}$  in (b) and 7  $\mu\text{m}/\text{min}$  in (c).

### 1.6.1 Diffusion - migration down a concentration gradient

Diffusion is transfer of species' particles caused by differences in the species' concentration within the domain in question. The driving force for diffusion is thus the concentration gradient and the particles tend to move against the gradient—towards lower concentration.

Speed of diffusive mass transfer is determined by the diffusivity of a species in a certain surrounding matter. In our case of copper electroplating, the interesting species are the cupric ( $\text{Cu}^{2+}$ ), sulphate ( $\text{SO}_4^{2-}$ ), hydrogen ( $\text{H}^+$ ), hydrogen sulphate ( $\text{HSO}_4^-$ ) and chloride ( $\text{Cl}^-$ ) ions as well as the additive molecules. The surrounding matter is liquid, mostly consisting of water. Diffusivity of species  $i$  in the electrolyte solution is denoted by  $D_i$ . The system is presumed homogenous ( $D_i$  equal in every direction).

The amount of species  $i$  travelling over a certain domain in a certain time determines the diffusion-dependent behavior of the species in question. This amount, known as the species' diffusive material flux,  $N$ , is given by *Fick's first law of diffusion* where  $c_i$  is the species' concentration.

$$N_{\text{diff},i} = -D_i \nabla c_i \quad (1.11)$$

For electrically neutral particles, diffusivity is determined mainly by their molecule size. As mentioned, diffusivity also depends on the solvent properties as well as temperature.

#### Diffusivity approximations for additives

Obtaining numerical values for diffusion coefficients of electrically neutral species was done by estimating the coefficients based on two semi-empirical equations found in the literature [40].

The Einstein-Stokes relation was used for the large-sized polymer additives:

$$D = \frac{9.96 \cdot 10^{-16} T}{\mu V_m^{1/3}} \quad (1.12)$$

Here  $V_m$  is the polymer's molar volume multiplied by 1000 ( $V_m = n/V$ , where  $n$  is the

number of moles of the species with volume  $V$ ,  $\text{m}^3/\text{mol}$ ),  $T$  is absolute temperature (K) and  $\mu$  the solvent viscosity (Pa·s). The equation is suitable for estimating diffusivities of species with a molar volume ( $\times 1000$ ) over  $0.5 \cdot 10^{-3} \text{m}^3/\text{mol}$ .

For species with smaller molar volumes there are no equations that predict diffusivities accurately. However, the semitheoretical Wilke-Chang correlation equation can be used in several cases to estimate the diffusion coefficient.

$$D = 1.173 \cdot 10^{-16} (\varphi M_{\text{solvent}})^{1/2} \frac{T}{\mu V_m^{3/5}} \quad (1.13)$$

$V_m$ ,  $T$  and  $\mu$  are as before but  $\varphi$  is an "association parameter" depending on the solvent and  $M_{\text{solvent}}$  is the solvent's molar weight (g/mol). Values for  $\varphi$  can be found in the literature and e.g. for water it is 2.6.

In the thesis  $\varphi$  is taken as for water but the solvent's molecular weight and viscosity are considered as for 1.0 M aqueous sulfuric acid.

### The diffusion layer thickness

The physical thickness of the layer of the quiescent solution covering the electrodes depends mainly on solution agitation and, on micro-scale, on the electrode surface geometry.

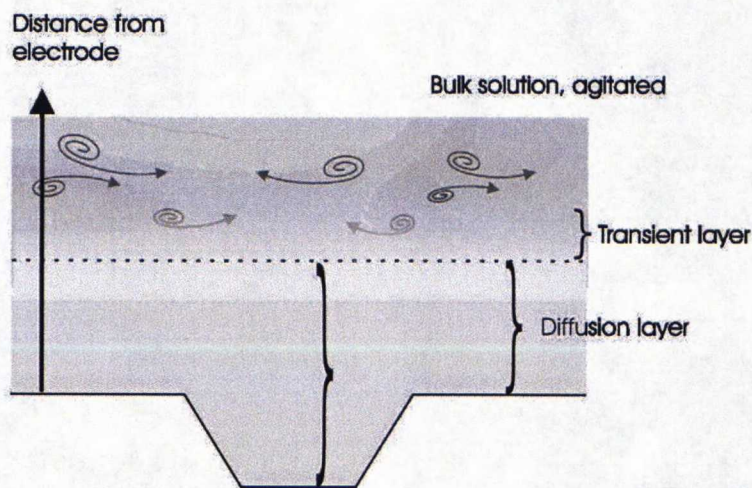


**Figure 1.19:** A picture illustrating physical thickness of the diffusion layer.

The theoretical background for estimating the effective diffusion layer thickness,  $\delta$ , is based on the *Nernst's diffusion layer* theory. Generally the theory is presented for a situation where species are extracted from the solution at the electrode surface (e.g. metal reduction at the cathode), the concentration gradient being towards the bulk solution. According to the theory,  $\delta$  is essentially unique for every species present in the solution, and diffusivity of the species in question as well as its concentration in the bulk and on the solid surface are assumed known. If the species' concentration at the metal surface is assumed zero and  $c_{i,b}$  is the species concentration in the solution

bulk,  $\delta$  has the following form.

$$\delta = \frac{z_i F D_i c_{i,b}}{i_l} \quad (1.14)$$

Here  $i_l$  is the limiting current density corresponding to the depletion of species on the electrode surface.  $z_i$  and  $F$  are the electron number of species  $i$  and Faraday's constant, 96485 As/mol.

Practical estimations of effective diffusion layer thickness are based on measuring the limiting current density under certain conditions. A common estimation method for the diffusion layer thickness is based on using a rotating disc electrode (RDE), which enables good control and prediction of solution flow and other mass transfer conditions. [2]

### 1.6.2 Migration along an electric potential gradient

Due to the potential difference between the cathode and the anode, the whole electrolyte bath is under the influence of an electric field. The field induces a force on the electrically charged particles in the bath, causing them to start migrating towards the direction of less potential difference between the particles charge and the field (towards a state of lower chemical potential).

In this thesis, electric potential is denoted by  $\phi$  and thus the electric field is expressed using the potential gradient  $\nabla\phi$ .

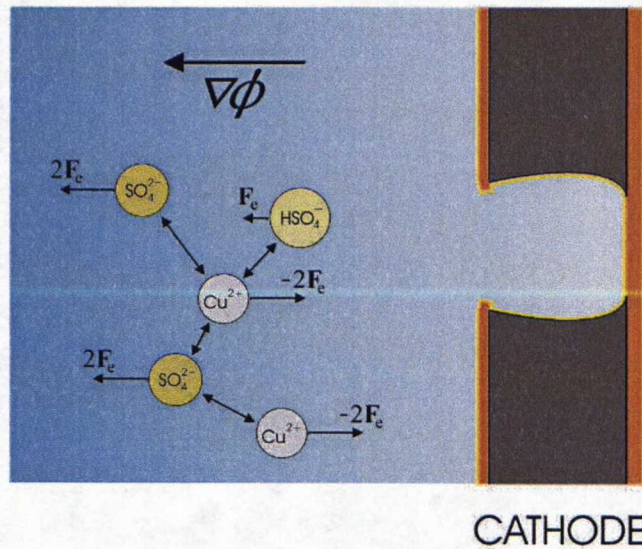


**Figure 1.20:** An illustration describing ion migration in an electric field and ion-ion interactions.

The velocity a particle gains in the environment it traverses in, depends of course on the strength of the electric field but also on the particle size and charge as well as the surrounding particles sizes and charge. In the case of copper electroplating, the interesting particles are the ions previously mentioned, (surrounded by each other while) travelling in an aqueous solution.

It is clear that though diffusive and migrative fluxes are caused by different phenomena, the eventual result is the same: mass transfer. It is also clear that migration cannot occur in the case of electrically neutral species since their charge is zero.

The speed of migrative mass transfer of a certain species  $i$  is determined by its *mobility* or *ionic mobility*,  $u_i$ . A relation known as *the Einstein relation* connects the species mobility with its diffusion coefficient:

$$u_i = \frac{D_i}{RT} \quad (1.15)$$

Therefore, diffusion and migration are tightly coupled for electrically charged species. In this thesis, the Einstein relation is used to calculate the diffusion coefficients of ionic species based on electrolyte conductivity.  $R$  in the equation denotes the ideal gas constant, 8.314 J/molK.

Electrolysis always includes charge transfer, i.e. a current, and in the copper electroplating electrolyte, charge is transferred by the charge-carrying  $\text{Cu}^{2+}$  ions.

Since current in the electrolyte is the stoichiometric multiple of charge carriers' material flow and thus directly related to the ion concentration change in the electrolyte domain, a relation between the current and the charge carriers' material flux can be formulated.

$$\mathbf{N}_{\text{mig},i} = -z_i F u_i c_i \nabla \phi \quad (1.16)$$

Applying the Einstein relation (1.15) to this equation further simplifies it.

$$\mathbf{N}_{\text{mig},i} = -\frac{z_i F}{RT} D_i c_i \nabla \phi \quad (1.17)$$

### 1.6.3 The Nernst-Planck equation

Combining the two means of mass transfer explained above yields us the so called *Nernst-Planck equation*. This equation describes diffusion and migration together in the quiescent diffusion layer covering the electrodes where convection is insignificant.

$$\mathbf{N}_i = \mathbf{N}_{\text{diff},i} + \mathbf{N}_{\text{mig},i} \quad (1.18)$$

$$= -D_i \nabla c_i - \frac{z_i F}{RT} D_i c_i \nabla \phi \quad (1.19)$$

### 1.6.4 Electrical conductivity of electrolyte

The property called *electrical conductivity*,  $\sigma$  couples the electric potential  $\phi$  and current density  $\mathbf{J}$  in the electrolyte bath, according to the electric field equation (1.20).

$$\mathbf{J} = -\sigma \nabla \phi \quad (1.20)$$

As described, the current in the electrolyte is nothing but the material flux of

charge carrying ions caused by the electric field over the electrolyte. A mass flux of charge carriers due to e.g. convection is not considered as current in this respect; only the mass flux caused by the potential gradient is. The equation for this mass flux is given in (1.17).

A formula for solution conductivity  $\sigma$  can be derived by combining the electric field equation (1.20) and the migration flux equation (1.17). The two equations are bound together by the relation  $\mathbf{J} = z_i F \mathbf{N}_{\text{mig},i}$ , which yields  $\sigma$  as follows:

$$\sigma = \frac{F^2}{RT} \sum_i z_i^2 D_i c_i \quad (1.21)$$

Electric conductivity of the copper electroplating bath is mainly determined by the sulphuric acid concentration but also copper sulphate concentration is considered in the thesis model. Other species are ignored due to their very low concentrations with respect to the two other mentioned.

An ionic species' diffusivity ( $D_i$ ) changes along with its concentration  $c$ . This is due to increasing ion-ion interactions and increasing drag effect. Generally  $D_i$  tends to decrease as concentration of species  $i$  increases, and generally the relation between the two is not linear.

### 1.6.5 Mass transfer related issues summarized

The Fick's diffusion law as well as the Nernst-Planck equation for mass transfer in a media under an electric field govern the mass transfer within the diffusion layer that covers both electrodes in the electroplating bath. The physical thickness of the diffusion layer is determined by the solution flow velocity in the very vicinity of the cathode, i.e. mainly by how strongly the electrolyte is agitated. Also the species' diffusivity affects its effective diffusion layer thickness.

All of the aforementioned equations can be solved numerically, thus enabling the first principles modelling of mass transfer. The time-dependent behavior of species' concentration can be obtained from the Nernst-Planck (1.19) equation by taking the spatial differential over it. This yields

$$\frac{\partial c_i}{\partial t} = \nabla \cdot (-D_i \nabla c_i) + \nabla \cdot \left( -\frac{z_i F}{RT} D_i c_i \nabla \phi \right), \quad (1.22)$$

which can be solved numerically.

The electric conductivity (1.21) of the solution depends on both local concentration and diffusivity of species present. Therefore the electrolyte conductivity is not equal all over the solution and this also has to be accounted for in the model. The electroplating bath is a very strong electrolyte and the relation between species (molar) conductivity and their concentration is not linear, which requires experimental verification of any estimate created for bath solution electric conductivity.

Outside the diffusion layer, in the solution bulk, convective mass transfer due to

agitation keeps solution conductivity, species concentrations as well as other thermodynamic properties of the electrolyte constant over the whole bath.

## 1.7 Electrode processes

After considering mass transfer of ions in the electrolyte, it is clear how current flows in the electrolysis circuit. In the electrolyte, current is carried mainly by copper ( $\text{Cu}^{2+}$ ) ions flowing from anode to cathode due to convection, diffusion and migration in the electric field. The circuit is completed by the interconnections that connect the electrodes outside the electrolysis bath and where current is carried by free electrons ( $e^-$ ). This is where the current direction is set by a current rectifier.

### 1.7.1 Deposition growth and current

Each copper ion carries a positive charge of two unit charges  $e$  and each electron carries one negative unit charge. When ionic copper is reduced from the electrolyte according to the copper reduction reaction,  $\text{Cu}^{2+} + e^- \rightarrow \text{Cu (s)}$ , two unit charges are transferred between the liquid phase and the solid metal lattice. The relation between amount of copper reduced and current, is given by the *Faraday's law*, which can be expressed as follows.

$$n_{\text{Cu}} = \frac{Q}{z_{\text{Cu}}F} = \frac{\int I(t)dt}{z_{\text{Cu}}F} \quad (1.23)$$

$n_{\text{Cu}}$  is the number of copper moles reduced and  $z_{\text{Cu}}$  is the cupric ion electron number or valence number, which is 2.  $Q$  is total charge transferred during reduction, and it is more conveniently expressed as integral of current,  $I$ , over time,  $t$ .

When knowing the density ( $\rho_{\text{Cu}}$ ) and atomic weight ( $M_{\text{Cu}}$ ) of copper, the copper deposit growth velocity  $\mathbf{v}$  on a deposition surface with the area  $A$  can be derived upon Faraday's law. Considering current density ( $i = I/A$ ) instead of absolute current simplifies the formula even further.

$$\mathbf{v} = \frac{IM_{\text{Cu}}}{Az_{\text{Cu}}F\rho_{\text{Cu}}} = i \frac{M_{\text{Cu}}}{z_{\text{Cu}}F\rho_{\text{Cu}}} \quad (1.24)$$

### 1.7.2 Current in an electrochemical system

When an electric field is forced over an electrochemical system, the system naturally changes in order to reach a chemical equilibrium with the imposed external conditions. This results in current and mass flowing to certain directions and electrochemical reactions happening at certain rates on the electrodes.

The rates of the electrochemical reactions taking place on the electrode-electrolyte interphases depend, as do all the reaction rates, on the energy available for the reacting system. Besides heat, also the potential difference (i.e. voltage) forced over the system brings energy into electrochemical systems.

The potential difference over a metal-solution interphase can be considered as a straight-forward measure of (potential) energy available for the electrochemical reaction taking place there.

For an electroplating bath, the energy required to transfer charge between the cathode and the reducing species in the electrolyte, determines the minimum potential difference required for the plating reaction to occur at a certain rate. This potential difference is known as the *charge transfer overpotential* or *activation overpotential*. It characterizes the nature of the electrochemical reaction in question by describing how high the chemical activation energy of the reaction is.

When the activation overpotential is available for a reaction, mass transfer can become a reaction rate-limiting factor. For instance, copper can be reduced from the electrolyte into solid metal only as fast as diffusion and migration can provide the metal-solution interphase with copper ions. Therefore, the thermodynamic properties of the system also determine a limit for how fast electrolysis can be carried out and how big a current can flow in a certain system. The theoretical maximum current, determined by limited mass transfer according to the Nernst diffusion layer theory, was explained earlier (1.6.1).

In practice, mass transfer limitations can be reduced by using good agitation, high solution concentration and low enough external electromotive force (EMF). Then the current over a metal-solution interphase is determined by the activation overpotential mechanism described by the *Butler-Volmer equation*.

$$i_i = i_{i,0} \left( e^{\left( \frac{(1-\alpha_{i,a})z_i F}{RT} \eta_i \right)} - e^{\left( \frac{-\alpha_{i,c} z_i F}{RT} \eta_i \right)} \right) \quad (1.25)$$

The  $\eta_i$  in the Butler-Volmer equation is the overpotential over the metal-solution interphase on electrode  $i$ , of the chemical system in question.  $\alpha$  is the transfer coefficient of the system and  $\alpha$  describes to which direction over the interphase charge is *more easily* transferred. The subscripts  $a$  and  $c$  of  $\alpha$  denote whether it is the transfer coefficient of the anodic or cathodic reaction that is in question ( $\alpha \in [0, 1]$ ).  $i_{i,0}$  is the exchange current density of system  $i$ , which is the density of the current flowing through the system when it is in equilibrium ( $\eta_i = 0$ ).

The Butler-Volmer equation thus describes a net current that follows as various electrochemical reactions take place at an interphase. The numeric value for a current yielded by the equation may be negative or positive, depending on whether the system is *anodic* (i.e. releasing charge transferrers) or *cathodic* (consuming charge transferrers). When applying the equation in combination with the electric circuit interpretation of the electroplating system, one must reconsider the current direction on each electrode. (It would be bizarre to have current flow in opposite directions on cathode and anode, though they both are part of the same electric circuit.) Naturally, the absolute value of the current magnitude does not change depending on interpretation.

In theory, the Butler-Volmer equation should be used to compute the current on

both the anode and cathode, for each individual species separately. The total current density would then be the sum of all the individual current densities. Often, however, an approximation of the total system must be made because determining  $\eta_i$ ,  $\alpha$  and  $i_{i,0}$  parameters separately for all individual species, included in even a simple electrolyte bath, is impossible due to species' interactions.

### Potential, voltage, overpotential and current

Obviously the fundamental reason for (net) current flow is the potential difference between the electrodes. But because electrochemical reactions are required for current to flow, the reaction energies, described by overpotentials, create a resistance for current flow in the electrolysis circuit. The reactions take place within the *electrochemical double layer* on cathode and anode and the situation is illustrated in Figure 1.21.

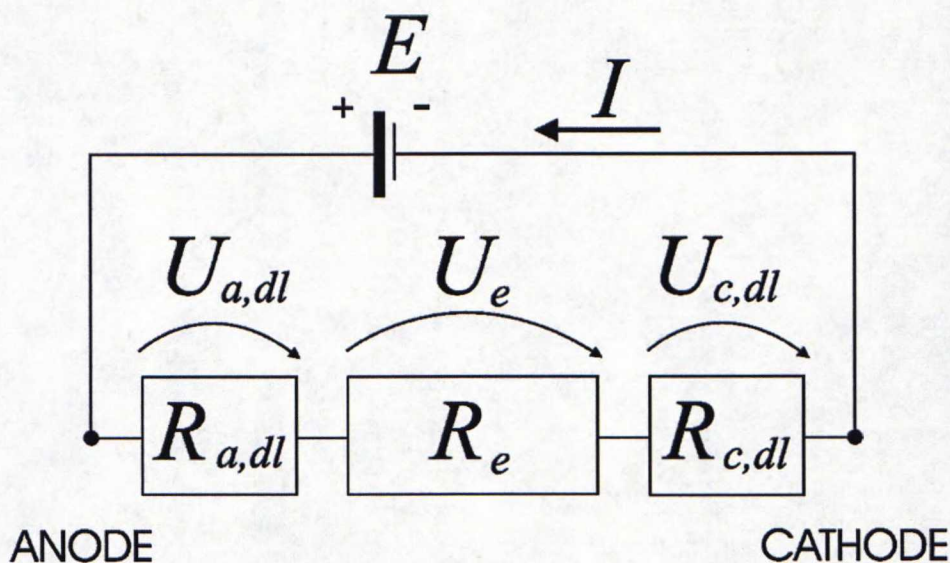


**Figure 1.21:** An schematic illustration of the electrolysis' electric circuit including the double layer resistances for current flow. (The subscripts of  $U$  and  $R$  denote  $a$  for anode,  $c$  for cathode,  $e$  for electrolyte,  $dl$  for double layer).

The  $U$  with different subscripts in Figure 1.21 denote voltage drops experienced in different sections of the electrolysis circuit.

The overpotential ( $\eta$ ) of a system is defined as the deviation between the potential difference over the electrodynamic double-layer when current is forced through the system, and the same difference when the system is in equilibrium ( $\Delta\phi_{eq}$ ).

$$\eta = \Delta\phi - \Delta\phi_{eq} \quad (1.26)$$

When submitted to an external electromotive force (EMV), the potential drop depends mainly on the imposed EMV, but can also be influenced by e.g. local surface chemistry (a.k.a polarization of electrode).

For copper the standard equilibrium potential  $\Delta\phi_{eq}^0$  (measured against a standard

hydrogen electrode (SHE)) is approximately 0.337V. This potential is measured in a standardized system, where the activity of solvated copper (ions) and metallic copper are known. (By definition, activity of a metal electrode is always 1.)

Hence, the equilibrium potential  $\Delta\phi_{eq}$  of a real system depends on the ion activities of the electrolyte. The dependency is described by the *Nernst equation*, which for a redox system of species  $i$  on a metal-solution interphase can be formulated as follows.

$$\Delta\phi_{eq,i} = \Delta\phi_{eq,i}^0 + \frac{RT}{z_i F} \ln(a_i) \quad (1.27)$$

Here  $a_i$  is the species' activity, which can be approximated based on the species' concentration.

### Connecting chemistry and current

The chemical environment on the metal-solution interphase can significantly alter the rates of electrochemical reactions taking place there. As described in Section 1.5, though some chemical species wouldn't downright take part in the reduction of metal ions, the species present can hinder the rate of metal reduction markedly by inhibiting charge transfer through some mechanism. This kind of a situation would mean that the activation overpotential (in the inhibited sites and thus also generally) is elevated, or conversely the current density is reduced.

Combining the capability of other chemicals to inhibit electrochemical reactions with the capability of others to deactivate these inhibiting chemicals, creates electrochemical systems, where reaction rates are determined not only by thermodynamics and the external EMV, but also chemical and geometrical properties of the system.

Since the rate of redox reactions taking place at the metal-solution interphases have to match with the corresponding currents, the mentioned properties have to be accounted for in the electrode equations.

In order to account for the chemical effects of additives, a *chemical term*,  $\mu$ , is introduced in the Butler-Volmer equation (1.25) for the system current.

$$i_i = i_{i,0}\mu \left( e^{\left(\frac{(1-\alpha_{i,a})z_i F}{RT}\eta_i\right)} - e^{\left(\frac{-\alpha_{i,c}z_i F}{RT}\eta_i\right)} \right) \quad (1.28)$$

$\mu$  is introduced in the equation on both cathode and anode separately.  $\mu$  accounts for whatever effects the electrode surface chemistry has on current flowing through the metal-solution interphase on that electrode.

### 1.7.3 Summary of the relevant electrode process principles

When the applied plating current density is known, the copper deposit growth velocity can be calculated based on Faraday's law (1.23), copper density and copper's molecule mass.

The plating current density depends on the local surface chemistry, solution chem-

istry as well as other operating conditions and is described by the Butler-Volmer equation (1.28). The Nernst equation (1.27) is applied to describe the effects of solution electrochemistry.

The electrode current system can and must be simplified assuming a one-directional total system as well as considering, in terms of current flow, only the most dominating electrochemical process, namely the copper reduction reaction (1.2).

## 1.8 Previously done modelling work and existing models

According to [41], mathematical models describing feature filling during electrodeposition have been developed at least since 1990. The first models describe *geometric levelling*, meaning metal surface smoothening that happens when deposited metal accumulates in grooves and holes on the original substrate surface. Irregularities of the metal surface gradually even up as the deposition process proceeds. Reaching a flat deposit surface this way, without using additives, requires a long time and subsequently the deposits become too thick for practical purposes.

### 1.8.1 The diffusion limited mass transfer of additives model

In 1998 a model based on *diffusion limited mass transfer of an inhibiting additive* was developed by Andricacos et al. at IBM research division [1]. The model assumes additive consumption on the metal surface which leads to an additive flux from the bulk solution through the diffusion layer, and thus an additive concentration difference between sites, where the effective diffusion layer thickness varies. The inhibitor concentration difference enables far faster levelling of surface irregularities than plain geometric levelling.

The reported results obtained with Andricacos' model corresponded with experimental deposition results obtained for partially filled 1  $\mu\text{m}$  wide interconnect trenches.

Andricacos' model had a strong influence on the nomenclature of copper electroplating for microchip-scale applications. Terms like *superfill* for describing faster than conformal deposition growth in blind holes and trenches on the chip, and *damascene electroplating* denoting the whole copper on-chip interconnection electroplating process stem from his paper.

Soon after the '98 model, other more complex models considering accelerator additives, precise mass transfer and the surface shape change were developed. One developed by Georgiadou et al. was published early 2001 [42]. This model did include an additive species but emphasized geometric properties (aspect ratio) and mass transfer phenomena, incorporating not only diffusion and migration but also convection<sup>5</sup>. Two different numerical implementations of the model were carried out and compared in the same context. Essentially, Georgiadou's model relied on limited mass transfer of

---

<sup>5</sup>despite the fact that also this model discussed submicron dimensions

additives.

### 1.8.2 The curvature enhanced accumulation of accelerator model

Later in 2001 (at least) two more significant models for simulating shape evolution of electroplated surfaces were published. The first one presented by Moffat et al. [29] considered surface coverage of an accelerating additive coupled with the modelled surface arc-length change. The accelerating additive was presumed to accumulate during the deposit growth there where the deposit surface had a concave shape.

Moffat's first generation model had deficiencies, e.g. not considering diffusion or depletion of cupric ions in the solution, but the model was a big step forward in modelling the "superfill" of nanometer-scale features. The model was later entitled *curvature enhanced accumulation of accelerator* (CAEC) model.

In 2001 also West et al. formulated a similar model to Moffat's, based on the CAEC principles [43]. From the viewpoint of a common reader, West's model was greatly simplified from the previous models and better highlighted the main principles of modelling microchip-scale electroplating. As Moffat used a specific *local curvature coefficient* for imposing increased deposit growth on concave surfaces, West implemented the CAEC effect via area computation. (No formulae for either of these were given in the published articles, however.) West's model lacked quantification of model parameters and was thus as such of rather little practical use.

### 1.8.3 Status quo

None of the models developed by early 2006 considered the whole range of additives in the electrolyte cocktail used in industrial interconnection plating baths. This is most likely due to insufficient knowledge of the actual chemical mechanisms that lie under superconformal electrodeposition of features, especially regarding the additive interactions and surface chemistry.

A great deal of effort has been put into inspecting the aspects of copper electroplating and gradually the work of Moffat et al., Vereecken et al. [6] and Dow et al. [13, 15, 44, 32] are yielding complete mechanism theories that incorporate several bath additives and their effects – at least in principle.

At the time of writing, the most recent model found for simulating nanometer-scale feature filling is from January 2006 [24]. The model discusses surface coverage of all, suppressing, accelerating as well as levelling additives and includes the deposit surface shape change effect. The extended CEAC model is developed for a specific "base" electrolyte composition (PEG,  $\text{Cl}^-$ , SPS) and includes a hypothetical, generic leveller species to account for the leveller's disruptive effect on accelerator influenced deposition increase. As in the very first CEAC models, also this model applies a special *curvature factor* to account for the deposit surface shape change.

Still, despite all research done on the subject, a mutual consensus over what phe-

nomena actually dominate the plating process, what additives are required and in what conditions to reach the desired plating result, does not yet exist. The modern models generally only consider systems with at least three additives, but reports show successful feature fill with only two additives [20, 45]. Various optimum values for additives, especially in regard to the chloride ion concentration are proposed [15].

Some studies say that aging time of the accelerator additive in the bath is a critical factor for desired fill result [46, 47]. Others emphasize convection as means of mass transfer [32, 42] or suppressor polymer molecule size [16, 45]. Also the difference between rate of the surface adsorption has been proposed as the dominant factor of superconformal copper electrodeposition [27], and all of these rather recently.

#### 1.8.4 Implementation techniques

Several techniques for actually numerically solving the models presented above have been tried out. In [35] a level set based implementation was developed. The level set computation relies on discretizing the solution space but no mesh restructuring is required during solution as the boundary, the movement of which is to be modelled, is described by a contour line of a suitable function. Because the boundary is just a contour line – a level line – of a function, it can easily have any shape desired for. No problems caused by overlapping mesh elements or infinitely small mesh elements thus occur.

The level set method is, however, rather hard to formulate and when e.g. inspecting effects of or trying to optimize geometrical properties of a feature to be plated, the model must be easily and broadly modifiable. In order to be sufficiently accurate, the level set method is also inherently demanding to compute. For model based control purposes for instance, it is rather inconvenient to use a computer model requiring three days on an up-to-date PC [35] to solve.

The finite element method, also applied in this thesis, was tried out by e.g. Georgiadou [42]. He compared the FEM solutions with another method called *etching and reaction modelling for electrochemical systems* (ERMES) method, specially designed for problems of this nature. Both computational methods performed adequately and neither of these proved superior to the other. The finite element method calculation was concluded to be less dependent on mesh type (discretization). No information about computation time or equipment requirement was given in the publication.

Also a Monte Carlo based implementation for simulating electrodeposition of copper on submicron trenches has been created [48]. The implemented model included only one hypothetical suppressing additive whose concentration, adsorption and consumption were investigated in combination with effects of trench aspect ratio. A typical trench filling simulation run on a fast computer took two days.

A significantly simplified implementation of the CEAC model (implemented e.g. with the level-set code in [35]) was also provided by Moffat's team in [34]. The *simple model*, as entitled, reduced computation time of the model to seconds, but the whole so-

lution essentially relies on one differential equation, thus also neglecting a large portion of the problem dynamics and governing chemical phenomena.

## Chapter 2

# Modelling microvia filling

Only a minor part of the research related to copper electroplating interconnect technologies concentrates on micro-scale electroplating. The majority discusses chip-scale systems, but luckily the essential chemical and electric problems and principles are somewhat the same in both domains.

When proceeding from nanometer-scale dimensions to micrometers, several aspects regarding mass transfer and time scale still need to be reconsidered. For example, filling of 100nm wide interconnect trenches on a silicon chip happens within minutes when a 130 $\mu\text{m}$  in diameter micro via requires about an hour to be filled. Further, a trench filling process is much more easily approximated as a 2D-problem than filling a round hole, which is essentially more three-dimensional than a trench. Also surface area changes are significantly faster and greater in nanometer-scale systems with high aspect ratios, than in a 100 $\mu\text{m}$ -microvia, whose aspect ratio is often below one.

### 2.1 The microvia filling process model

One aim of this thesis is to develop a model of the micrometer-scale via filling process, that is sufficiently accurate and versatile for process control purposes. As it is clear upon the literature review regarding electrochemistry, additive chemistry and thermodynamics, only the very fundamental parts of the model are understood, namely the mass transfer related principles. The electrochemistry related to charge transfer required for copper reduction is a well established concept, but principles for calculating the overpotential and the chemical mixed potential values in the additive-influenced system is still based very much on assumptions and educated guesses. The least well known factors and most uncertain assumptions in modelling the via fill process are related to the chemistry of additives involved in the process.

#### 2.1.1 Assumptions, exclusions and simplifications – scope of the model

A plain fact is that neither the process operators at the example case production line nor the process control developers know what is the actual composition of the elec-

troplating bath solution. Though additive concentrations for two electrolyte additives are measured on-line for control purposes, the names of these additives are generic, non-describing identifiers and the concentration values measured have no meaningful unit (ml/l). Hence, only indicative values of e.g. additive consumption or conservation can be obtained, though again the question of knowing what additive solution includes what chemical compound arises.

To tackle the problem of the unknown electrolyte additive composition, the modelled bath includes only one generic additive species, which is presumed to sufficiently describe the relative behaviour between the suppressor and accelerator (i.e. suppressor negating) additives. A single electrolyte additive is assumed to sufficiently capture the phenomena related to additives' mass transfer. Having several additives in the electrolyte solution domain only increases the number of mass transfer equations to be solved as well as free parameters, while keeping the fundamental phenomenon the same.

Since the superconformal deposition in microvias is not completely driven by phenomena related to mass transfer of additives, also the local area change in different parts of the plated surface is considered in the model. One can consider the balance between these two - mass transfer phenomena and local area change - as something determined by the relative concentrations of suppressing and accelerating additives in the electrolyte. As explained in Section 1.5.2, the suppressing and accelerating additives seem to have distinctively different affecting mechanisms, where the former type's effect is more governed by mass transfer and the latter's by surface adsorption and surface area change related factors.

The simplifications presented above enable a robust, but under appropriate interpretations meaningful study of the model and the process, even in the shadow of unawareness over absolute solution composition.

The problem of only considering relative values instead of absolute values is of course, that no information of absolute values is either obtained. However, as the production line process is always controlled somewhat close to the optimum values given by the equipment supplier, even the relative values can be used to judge what variable should be controlled and to what direction, if control actions are needed. Obviously, keeping the closer-to-optimum variables untouched while trying to optimize the relative values by changing the further-from-optimum variables is the simplest strategy.

Electrochemical properties of the plating system are implemented as precisely as possible. However, lacking the possibility for extensive laboratory analyses, voltammetric experiments etc. several assumptions have been made when determining parameters for the initial model. The current density used for process control on the production line is known.

Parameters related to thermodynamics, namely diffusivities of species, are estimated based on conductivity measurements done on the bath solution samples taken from the production line. Also empirical correlation equations are used.

Solution temperature is measured and controlled continuously on the production line, and it is assumed constant in the model due to its small actual variation.

Density and average molecule mass of the electrolyte is calculated by assuming the bath solution as an aqueous solution of copper sulphate and sulphuric acid. Volume of individual species is assumed to remain constant during solution mixing. Viscosity for the electrolyte is taken as the viscosity of sulphuric acid of equal concentration with the electrolyte. Both density and viscosity are assumed independent of temperature due to continuous temperature control on the production line.

All model parameters are considered free parameters as long as their numerical values are within reasonable physical restrictions (e.g. cathodic overpotential cannot be positive). An effort to correct them will be made afterwards on the basis of via filling experiments done on the production line, as well as other experiments.

### 2.1.2 The finite element method

The finite element method (FEM) is a numerical solution method for solving partial differential equations (PDEs). Once a phenomenon occurring in space and time, for example diffusion, is formulated as a PDE model, e.g. the diffusion equation, problems related to this phenomenon can be solved by applying FEM.

The finite element method was chosen as the solution technique for the model because it is well documented in the literature and there are several FEM-based modelling tools, easy to apply to even complicated problems. Further, none of the other examined applicable method was found superior to FEM.

The starting point of a FEM solution is the *mesh*, i.e. a discretization of the original problem domain into small units of simple shape. This results in a net of nodes with nearly equal distances between each other. Roughly put, each node of the net is a solution point for the problem and each distance is a discretization step in space. Finally, in addition to the spatial problem, there is the problem in time, and a proper PDE can model the phenomenon accurately in all these dimensions.

Converting a real world problem into a FEM model requires defining all the equations that describe the problem phenomena in the correct format at every point of the modelling domain. In the via fill model case, this means creating initial and boundary conditions and formulating PDEs for mass transfer of all species, the electric potential field as well as the mesh shape evolution during model solution. In addition, regular expressions are used to compute several static relations, e.g. additive effects.

### 2.1.3 Implementation of the model

Despite that the real world problem being in three dimensions, the model is built in two dimensions, in a cartesian coordinate system. The three-dimensional problem is simplified by considering the microvia perfectly symmetrical over the real world  $zx$ -plane. The coordinate change from  $xyz$ -coordinates to  $xy$ -coordinates is illustrated in

Figure 2.1.3.

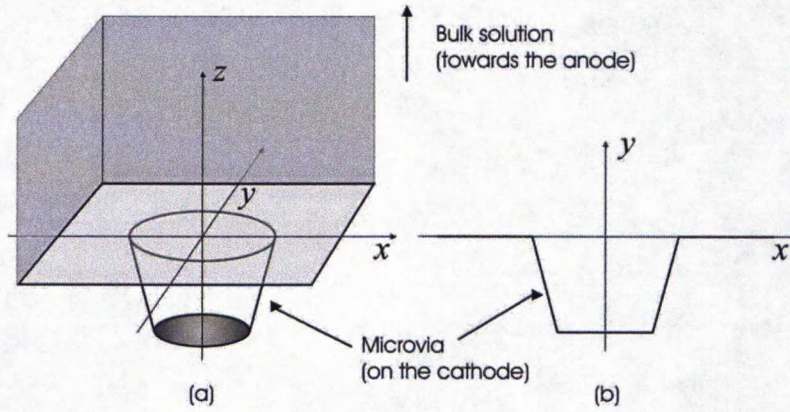


**Figure 2.1:** The coordinate transformation done when simplifying the real world 3D-problem (a) into two dimensions (b).

In total there are three independent variables in the model, the spatial coordinates  $X$  and  $Y$ , and time  $t$ . Depending on the model configuration, there are approximately 250 to 1000 mesh elements and the number of degrees of freedom to be solved ranges from approximately 5000 to 20000.

It is noteworthy that modelling the electrochemical double layer is not implemented as a FEM problem but only through the current equation (2.12). This is justified by the dimensions of the electrochemical double layer, its thickness being within only tens of Ångströms [41]. The current equation sufficiently captures the physical effects brought to the model by the layer and no spatial gradients need to be solved within the model.

Neither is the electroneutrality condition ( $\sum c_i z_i = 0$ ) enforced in the diffusion layer. This simplification can be justified by assuming concentration and diffusivity of hydrogen ions to be so high (compared to cupric ions) that the electroneutrality requirement does not pose a limitation for mass transfer of cupric ions. Further, the electroneutrality condition can be approximated by always presuming the sulphate ion concentration equal to copper ion concentrations. (These two are counter ions in copper sulphate.)

On a regular 2.66GHz desktop PC with 1GB RAM, the model is solved within one to five minutes, depending on the model configuration.

The Comsol Multiphysics [49] graphical modelling environment was used to create the FEM implementation of the presented model.

### Computing mass transfer

Mass transfer of components is calculated based on the Nernst-Planck equation (1.19) explained earlier.

$$\frac{\partial c_i}{\partial t} = \nabla \cdot (-D_i \nabla c_i) + \nabla \cdot \left( -\frac{z_i F}{RT} D_i c_i \nabla \phi \right) \quad (2.1)$$

Specifically, the dependent variables to be solved are the concentration of cupric

ions  $c_{Cu}$  and additive species  $c_{Add}$ . The molecular charge of the latter equals zero, and thus its mass transfer equation becomes the diffusion equation.

All concentrations are restricted to equal a constant bulk solution concentration on the diffusion layer outer boundary, a.k.a. the anodic boundary.

$$c_i = c_{b,i} \quad (2.2)$$

The diffusion layer cross-section boundaries are formulated as symmetry boundaries, hence the concentration gradients over these boundaries are not restricted in any way.

On the cathode boundary, the boundary of interest, the boundary normal concentration gradient is restricted to equal species' flux over the boundary,  $N_i$ . ( $\mathbf{n}$  is the boundary normal vector.)

$$N_i = \mathbf{n} \cdot (-D_i \nabla c_i) + \mathbf{n} \cdot \left(-\frac{z_i F}{RT} D_i c_i \nabla \phi\right) \quad (2.3)$$

For the cupric ion this is the reduction flux (i.e. rate of deposition), for other species the flux is either their rate of adsorption on the metal surface possibly combined with their desorption rate from the surface and/or decomposition rate on the metal surface.

### Computing electric potential

Electric potential in the modelling domain is computed based on the electric field equation (1.20). Only one dependent variable, the potential  $\phi$ , is included in the model. As denoted by the equation, potential is coupled with current in the electrolyte, which in turn is mostly determined by current flowing over the cathode metal-solution interphase. In the modelled system, the continuity equation for charge is considered (in two dimensions), which in the modelling domain reduces into solving the Laplace's equation for electric potential  $\phi$ .

$$\nabla \cdot (-\sigma \nabla \phi) = 0 \quad (2.4)$$

On the anodic modelling boundary, the electric potential is fixed to the anodic boundary potential  $\phi_{anodicboundary}$ , which is calculated based on the measured potential difference between the anode and cathode (i.e. the EMV,  $E = \phi_a - \phi_c$ ), the cathode potential  $\phi_c$  to be solved and the dimensions of the real world deposition apparatus.

The bulk solution is assumed homogenous and thus its electric conductivity is constant over the whole bath. Constant conductivity results in a linear drop of the electric potential when moving from anode to cathode. The anodic boundary voltage is thus obtained simply as a share of total voltage drop over the electrolyte, the share corresponding to the quotient of the physical diffusion boundary thickness and the electrodes' distance, as follows.

$$\phi_{anodicboundary} = \phi_c + (\phi_a - \phi_c) \frac{\delta}{d_{electrodes}}. \quad (2.5)$$

$\delta$  is the average thickness of the physical diffusion layer and  $d_{electrodes}$  is the distance between anode and cathode.

Potential over the symmetry boundaries is not restricted in any way.

On the cathode, the potential is fixed. The potential gradient over the cathode (multiplied by local conductivity) must equal the cathode normal current density flux over the boundary.

$$-\sigma \nabla \phi = \mathbf{n} \cdot i_{cathode} \quad (2.6)$$

The cathode current density  $i_{cathode}$  is calculated with the current equation (2.12) derived upon the Butler-Volmer equation. Current is always assumed to flow normally to the metal surface.

Note, that here the *boundary* comprises, inclusively, everything in between the very nearest-to-cathode liquid layer and the outermost metal lattice layer – including the electrochemical double layer. Therefore the presented reasoning is justified, though one can question what might be the *conductivity of the electrochemical double layer?*.

### Computing electric current

Calculation of current in the electrode processes is done based on the Butler-Volmer equation (1.25). The equation can be solved with respect to the total electromotive force applied over the plating bath.

First, the total chemical system is simplified by approximating it based on the dominating elements found in the system. Parameters of individual chemical components are approximated by setting them equal to those of the dominating system, or to that of the measurable total system. This procedure reduces the Butler-Volmer system into one equation for both the anode and cathode (2.7). The chemical term  $\mu$  stays in the equation as such.

$$i_i = i_0 \mu \left( e^{\left( \frac{(1-\alpha)zF}{RT} \eta \right)} - e^{\left( \frac{-\alpha zF}{RT} \eta \right)} \right) \quad (2.7)$$

Here  $\alpha$  and  $i_0$  are parameters that need to be determined experimentally, and  $\eta$  becomes the overpotential measured or calculated based on the overall system. (Note that now, the  $\alpha$ -parameters of the anodic and cathodic processes are assumed to add up to unity, i.e. the *bias* of the system is known.)  $z$  can in this case be assumed as 2 which corresponds to the electron number of copper, the main component in the electrode reaction.

In a real electroplating system the total current density as well as the current flow direction is always known. Because the system is operated significantly far away from its chemical equilibrium, the two-directional Butler-Volmer equation can be approximated

by only taking its one-directional parts, separately on the anode and cathode. This operation reduces equation (2.7) to

$$i_a = i_{0,a} \mu_a e^{\left(\frac{\alpha_a z F}{RT} \eta_a\right)} \quad (2.8)$$

on the anode and

$$i_c = -i_{0,c} \mu_c e^{\left(\frac{-\alpha_c z F}{RT} \eta_c\right)} \quad (2.9)$$

on the cathode. The subscripts  $a$  and  $c$  denote anode and cathode respectively.

After simplifying the current equation, constraints for coupling overpotentials ( $\eta$ ) with properties that can be estimated, measured or are known, must be formulated. These properties are: total electromotive force (EMV) applied over the bath, electrolyte conductivity and electrolyte copper activity derived upon concentration and temperature. The coupling can be derived as follows.

First, the electric circuit diagram given in Figure 1.21 allows us to obtain an equation based on Kirchoff's law over the circuit:  $E = U_{a,dl} + U_e + U_{c,dl}$ .

$U_e$  here is the voltage drop experienced due to ohmic loss in the electrolyte, which is dependent on the electrolyte section *size* as well as conductivity of and current density in the electrolyte.  $U_e$  can be formulated as follows:  $U_e = i \frac{l}{\sigma}$ . In practice,  $l$  is the distance between anode and cathode ( $d_{electrodes}$ ) and  $i$  is the control current density ( $i_{control}$ ).  $\sigma$  is the electrolyte conductivity which is determined by the electrolyte's chemical properties as described in Section 1.6.4.

$U_{a,dl}$  and  $U_{c,dl}$  are the voltage drops when moving over the electric double layer on each electrode, which in fact equal  $\Delta\phi_{a,i}$  and  $\Delta\phi_{c,i}$  in magnitude (eq. 2.10), respectively. However, it must be noted that  $U_i$  is defined as voltage *drop* in the direction of current and since  $\Delta\phi$  is defined as the potential *difference* when moving *from solution to metal*,  $\Delta\phi_{c,i}$  changes sign, i.e.  $\Delta\phi_{c,i} = -U_{c,dl}$ .

Second, the overpotential terms, earlier defined as  $\eta = \Delta\phi - \Delta\phi_{eq}$  can be simplified by substituting the Nernst equation (1.27) into  $\Delta\phi_{eq}$ .  $\eta$  becomes as follows.

$$\eta_i = \Delta\phi_i - \Delta\phi_{i,eq}^0 - \frac{RT}{z_i F} \ln(a_i) \quad (2.10)$$

Here again the subscript  $i$  refers to either anode or cathode, and activity is the copper ion activity on either anode or cathode.

Now substituting  $E$  into  $\Delta\phi$  gives us  $\eta$  finally as a function of known properties.

The final equation, upon which the system is solved, is obtained based on the condition that total current on both anode and cathode must be equal ( $I_a = I_c$ ). A relation coupling the anode and cathode *average* current densities ( $i_a, i_c$ ) can be derived when the surface areas of the electrodes (or their ratio) are known,  $i_a A_a = i_c A_c$ .

Here it is important to notice, that the current densities applied do not contain any information about the (absolute) current flow direction. Because the current equality

equation is based on the circuit interpretation of the electrolysis system, the equation only states that the current direction on both anode and cathode must be the same. Therefore, only their magnitude is considered and an interpretation for determining the current flow direction upon physical conditions is made afterwards.

By substituting  $\eta_a$ ,  $\eta_c$  from (2.10) for anode and cathode, and  $i_a$  (2.8) and  $i_c$  (2.9) respectively into  $i_a A_a = i_c A_c$  and solving the equation yields us the one-directional cathodic current equation as follows.

$$i_c = \left( i_{0,c}^{\frac{\alpha_a}{\alpha_c}} i_{0,a} \mu_c^{\frac{\alpha_a}{\alpha_c}} \mu_a \frac{A_a}{A_c} \left( \frac{a_c}{a_a} \right)^{\alpha_a} e^{\left( \frac{\alpha_a z F (E - U_e)}{RT} \right)} \right)^{\frac{\alpha_c}{\alpha_a + \alpha_c}} \quad (2.11)$$

To formulate the final current equation, the following assumptions are made and notations are used.

- The chemical term  $\mu_a$  is assumed constant and equal to 1. All surface chemical effects are considered to take place on the cathode.
- The exchange current densities  $i_{0,c}$  and  $i_{0,a}$  are considered constant and equal, and the notion  $i_{0,a} = i_{0,c} = i_0$  is applied. This simplifies the  $\left( i_{0,c}^{\frac{\alpha_a}{\alpha_c}} i_{0,a} \right)^{\frac{\alpha_c}{\alpha_a + \alpha_c}}$  term into  $i_0$ .

Based on the above presented simplifications, assumptions and justifications, the final one-directional equation for magnitude of the current density on the model cathode boundary can be formulated as follows.

$$i_c = i_0 \mu^{\left( \frac{\alpha_a}{\alpha_a + \alpha_c} \right)} \left( \frac{A_a}{A_c} \left( \frac{a_c}{a_a} \right)^{\alpha_a} e^{\left( \frac{\alpha_a z F (E - U_e)}{RT} \right)} \right)^{\frac{\alpha_c}{\alpha_a + \alpha_c}} \quad (2.12)$$

The equation includes three parameters that need to be identified based on voltammetric experiments, namely the exchange current density  $i_0$  and the transfer coefficients  $\alpha_a$  and  $\alpha_c$ . For the first-generation model, these parameters are estimated based on gathered preliminary voltammetric data.

The  $E$ ,  $A_i$ , and  $T$  parameters can be measured directly but copper ion activity (on both anode and cathode) as well as the ohmic potential loss must be estimated based on measurements.

The chemical term  $\mu$  is used to implement surface chemistry phenomena, and is described in below.

When implementing the current calculation, the total system is assumed symmetrically reversible so that the one-directional current equation obtained above can be *mirrored* to form a two-directional current equation. The assumption is justified by the fact that the system truly is a copper-copper electrode system and further because voltammetric measurements (reported in Chapter 3) show symmetric behavior.

## Modelling current control

The real production line process is a *galvanostatic* process, i.e. current density on the cathode is kept constant by adjusting the cell potential. Though current density is being controlled on equipment level, local current density on the cathode still varies significantly. Inside the microvias current density can rise due to surface chemical effects up to as high as five or seven times that on the board surface bulk. Local current density peaks still have no significant effect on the control system because the absolute area encompassed by microvias is so small compared to the total area of the cathode boards.

The current control implementation relies on the aforementioned principles. In the model, the cathodic current density ( $i_c$ ) on the level board surface section of the cathode is constrained to equal the control current density ( $i_{control}$ ). The required electromotive force is then solved from the current equation (2.12) based on desired control current density, after which it is applied over the whole cathode surface. In the one-directional cathodic current system, the control law upon which applied electromotive force is calculated becomes as below.

$$E = \frac{RT}{zF} \frac{\alpha_a + \alpha_c}{\alpha_a \alpha_c} \left( \ln(i_{control}) - \ln \left( i_0 \mu^{\frac{\alpha_a}{\alpha_a + \alpha_c}} \left( \frac{A_a}{A_c} \right)^{\frac{\alpha_c}{\alpha_a + \alpha_c}} \left( \frac{a_c}{a_a} \right)^{\frac{\alpha_a \alpha_c}{\alpha_a + \alpha_c}} \right) \right) + U_e \quad (2.13)$$

The procedure keeps current density on the board surface bulk, where surface chemical factors remain unchanged over the process, as desired and allows current density inside the via to alter according to surface chemical effects.

## Computing copper ion activities

Electrolyte copper ion concentration is converted to molality, assuming only a binary aqueous solution, as in the linear-fit in (2.14). The fit is based on experimental data found in [50].

$$m_{Cu} = 1.01 \cdot 10^{-3} c_{Cu} \quad (2.14)$$

Here concentration of copper is given as mol/m<sup>3</sup> and molality has the dimension mol/kg.

The activity of a species is defined in (2.15).

$$a_i = \gamma_i \cdot m_i / m^\circ \quad (2.15)$$

Here  $m^\circ$  denotes unit molality,  $m^\circ = 1$  mol/kg and  $\gamma_i$  is the activity coefficient of species  $i$ .  $\gamma_i$  also depends on the species' concentration and in the model it is therefore calculated based on the exponential fit (2.16), created upon experimental data found in [50].

$$\gamma_{Cu} = 1.95c_{Cu}^{-0.5554} \quad (2.16)$$

By calculating  $\gamma_{Cu}$  and  $m_{Cu}$  from  $c_{Cu}$  based on the fit equations (2.16) and (??), and substituting the values into the activity equation (2.15), an estimate for copper ion activity is obtained as (2.17).

$$a_{Cu} = 1.96 \cdot 10^{-3} c_{Cu}^{0.4446} \quad (2.17)$$

It must be noted that e.g. temperature (as well as other species present in the solution) affect a species' activity and therefore there is inaccuracy in the estimate.

### Calculating solution conductivity

Literature values for a ions' diffusivities in very dilute concentrations can be found. The copper plating electrolyte is, however, anything but a dilute solution which is why experimental measurements were required to determine correction factors for the literature values. A linear approximation for species' mobility based on their concentration was created upon electrolyte conductivity measurements conducted in Aspocomp laboratory and conductivity reference data found in [50].

Since electrolyte conductivity and mass transfer of ions are coupled by the Einstein relation (1.15) and the conductivity equation (1.21), it was considered meaningful to construct estimates for  $Cu^{2+}$ ,  $SO_4^{2-}$ ,  $HSO_4^-$  and  $H^+$  ions' diffusivities - i.e. their diffusion coefficients - within a certain range of operating concentrations. Knowing the nonlinear nature of this property (in respect to concentration) an exponential fit was created.

Because only little measurement data was available (two conductivity measurements), the reference data found in [50] was used for creating the fit and afterwards the fit was validated against the measured data points.

First the molar conductivity,  $\Lambda_i$ , was determined for each ion species based on the concentration-conductivity reference data found for binary copper sulphate and sulphuric acid solutions.  $\Lambda_i$  for each ionic species was determined by weighting the stoichiometric proportion of the total binary solution molar conductivity by each of the ion's molar conductivity,  $\Lambda_{i,0}$  measured in an infinitely dilute solution. Hence, for example, the molar conductivity of copper ion becomes

$$\Lambda_{Cu^{2+}} = \frac{\sigma_{CuSO_4}}{c_{CuSO_4}} \frac{\Lambda_{Cu^{2+},0}}{\Lambda_{CuSO_4,0}}, \quad (2.18)$$

where  $\sigma$  is the binary solution conductivity.

The obtained diffusivity estimation equations are listed in Table 2.1.

The obtained molar conductivities for each species are then applied in a normal manner to calculate the species' diffusivities and further the total solution conductivity.  $D_i = (RT/F^2)(\Lambda_i/|z_i|)$ , where  $z$  is the electron number of the species. Total

solution conductivity  $\sigma$  is calculated with the total conductivity equation (1.21).

$$\sigma = \frac{F^2}{RT} \sum_i z_i^2 D_i c_i \quad (2.19)$$

The diffusion coefficients obtained here are applied also in the mass transfer field equations.

### Calculating ohmic potential loss over the electrolyte

With the solution conductivity estimated obtained above, the ohmic potential loss  $U_e$  that occurs when moving from anode to cathode, over the electrolyte, can be formulated as follows.

$$U_e = i \frac{d_{electrodes}}{\sigma} \quad (2.20)$$

Here  $i$  represents the average current density in the electrolyte, which in practice is the control current density ( $i_{control}$ ) of the plating process set by the process operator.

### Implementing copper consumption effects

The most problematic nonlinearity in the model is introduced by the *copper ion depletion* phenomenon. That is, when the control current density is set too high, the cathode effectively depletes the diffusion layer from copper ions, meaning that reduction cannot continue anymore.

Copper ion activity is used to numerically implement effects caused by deviation in cupric ion concentration, i.e.  $a_c$  is a factor in the chemical term  $\mu$ , accounting for copper's chemical effects.

$$\mu_{Cu} = a_c \quad (2.21)$$

Copper ion activity is estimated with an exponential fit based on measurement data for copper sulphate, as in (2.17). Activity of copper goes to zero along with copper concentration, thus slowing down the reduction process as the diffusion layer depletes of copper ions.

---

|                 |   |
|-----------------|---|
| $D_{Cu}$        | $= 4.51 \cdot 10^{-10} \cdot 0.9992^{c_{Cu}}$         |
| $D_{SO_4^{2-}}$ | $= 6.73 \cdot 10^{-10} \cdot 0.9992^{c_{Cu}}$         |
| $D_{H^+}$       | $= 5.54 \cdot 10^{-9} \cdot 0.9998^{c_{b, H_2SO_4}}$  |
| $D_{HSO_4^-}$   | $= 8.24 \cdot 10^{-10} \cdot 0.9998^{c_{b, H_2SO_4}}$ |

---

**Table 2.1:** Ionic species' diffusion coefficient estimates.

$$a_{Cu} = 1.96 \cdot 10^{-3} c_{Cu}^{0.4446} \quad (2.22)$$

In the real process, copper depletion is not a problem as such. After depletion, the copper reduction rate is just completely determined by mass transfer of copper ions (and not by control current anymore). Depletion of copper can still lead into a bad fill result and void vias, which is why it is important to spot such situations.

In the model, then again, depletion itself is a nuisance since numerical problems occur as a species' concentration at the cathode boundary approaches zero (concentrations can even go below zero). Usually such a situation interrupts the model solution and no final result is obtained. Based on the last solved values, however, the model user can deduce that copper depletion occurred and that a smaller control current density (or different electrolyte chemistry) should be applied.

### Implementing surface chemistry

As explained in Section 1.5.3, a static coupling between a species concentration in the very vicinity of a surface and the surface concentration of its adsorbed-to-surface species can be formulated when the adsorption process is assumed to have reached steady state. The coupling is called the adsorption isotherm and can be formulated as follows (the Langmuir isotherm, 1.9).

$$\Gamma_i = \frac{\beta_i c_i}{1 + \beta_i c_i} \left( \Gamma_{s,i} - \sum_{j \neq i}^N \Gamma_j \right) \quad (2.23)$$

It is assumed that even the slowest chemical phenomena included in the system occur within minutes, and that the chemical dynamics can be neglected in the one-hour-scale microvia filling process. With this (steady state of adsorption) assumption, it is justified to approximate the surface concentration of an adsorbed species based on its solution concentration very close to the boundary.

In Chapter 3 it is shown that additives are being consumed during the process, therefore the net mass flux of additives can be assumed one-directional, from solution to surface. (Once adsorbed on the surface, the additive is either decomposed chemically or incorporated into the copper layer, thus being effectively consumed.)

As explained earlier in Section 2.1.3, the real two-additive system is modelled with only one *pseudo-additive*, which is effectively a suppressor. The modelled additive effect on the cathode surface depends on the additive's surface concentration (amount of additive per unit surface, mol/m<sup>2</sup>), which is regarded as a static dependency of the additive's volumetric concentration on the cathode boundary.

The differences in surface concentration are caused by consumption of the additive on the cathode. Additive consumption is modelled as a material flux whose net direction on the cathode is away from the modelling domain. The flux is implemented as a first order reaction rate flux of the additive over the cathode boundary.

$$N_{Add} = \mathbf{n} \cdot (-D_{Add} \nabla c_{Add}) \quad (2.24)$$

The additive flux  $N_{Add}$  is calculated based on the principles explained in Section 1.5. Since the effects of two additives are now incorporated into one, the additive flux is also made dependent of all the factors that the fluxes of several real additives would be dependent of, namely the additive concentration and the local cathode surface area change.

In the real system, the accelerator additive is assumed to (i) cancel the suppressor's effect and (ii) to accumulate around sites where the cathode surface area diminishes locally. Therefore the modelled additive flux increases where the local surface area diminishes - causing the suppressing effect of the additive to diminish around these sites.

Further, as the experiments show, all additives are consumed during deposition which is why a constant flux term is also incorporated in the total additive flux. This results in a concentration gradient all over the modelling domain and not only around the sites where the surface area changes.

$$N_{Add} = k_1 c_{Add} \left( k_2 + \frac{A_0}{A} \right) \quad (2.25)$$

$k_i$  are constant parameters,  $k_1$  determining the magnitude scale of the total additive flux and  $k_2$  setting the ratio between continuous area-independent consumption of additives and area-change-dependent additive consumption.

$k_2$  is determined based on the concentration values of additives in the two-additive system, specifically their ratio.  $k_2$  implements the effect of the accelerator cancelling the suppressor's effect. In order for the microvia to become properly filled, the suppressor and accelerator additives need to be present in the electrolysis bath in correct (proportional) concentrations. If the accelerator concentration is too small, the suppressing effect dominates, resulting in conformal or only slowly levelling fill. If the accelerator concentration is too high (compared to the suppressor concentration), deposit growth inside the via is slowed down due to copper depletion; all copper is reduced already on the level surface because the suppressing effect is diminished there.

The final suppressing effect of the additive is calculated based on a saturation-type equation, which is further scaled by a power term that depicts the multiplicative nature of having several additives' combined effect present simultaneously.

$$\mu_{Add} = \left( \frac{c_{b,Add} - k_3 c_{Add}}{k_4 + c_{Add}} \right)^{k_5} \quad (2.26)$$

Here  $k_3$  is a coefficient determining the maximum degree of reduction reaction suppression caused by the additive - i.e. it sets the maximum suppression, reached at saturated additive coverage.  $k_4$  is a constant that describes the balance between adsorption and desorption (or formation and degradation) of additive species, based

on the corresponding reaction rates. ( $k_4$  is analogous to the *Michaelis* constant in the *Michaelis-Menten* reaction mechanism defined for enzyme action.)  $k_5$  is a power-term denoting the combined effect of several additives present simultaneously.

The total chemical effect implemented is a product of both copper ion depletion effects and surface chemical effects.

$$\mu = \mu_{Cu}\mu_{Add} \quad (2.27)$$

No surface quantities, such as surface concentration (mol/m<sup>2</sup>), surface coverage (no dimension) or diffusion of surface-adsorbed species (surface diffusion) are computed explicitly. Neither is the surface area time derivative, which as such would be more reasonable, applied in modelling surface shape change effects. The reason for both of these exclusions is similar; neither of them proved ultimately necessary in the first generation model and both of them bring along a heavy computational load to the model.

### Moving the mesh, ALE method

The model is implemented applying the *Arbitrary Lagrange-Eulerian* (ALE) method in order to account for the geometric changes that take place in the modelling domain during electrodeposition, namely the deposition growth and via filling.

The ALE method is basically a geometric transformation operation done on the basic rigid discretization grid (the mesh). The idea is to continuously, during model solution, keep track of a moving coordinate system (which is a transformation of the original, fixed, coordinate system) and virtually solve all physics equations in the moving coordinates system. Hence, all geometry changes actually affect the solution of the physical phenomena.

The ALE formulation introduces four dependent variables to be solved in the model, namely the moving coordinates  $x$  and  $y$  as well as the velocity of the moving mesh  $\psi_x$  and  $\psi_y$ . The variables can be understood as functions of  $X$ ,  $Y$  and  $t$ , but since they are only viewed as a part of the spatial system, it is more convenient to leave time out.  $x$  and  $y$  become  $x(X, Y)$  and  $y(X, Y)$ . The values of these functions are computed by integrating over a mapping between the original, fixed coordinate system and the moving coordinate system. The following mapping is obtained by applying the differential chain rule in differential form on  $x$  and  $y$  [51].

$$\begin{bmatrix} dx \\ dy \end{bmatrix} = \begin{bmatrix} \frac{\partial x}{\partial X} & \frac{\partial x}{\partial Y} \\ \frac{\partial y}{\partial X} & \frac{\partial y}{\partial Y} \end{bmatrix} \begin{bmatrix} dX \\ dY \end{bmatrix} \quad (2.28)$$

The matrix introduced is a Jacobian matrix  $J$  containing the (fixed) spatial derivatives of both moving coordinates. By solving the inverse of the Jacobian matrix,  $J^{-1}$ , a mapping from the moving coordinate system to the fixed coordinate system, where

all actual computation is done, is obtained.

$$\begin{bmatrix} dX \\ dY \end{bmatrix} = J^{-1} \begin{bmatrix} dx \\ dy \end{bmatrix} \quad (2.29)$$

By multiplying all differentials formulated for the moving coordinate system with the transformation matrix  $J^{-1}$ , one can actually solve them in the fixed coordinate system – which is what the finite element solver does. Interpreting this the other way, by including the transformation in the differential equation formulation, one can formulate an equation (to be solved in a fixed coordinate system) that corresponds to the situation in the moving coordinate system – which is what the modeler will have to do.

There is still an additional modification that needs to be done to the re-formulated equations in order to maintain physical sensibility of the model. Due to the geometric changes in the mesh, also the actual discretization (the moving grid) changes and this must be accounted for by using an appropriate scaling factor when integrating the differential equations. The scaling factor is given by the determinant of the previously presented Jacobian matrix  $J$ . Hence, by multiplying the equations with  $\det(J) = \partial x/\partial X \cdot \partial y/\partial Y - \partial y/\partial X \cdot \partial x/\partial Y$  enables keeping the numerical values of all integrals also physically correct.

To conclude the ALE formulation part, in order to solve for variables in the changing modelling geometry, their corresponding differential equations must be transformed to the moving coordinate system and to maintain correct numerical values of variables, the equations have to be scaled by a factor that accounts for changes in the geometry discretization. The transformation is obtained by multiplying all differentials with the corresponding elements of the Jacobian matrix inverse  $J^{-1}$ , and the scaling factor is  $\det(J)$ .

The moving mesh velocity variables  $\psi_x$  and  $\psi_y$  are obtained simply by taking time derivatives of the corresponding moving spatial coordinates.

$$\psi = \begin{bmatrix} \psi_x \\ \psi_y \end{bmatrix} = \begin{bmatrix} \frac{\partial x}{\partial t} \\ \frac{\partial y}{\partial t} \end{bmatrix} \quad (2.30)$$

The variables  $x$ ,  $y$ ,  $\psi_x$  and  $\psi_y$  can be restricted and solved for in a similar manner as any other variables in the finite element problem domain.

In the model, the mesh movement is generally free except for on the boundaries. On the symmetry boundaries movement is restricted on the symmetry axis. Specifically, movement velocities in the direction of the  $x$ -axis are limited to zero on diffusion layer cross-section boundaries.

$$\psi = \begin{bmatrix} 0 \\ \psi_y \end{bmatrix} \quad (2.31)$$

On the anodic modelling boundary, movement velocity is restricted to zero in the  $x$ -axis' direction. In order to keep the diffusion layer and thus mass transfer properties reasonable, the anodic boundary movement velocity in the  $y$ -axis' direction is restricted to equal the cathode boundary movement velocity  $\psi_{y,cathode}$ , observed on the level board surface.

$$\psi = \begin{bmatrix} 0 \\ \psi_{y,cathode} \end{bmatrix} \quad (2.32)$$

On the cathode boundary, where all mesh movement eventually originates from, mesh velocity is restricted to equal the copper deposit growth. Copper deposit growth velocity is derived from Faraday's law (1.23).

$$\psi \cdot \mathbf{n} = -N_{Cu} \frac{M_{Cu}}{\rho_{Cu}} \quad (2.33)$$

Besides these restrictions, the moving coordinate mesh is allowed to move freely.

Of course, also all other equations of the dependent variables included in the model have to be modified to apply for the moving coordinate system before being solved. The modification is identical to that of the coordinate variables themselves.

More information about the ALE method can be found for example in references [52, 51].

### Computing local area change

As described in [29], the local deposit surface shape change affects how the additives there interact. Basically the idea boils down to local surface concentration changes inflicted by local surface area decrease or increase, which occurs as either a concave or convex deposit surface grows, respectively.

The ALE method enables formulating an extra dependent variable to denote local boundary mesh element length on a modelling boundary in the moving coordinate system. By appropriate use of model symmetry, the boundary element length gives means to compute local area and its dynamics, even though the model is a two-dimensional model.

By fixing the mesh boundary element length to an appropriate value  $l_0$  during mesh initialization, at the same time we obtain the spatial discretization step of the fixed, non-moving mesh. Based on this knowledge, the element length  $l$  on the moving boundary can then be computed by solving a simple equation with the spatial differentials of the moving coordinates (eq. 2.34).

$$l = \sqrt{\left(l_0 \frac{\partial x}{\partial X}\right)^2 + \left(l_0 \frac{\partial y}{\partial Y}\right)^2} \quad (2.34)$$

Extending the boundary element length to correspond to local area is based on a symmetry assumption. The micro via is assumed perfectly round, with its center in the origin. The radius of the via is thus always  $|x|$  and now each boundary element can be considered to be the cross-section of a circular *belt*, with radius  $x$ , going around the via on the via surface (see Fig. 2.2). The area of such a belt is given by equation (2.35).

$$A = 2\pi l|x| \quad (2.35)$$

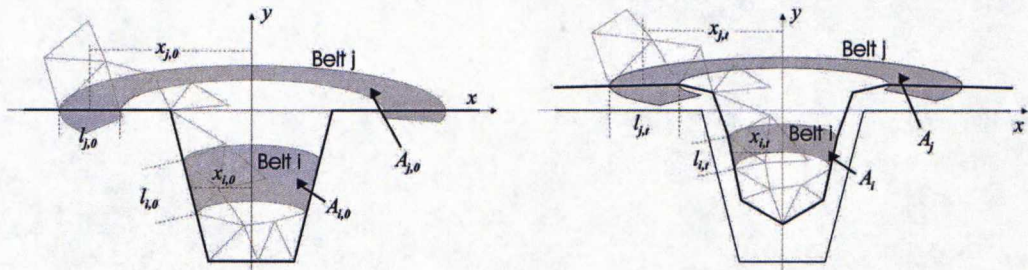


**Figure 2.2:** An illustration showing how the three-dimensional local area change is taken into account in the model. As deposition proceeds, the via shape changes and the local area term  $A$ , dedicated to every model boundary element changes accordingly.

The solution is not perfectly precise because the initial mesh element size cannot be explicitly fixed in the application environment used. The method proved sufficiently accurate, and since absolute accuracy is not as critical here as the relative accuracy, this loss of precision cannot be considered a problem.

The method allows for both the local area time derivative and the local area to be computed for each mesh boundary element. Also the initial local area is known for each element. This enables keeping track of where area shrinkage or enlargement is greatest and at what time instant. Combining area change with surface chemical effects enables modelling surface interactions between the additives during plating.

#### 2.1.4 Modelling principles summarized

The finite element method is used to model the problem, which has derivatives in both time and space dimensions. The Arbitrary Lagrange-Eulerian formulation is applied to solve the problem in a moving coordinate system, which is required to account for geometric changes in the problem domain.

Via fill modelling is divided into three separate parts: (i) the mass transfer model, based on the Nernst-Planck equation (1.19), (ii) the electrostatics model, based on the electric field equation (1.20) and (iii) a model for various, static, surface chemical relations, based on the current equation (2.12) and several surface chemical equations.

Surface area change is computed and its effect is implemented with a computational method developed specifically for the purpose.

## Chapter 3

# Experimental verification and discussion

Experiments carried out during the course of modelling work are explained here briefly. All experiments were made in order to confirm some part of the total model, therefore also the corresponding modelling or estimate-given results are presented and compared to the measured results.

The model's capability to correctly predict how well a process fills microvias depends on several other estimates. It is just as vital to assure correctness of *supporting parts* of the model as it is to get the final via filling estimate correct. Understanding and having the foundations right is especially important considering convertibility of the model for other types of via filling processes. Change on the production line never ceases.

### 3.1 Via filling experiments

The microvia fill model aims not only to predict the fill result of the process but also to capture the fill evolution during electroplating. In order to examine the fill evolution in the microvia and copper film growth on the board surface versus plating time, plating tests with varying plating time was conducted. All tests were made at the Aspocomp Salo plant production line and R&D Center Laboratory.

Two individual tests were conducted by the Aspocomp staff and both of these tests included a twelve-sample series of plating tests. The samples consist of electroplated microvias, the plating time varying from 6 minutes to 72 minutes, with a 6-minute interval (totalling 12 samples per test batch). The chemical composition of the electroplating bath as well as other process operating conditions were kept identical during both test runs (within production line control possibilities). The approximate electrolyte composition is shown in Table 1.1. The tests were conducted on the production line, applying impingement agitation as well as proper pretreatment of the samples. The resulted cross-section images are shown in A.1 and A.2.

Two more individual test runs were conducted by the author with the assistance of Aspocomp staff. Both of these two tests included a six-sample series of electroplated microvias. Now the electroplating time varied from 15 minutes to 90 minutes with a 15-minute interval. The bath composition was altered between the tests as shown in Table 3.1.

| Component                      | Electrolyte composition 1 | Electrolyte composition 2 |
|--------------------------------|---------------------------|---------------------------|
| CuSO <sub>4</sub>              | 0.814 mol/l               | 0.814 mol/l               |
| H <sub>2</sub> SO <sub>4</sub> | 1.05 mol/l                | 1.05 mol/l                |
| HCl                            | 1.3 mmol/l                | 1.3 mmol/l                |
| Additive A                     | 1.26 ml/l                 | 1.53 ml/l                 |
| Additive B                     | 16.6 ml/l                 | 15.7 ml/l                 |
| Add A / Add B                  | 0.075                     | 0.097                     |

**Table 3.1:** Electrolyte composition in test runs 1 and 2 of the second test series.

Before electroplating, the test boards were pretreated similarly to those at the production line by immersing the boards in a microetching solution detailed in Table 3.2 for one minute.

| Component                   | Concentration |
|-----------------------------|---------------|
| Sulphuric acid              | 0.21 mol/l    |
| Potassium monopersulphate   | 0.17 mol/l    |
| Potassium hydrogen sulphate | 0.11 mol/l    |

**Table 3.2:** The test board pretreatment solution (a.k.a. microetching solution).

The electrolyte used in the first six-piece test series was also analyzed after 90 minutes of electroplating. The analysis results on behalf of the additives, shown in Table 3.3 clearly indicate consumption of both additives, the absolute consumption of additive B being greater than that of additive A. However, the relative consumption of additive A is dramatically greater than that of additive B.

Electroplating was conducted with experiment-size equipment, using a Haring cell as the plating bath container and air pumping for solution agitation. Otherwise all process operating conditions were identical to those at the production line. The apparatus is shown in Figure 3.1 and two identical setups were used simultaneously to shorten the testing time.

After electroplating, samples were cut from the test boards and microsectioning was applied to bring out the cross-section of the filled microvias and the board surface

| Component     | Fresh composition | After 90 minutes of plating | Change              |
|---------------|-------------------|-----------------------------|---------------------|
| Additive A    | 1.26 ml/l         | 0.81 ml/l                   | -0.71 ml/l (-35.7%) |
| Additive B    | 16.6 ml/l         | 15.5 ml/l                   | -1.74 ml/l (-6.6%)  |
| Add A / Add B | 0.076             | 0.052                       | -0.024 (-31.2%)     |

**Table 3.3:** Electrolyte composition in test runs 1 and 2 of the second test series.

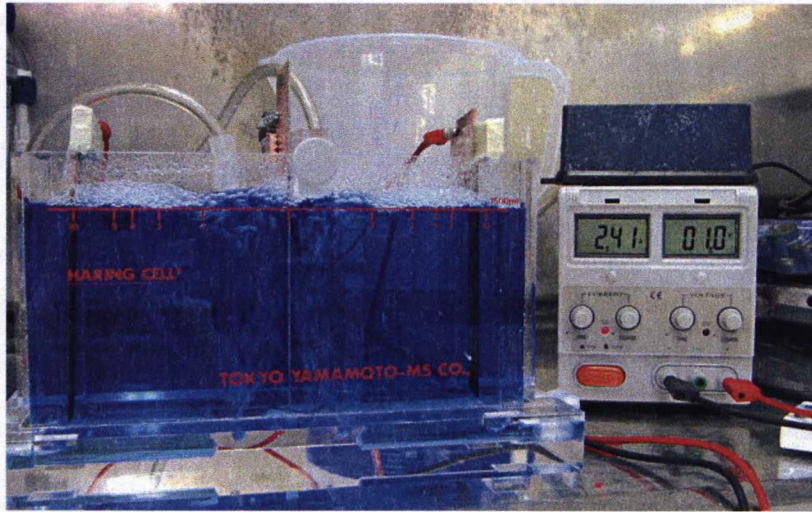


**Figure 3.1:** The experiment-size electroplating apparatus.

there. The samples were photographed with an optical microscope at the Aspocomp R&D facilities.

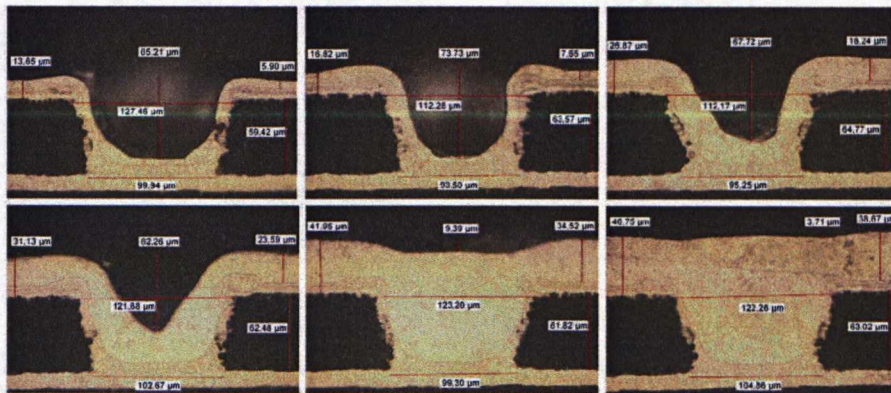


**Figure 3.2:** The cross-section images of sample pieces at a via fill plating test series. Images are taken with an optical microscope (with a 500x magnification).

The electroplating process evolution on both the wafer and inside the microvias was measured visually from the cross-section images. The SEM-images each include a scale (e.g. Fig. 3.3) enabling measuring with any measurement device, but samples photographed with an optical microscope (e.g. Fig. 3.2) were measured using an

appropriate software tool. The vertical growth of the deposit thickness at three points (marked in Fig. 3.3) was plotted in order to obtain a conception of how via filling takes place. An example plot is shown in Figure 3.4.

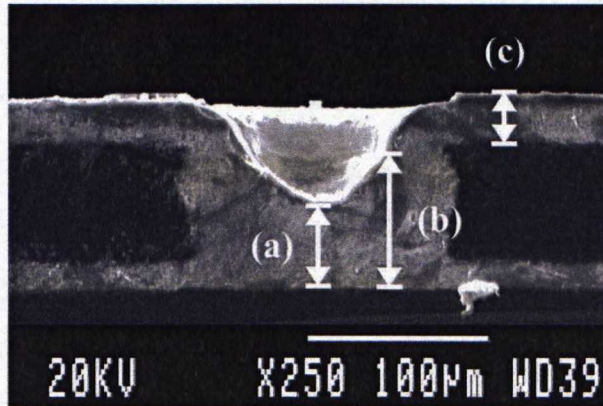


**Figure 3.3:** An example of a sample SEM-image. The deposit growth measurement sites are marked with white arrows. Point (a) is entitled *inside via*, (b) *midway-to-via-corner point (MCP)* and (c) is the *board surface* measurement point.

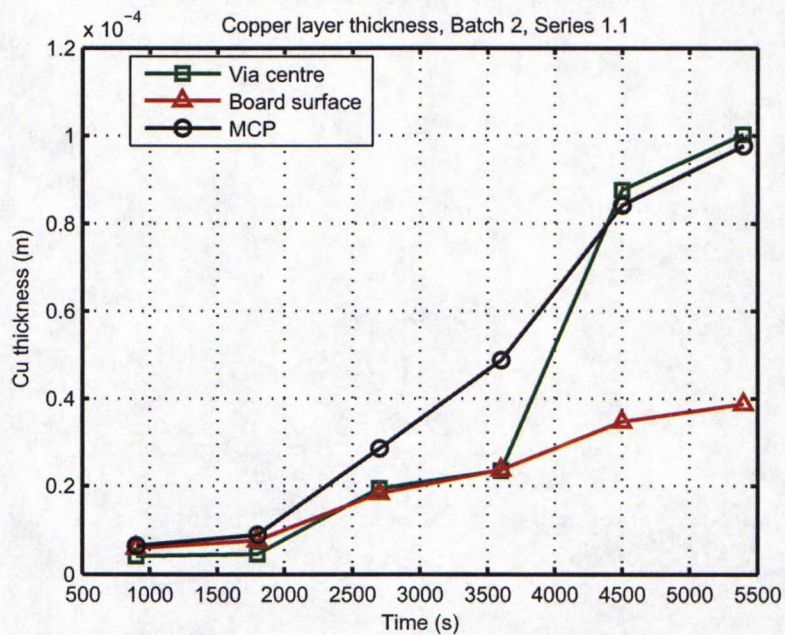


**Figure 3.4:** A typical plot with the deposited copper layer thickness (m) plotted against plating time (s). Dimensions are measured from picture material taken through an optical or scanning electron microscope (e.g. in Fig. 3.2).

After measuring the cross-section image dimensions, also via fill ratios were calculated. An example of a typical fill ratio plot is given in Figure 3.5.

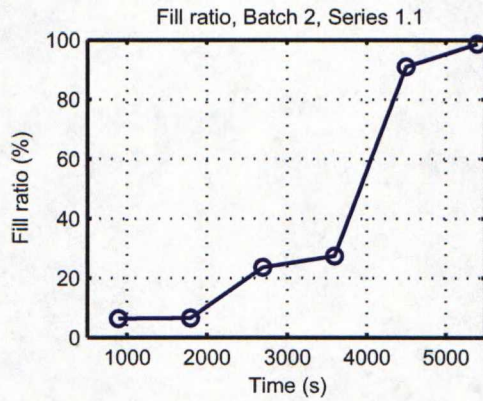


**Figure 3.5:** A typical via fill ratio plot with fill ratio (%) plotted against plating time (s). Fill ratio is calculated based on the same data as seen in figures 3.4 and 3.2.

### 3.1.1 Comparing via fill measurements to modelling results

The model is parametrized and compared against the two most recent via filling test runs, mainly because their chemistry is sufficiently well known. Specific chemical analysis of the first two test runs was never obtained.

The overall conclusion of the via fill model fill prediction performance may be put into one clause; the model can predict final fill result fairly well but has difficulties capturing the process dynamics during fast transient-type behaviour. This becomes evident when comparing measured and modelled curves showing deposit growth inside the microvia (Fig. 3.6).

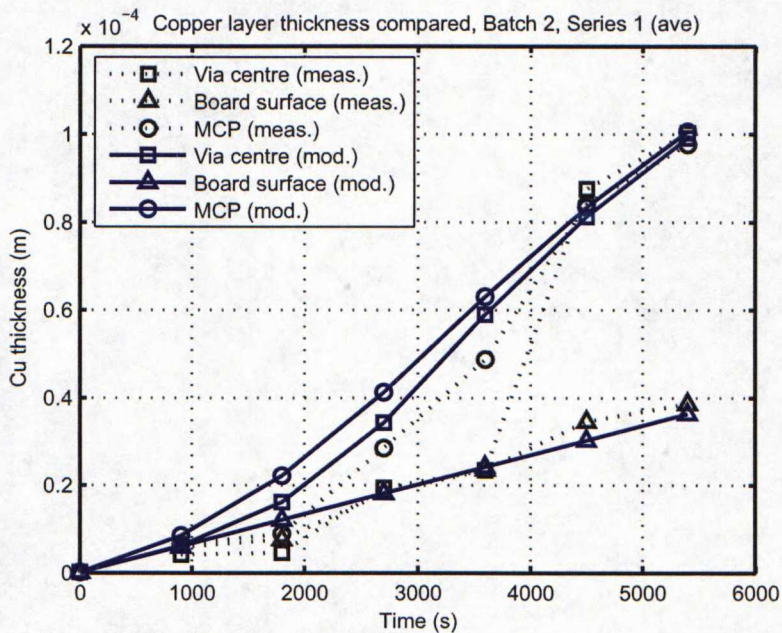


**Figure 3.6:** Measured and modelled copper deposit growth on various measurement points within the modelling domain.

On the level PCB surface, where the deposit growth is linear, the model follows

the measured deposit growth well (Fig. 3.7).

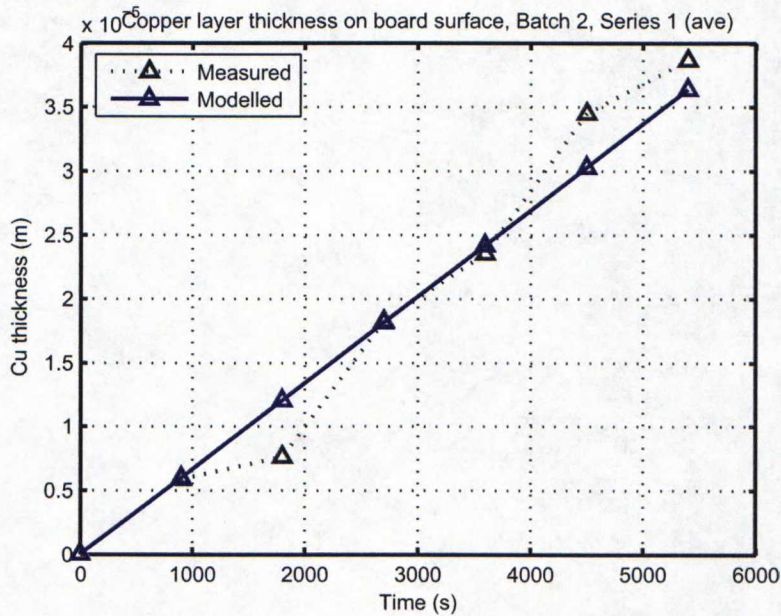


**Figure 3.7:** Measured and modelled copper deposit growth on the level board surface.

It is clear that on the board surface, where diffusion layer thickness, solution flow, local area and other affecting properties remain constant during the whole deposition process, whereas inside (and eventually on top of) the via all these properties change over time.

The model deposit thickness prediction capability seems to worsen as the deposit thickness measurement point is moved closer to the via centre. In the *midway-to-via-centre* point, the modelled growth curve is still rather similar to the measured one (Fig. 3.8), but when deposit thickness is modelled in the very centre point of the via, the modelled deposit thickness behaviour is not as nonlinear as observed in the experiments (Fig. 3.9).

The model can also output the via fill ratio but comparing the modelled ratio against the fill ratio measured from cross-sectional images requires some rearranging of measurement data. Since the model dimensions are initially configured to correspond to the dimensions the microvia has exactly before plating (i.e. already having the basis copper on the board surface as well as a chemical and a flash copper all over), an initial copper layer thickness must be subtracted from the total measured copper layer thickness. The initial copper layer thickness can also be measured from the cross-sectional images. Figure 3.10 displays the modelled and measured fill ratio plots.

It is clear that the model cannot sufficiently well follow the real growth process where its nonlinearity is greatest. Sharp-cornered cross-section profiles are caused by depletion of copper in the diffusion layer but the depletion phenomenon can only be modelled to some extent, which is one reason why serious nonlinearities do not show in the model.

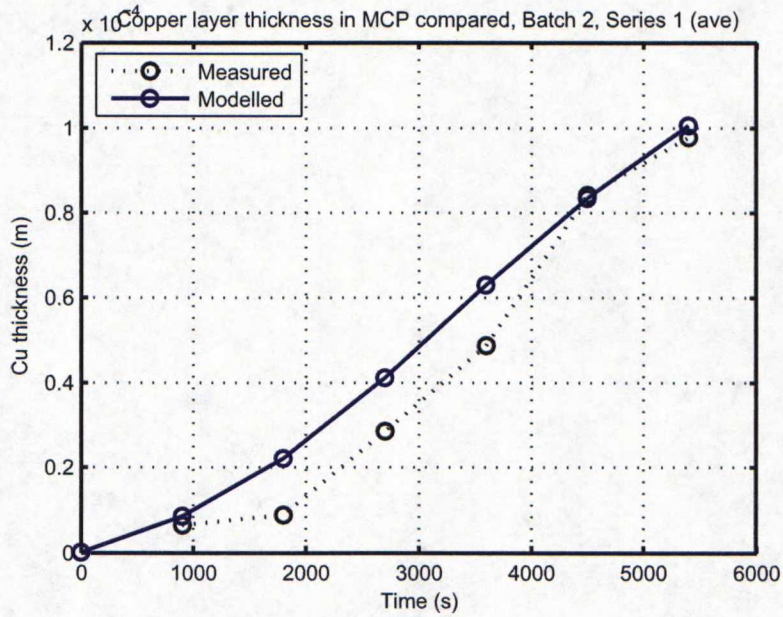


**Figure 3.8:** Measured and modelled copper deposit growth in the midway-to-via-centre point (see Fig. 3.3).

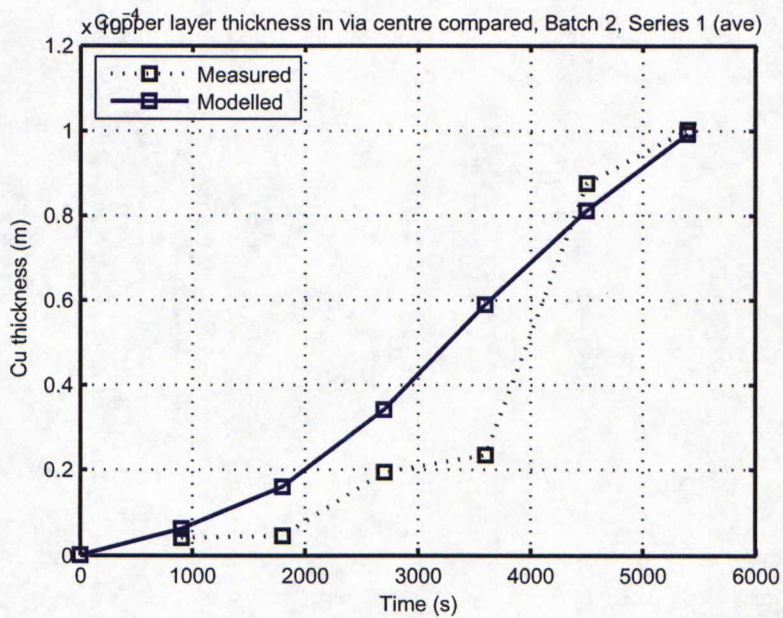


**Figure 3.9:** Measured and modelled copper deposit growth in the via centre.

The via surface area and shape changes are also much more nonlinear in the via centre compared to other locations in the modelling domain. On the board surface no such phenomena take place and in the via bottom corner and close to it (MCP) surface shrinkage and shape change is more continuous than in the via centre, where no such changes occur in the initial phase of the deposition. These parts of the model, require further work.

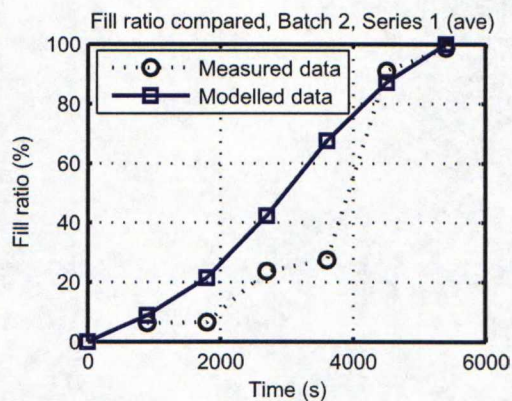


**Figure 3.10:** Measured and modelled via fill ratio vs. time.

### 3.2 Voltammetric measurements

In order to get a conception of practical values of the parameters in the current equation (2.12), linear potential sweep tests were conducted at the TKK Laboratory of Physical Chemistry and Electrochemistry. The tests were executed using an electrolyte solution sample taken from the factory production line.

A potential sweep test is basically done by posing a varying electro motive force ( $E$ ) over the examined system and then measuring the current ( $I$ ) flowing through the system. A current-voltage curve is obtained as a result. The voltage during a typical sweep is plotted against time in Figure 3.11.

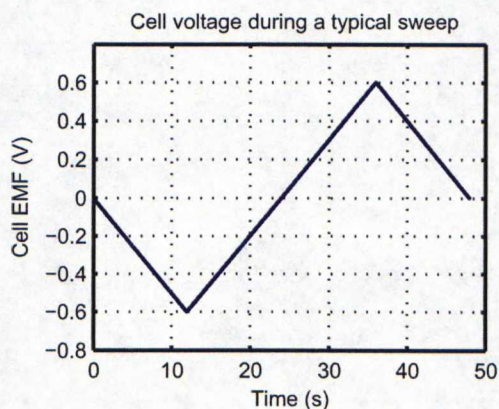


**Figure 3.11:** The cell voltage (V) against time (s) applied creating typical linear sweep voltammogram. The sweep rate is 0.05V/s.

When the electrode area is known, the current density ( $i$ ) on each electrode can be calculated ( $i = I/A$ ) and a current density-voltage curve ( $i$ - $E$ -curve) is obtained (e.g. Fig. 3.12).

Reasoning must be used when interpreting the absolute voltage values on the curve. The original current equation is based on the Butler-Volmer-equation (1.25), which is defined specifically for overpotential. However, minimizing ohmic loss by down scaling equipment size, and calculating or knowing the equilibrium potentials of electrode-

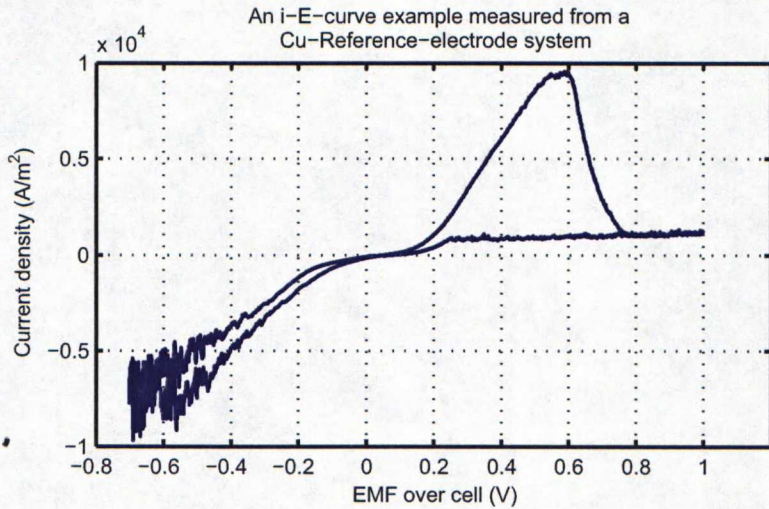


**Figure 3.12:** An example of the  $i$ - $E$ -curve measured from a system with a Cu-electrode against a standard calomel reference electrode.

electrolyte interphases enables obtaining a sensible physical meaning for the applied voltage.

Two types of tests were done; one with a symmetric system (as on the production line) with both electrodes being copper and another with the other electrode being a reference electrode whose standard potential is known. A standard calomel reference electrode was used. The tests were conducted in reduced dimensions, the distance between electrodes being approximately 1cm and cathode area varying from  $2\text{mm}^2$  to  $190\text{mm}^2$ . To enhance mass transfer properties, the solution was constantly stirred with a magnetic rod mixer. The electrolyte was renewed regularly between sweeps in order to reduce alterations in electrolyte chemical properties.

The obtained  $i$ - $E$ -curves can be used to identify the current equation parameters, namely the parameters  $i_0$  and  $\alpha_a$  and  $\alpha_c$ . The least-squares method was used to fit the current equation (2.12) with test data from several test runs. The results obtained and applied in the model are presented in Table 3.4. The presented parameters are average parameters of six similar runs.

| Parameter  | Identified value (E) | Deviation ( $\sigma^2$ ) |
|------------|----------------------|--------------------------|
| $i_0$      | $55 \text{ A/m}^2$   | $\pm 5.67$               |
| $\alpha_a$ | 0.13                 | $\pm 0.009$              |
| $\alpha_c$ | 0.16                 | $\pm 0.012$              |

**Table 3.4:** Values obtained for the current equation parameters.

The parameters are estimated numerically by fitting the current equation into measurement data so that the fitting error square sum becomes minimized.

The tests carried out on a symmetric Cu-Cu-electrode system show that the sym-

metry assumption applied in deriving the current equation is justified. The current curve is very similar in both the first and third quadrant of the  $i$ - $E$ -coordinate plane (Fig. 3.13) - as if "mirrored" over a diagonal line going through the origin.

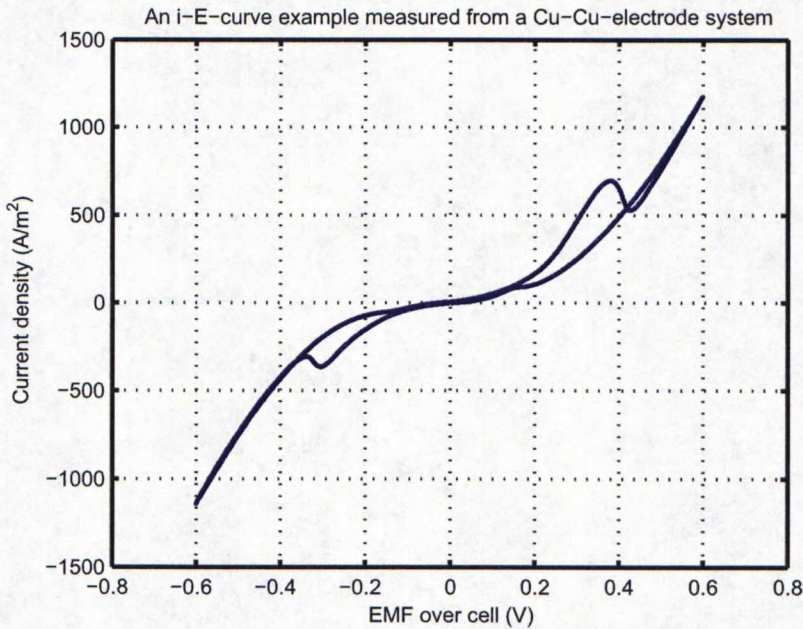


**Figure 3.13:** An example of the  $i$ - $E$ -curve measured from a symmetric Cu-Cu-electrode system.

### 3.3 Conductivity measurements

The conductivity of an electrolyte whose composition is known tells much about the electrolyte's mass transfer capabilities. Since diffusivities of the electrolyte species are estimated based on total electrolyte conductivity, experiments to determine the conductivity of the real electrolyte were carried out. The conductivity was measured from two different solution compositions detailed in Table 3.5. Also the respective conductivity values are given in the same table.

| Property                            | Electrolyte composition 1 | Electrolyte composition 2 |
|-------------------------------------|---------------------------|---------------------------|
| $c_{CuSO_4}$ (mol/m <sup>3</sup> )  | 845.0                     | 422.5                     |
| $c_{H_2SO_4}$ (mol/m <sup>3</sup> ) | 1099.1                    | 549.6                     |
| Measured conductivity (S/m)         | 28.9                      | 18.6                      |
| Estimated conductivity (S/m)        | 29.2                      | 17.2                      |

**Table 3.5:** Electrolyte compositions in conductivity experiments and corresponding measured as well as estimated values for conductivity.

When comparing the conductivity values obtained by using the estimate applied in the model (with equations presented in Section 2.1.3), an error is obvious and estimate correction needs to be made based on better measurement data.

Measuring conductivity itself is rather easy. The lack of extensive measurement data is explained by the fact that each solution analysis, which is a rather time consuming procedure, is carried out manually at the plant analysis laboratory. It is clear, however, that more measurement data are needed in order to correct and validate the estimate thoroughly (see Section 3.5).

### 3.4 Copper electrode equilibrium potential measurements

As explained in Chapter 2, copper ion activity is estimated based on experimental data found in reference material [50]. Measuring a species' activity in a solution directly (e.g. similarly as measuring its concentration from a sample) cannot be done, but the Nernst equation (1.27) couples a species' activity with its electrochemical equilibrium potential, which in practice is a measurable voltage. Hence, by measuring a voltage between a known reference electrode and the inspected copper-electrolyte solution - electrode, the activity estimate obtained based on literature data can be checked.

The copper electrode equilibrium potential was measured in the electrolyte sample solution against a silver chloride reference electrode (Metrohm 6.0259.100) with a reference potential of 0.222V. The measured equilibrium potential and the equilibrium potential calculated based on the copper activity estimate with Nernst's equation are shown in Table 3.6. The corresponding potentials *calculated* against a standard hydrogen electrode (SHE) are presented for comparison (assuming copper equilibrium potential is 0.337V).

|                                     | Against AgCl (real) | Against SHE (calculated) |
|-------------------------------------|---------------------|--------------------------|
| Measured equilibrium potential (V)  | 0.0750V             | 0.295V                   |
| Estimated equilibrium potential (V) | 0.0731V             | 0.297V                   |

**Table 3.6:** Preliminary result of copper equilibrium potential measurements for copper ion activity estimation. Measurement results are compared against equilibrium estimates based on the activity estimate given in (2.17).

Once again it is obvious that more experimental data are needed in order to sufficiently map the copper ion activity behaviour as electrolyte composition varies.

## 3.5 Discussion and future work

### 3.5.1 What the model does

The model can predict required fill time and control current density within a certain range of operating conditions. Geometric properties of the plated via as well as control properties of the production process are taken into account sufficiently.

The model provides good and versatile information of species' mass transfer as well as behaviour within the modelling domain that enable study of mass transfer properties' effect on the fill result. The extensive geometric abilities of the model enable studying mass transfer phenomena and their effect on the fill result also in bottleneck locations or untested via geometries.

The model incorporates a broad solution of the cathodic current and potential system, providing system analysts with good information of how electric potential and current behave in both the bulk system as well as within the modelling domain layer and even over the (not modelled) electric double layer. This information can be applied to verify correctness and sensibility of the model. Further, the potential system solution enables studying effect of protrusions and cavities on potential field and fill result.

The model implementation enables adding other surface chemical phenomena into the current, simplified surface chemistry model, even on a very complex configuration if considered necessary. Examining different additive mixtures or combinations of different additive effects is in this way straight-forward.

### 3.5.2 What the model does not and why

The model does not handle extremely difficult geometries such as pincushion-like surfaces or very high aspect ratio tunnels. The ALE-method applied to implement changing model geometry does not allow topological changes in the model and thus e.g. removing geometry elements during model solution is impossible.

Serious difficulties are also posed by the nonlinearity brought to the system by diffusion limited mass transfer at limiting current. The model does not have any mechanism to overcome a situation where the diffusion layer near the cathode is effectively depleted of copper ions during deposition, but usually ceases to solve as concentration of copper ends up negative. In order to run the model, control parameters (current density) have to be adjusted appropriately, not to deplete the diffusion layer of copper completely.

The model mass transfer and electric field equations are currently solved independently of the electroneutrality condition. Electroneutrality is considered only when computing conductivity of electrolyte and estimating diffusivities of copper and sulphate ions. The electroneutrality condition may be incorporated in the model by adding necessary equations if considered necessary.

Since current efficiency of copper electroplating baths is generally considered good

[2], this practical aspect of the process is completely ignored in the first generation model. Current efficiency of the process should be determined and incorporated in the model, as it is only a multiplier added to the cathode boundary copper flux equation.

### **3.5.3 Improving the model - outline of experiments required**

Many of the parameter values in the current model version are on a rather weak experimental basis. As the process itself is new, not much data of any aspect of the process was available during the first phase of model development. When the process is taken into production, plenty of systematic data are gathered for quality assurance and process monitoring purposes. The data are mainly numeric data gathered from cross-sectioned vias, sampled regularly during production as well as data regarding control parameters given on the production line. This data can as such be applied to improve the model, especially with respect to how via geometry and the control parameters effect fill result.

Some additional experiments should also be made, especially when the process set up changes, in order to initially correct the current model and in the future to update the model when needed.

#### **Determining current equation parameters**

It is obvious that the  $\alpha$  and  $i_0$  parameters in the current equation (eq. 2.12) vary as the electrolyte composition changes and that they play a key role in system accuracy. These parameters can be determined by conducting a rather simple and well-established current-potential test (as explained in 3.2) on the electrolyte solution as the solution composition changes.

An algorithm for numerical identification of the aforementioned parameters has been created and it can be applied to avoid manual identification work and to keep the procedure similar case by case.

The  $i$ - $E$ -curve should be determined from a similar system as is on the production line, albeit scale-down to laboratory-size equipment is beneficial in order to reduce error brought by ohmic loss of potential over electrolyte. A sufficiently small voltage sweep rate should be applied and care must be taken not to destroy the electrode surfaces by applying too high a voltage. For example the value of 0.01 V/s for sweep rate -0.5 V for minimum cathodic potential may be applied.

#### **Determining electrical conductivity of electrolyte**

The bulk solution composition can be determined easily based on the control configuration given on the production line. But as said, the copper reduction reaction takes place on the cathode, within the diffusion layer, where the electrolyte composition and thus its electrical as well as mass transfer properties differ significantly from those of the bulk. Therefore it is necessary to sort out how these properties change as the

electrolyte composition changes.

Electrical conductivity of a solution is simple to measure, and as it is known that conductivity is brought to the plating bath mainly by copper sulphate and sulphuric acid, the experiment procedures can be simplified significantly. Further, considering the fact that only copper ions are consumed on the cathode and no concentration gradient (caused by consumption) of sulphate, hydrogen sulphate or hydrogen ions should thus exist there, the main focus is on determining the effect of copper ions on electrolyte conductivity. However, the condition of electroneutrality requires an equal amount of oppositely charged ions to be *removed* from the solution as copper ions are consumed, hence it is not necessary to vary only the copper ion concentration but also the concentration of some oppositely charged ions may be varied. Specifically, with the assumption that the electroneutrality condition is kept by the copper counter ion, namely the sulphate ion, the experiment can be simplified into three test batches:

- In order to determine the copper ion effect, conductivity should be measured in a series of acid-copper solutions, with the sulphuric acid concentration being kept constant as copper sulphate concentration varies from bulk solution concentration to zero (depletion).
- In order to determine the effect of sulphuric acid on conductivity, conductivity should be measured on a test series of acid-copper solutions with the copper sulphate concentration being kept constant on an operating conditions level, and acidity being varied within operating conditions values.
- To test and validate the estimate created upon the above measurements, a series of solution compositions where both components concentrations are varied should be made.

All the experiment electrolytes can be prepared independently of production, in laboratory conditions. The solution compositions need not be measured from a finished solution but can be calculated with sufficient accuracy based on weight and volume of individual solution components. These aspects further simplify the experiment.

### **Determining mass transfer and consumption of electrolyte additives**

The basic electrolyte components' (acid and copper) mass transfer properties can be deduced based on conductivity measurements. The additives' mass transfer properties examination requires further tests. The organic additives are electrically neutral thus not showing up in conductivity-based measurements and in general, the additives are present in such minor quantities that their effect in bulk solution properties is difficult to detect. The additives' properties as well as effects should thus be examined based on surface chemical phenomena, specifically inhibition of current flow.

Since the organic additives are, without exception, proprietary information of the equipment supplier, applying chemical knowledge and theories as well as literature

data to work out the effect of additives is not a reliable method. Their effect has to be determined empirically and on a qualitative level. The experiments should be made when ever the additive recipe in the electrolyte changes, in order to be able to update the model appropriately.

Concentration step tests can be used to determine the surface chemistry dynamics of additives. The current model assumes that the cathode surface is constantly in steady state with respect to additives' adsorption and desorption balance. This assumption should be confirmed or corrected. Further, the model currently assumes that an inhibiting agent can literally stop reduction of copper if its surface concentration is sufficiently high. This assumption can easily be tested and corrected by for example doing current-potential tests in a system with electrodes surely saturated of the inhibiting agent.

Measuring additive consumption in a bath yields information necessary to determine the basic characteristics of each additive and the basic nature of the surface chemical system created by the applied additive recipe. Additive consumption can be measured in a laboratory-scale system as well as on the production line. However, it is important to take bath size and electrode area into consideration when comparing the results. A basic solution composition analysis performed on the electrolyte solution at different times during plating is enough to sort out additives' consumption rate versus e.g. supplied power, or other applicable control parameter.

Determining additive consumption also enables the production line to control additive concentration more accurately compared to the currently applied power supply-based control system given by the equipment supplier.

It goes without saying that, when considering the additive system it is absolutely necessary to include chloride into the analysis.

### **Determining activity of copper**

The same preparations that are made for the electrolyte conductivity measurements can be utilized when determining copper ion activity in the electrolysis system. Though also additives must be taken in concern now, adding them into the conductivity experiment solutions is a rather straight-forward procedure.

When an extensive series of acid-copper solution samples including additives are made, the copper equilibrium potential in the solution is measured against a reference electrode whose chemical potential is known. This enables solving copper ion's activity based on the Nernst equation (1.27).

If it becomes clear that additives do not affect the copper equilibrium potential, the activity estimate can be fixed and tests to examine copper activity need not further to be made.

### **Determining current efficiency**

Current efficiency is the ratio of actual current flow through the system and the equivalent charge flow based on the amount of deposited copper. This gives a figure describing how well the power supplied by the voltage source is applied to reduce copper on the cathode.

Current, or power supplied to the system is constantly measured and replenishment data on of the copper anodes can be retrieved from the process computer logs. Combining these two pieces of information can be used to estimate the long term current efficiency of the system. In order to obtain a more specific values, experiments should be made, simply by weighing the boards plated under known operating conditions.

### **Improvements in the computational implementation**

Based on the data described above, also computational improvements can be achieved. Instead of using only one additive to introduce additive chemistry effects in the model, acquiring extended data enables modelling at least the two-additive system as such. This enables inspecting additive interactions and better modelling of their absolute concentration values and consumption.

Surface chemical phenomena should also be implemented on the modelled surface domain. This means solving mass transfer equations on the model cathode boundary, introducing surface chemistry dynamics in the model. Surface diffusion phenomena can enable smoother solution of nonlinear additive effects on the cathode boundary.

The local area and shape change phenomena modelled on the cathode should also incorporate the area change dynamics. Currently local area change during solution is only compared to the model domain initial stage, which effectively reduces all surface effect dynamics. However, implementing surface chemistry dynamics through mass transfer equations or area change dynamics are somewhat optional.

## **3.6 Conclusion**

Based on the literature study and experimental work done within this thesis it is reasonable to say that a reliable and adjustable distributed parameter model of the via filling by copper electroplating process is possible. To enhance reliability and accuracy of the first-generation model, the electrolyte chemical components' effects on over all electrolyte conductivity, on species' mass transfer properties as well as on copper ion activity need to be worked out by extensive experiments. Not only a quantitative measure is sufficient, but qualitative dependencies between the aforementioned properties need to be disclosed.

Due to the proprietary nature of the production line processes, voltammetric experiments are required to correctly parametrize the electrochemical factors in the model for each application case. Surface chemical dependencies have to be examined case-wise

via either potential step voltammetry or concentration step tests.

The constructed model considers the most important factors in the process, namely plating time, control current density, mass transfer of copper and initial via geometry as well as via shape change. The model also provides information of the current-potential-relationship behaviour within the modelling domain. The biggest challenges to model applicability are posed by nonlinearities in the process, especially by copper depletion.

# Bibliography

- [1] Andricacos P. C., Uzoh C., Dukovic J. O., Horkans J., and Deligianni H. Damascene copper electroplating for chip interconnections. *IBM Journal of Research and Development*, 42(5):567–574, 1998.
- [2] Eds. Schlesinger M. and Paunovic M. John Wiley and Sons, 2000.
- [3] Sato A. and Barauskas R. Copper plating. 9999.
- [4] Coombs J.F. Jr. McGraw-Hill, 2001. ISBN 0-07-135016-0.
- [5] Timo Närhi. Double microvia build-ups with viafilling technology. Master's thesis, Tampere University of Technology, Department of Electrical Engineering, 2005.
- [6] Vereecken P. M., Binstead R. A., Deligianni H., and Andricacos P. C. The chemistry of additives in damascene copper plating. *IBM Journal of Research and Development*, 49(1):3–18, 2005. ISSN 0018-8646.
- [7] Lefebvre M., Allardyce G., Seita M., Tsuchida H., Kusaka M., and Hayashi S. Copper electroplating technology for microvia filling. *Circuit World*, 29(2):9–14, 2003. ISSN 0305-6120.
- [8] Reid J. Copper electrodeposition: Principles and recent progress. *Japanese Journal of Applied Physics*, 40(4), 2001.
- [9] Atkins P.W. Oxford University Press, 1998. ISBN 0-19-850101-3.
- [10] Bonou L., Eyraud M., Denoyel R., and Massiani Y. Influence of additives on Cu electrodeposition mechanisms in acid solution: Direct current study supported by non-electrochemical measurements. *Electrochimica Acta*, 47:4139–4148, 2002. ISSN 0013-4686.
- [11] Soares D.M., Wasle S., Weil K.G., and Doblhofer K. Copper ion reduction catalyzed by chloride ions. *Journal of Electroanalytical Chemistry*, (532):353–358, 2002. ISSN 0022-0728.
- [12] Moffat T. P., Bonevich J. E., Huber W. H., Stanishevsky A., Kelly D. R., Stafford G. R., and Josell D. Superconformal electrodeposition of copper in 500–90 nm features. *Journal of The Electrochemical Society*, 147(12):4524–4535, 2000. ISSN 0013-4651.
- [13] Dow W-P., Huang H-S., and Linb Z. Interactions between brightener and chloride ions on copper electroplating for laser-drilled via-hole filling. *Electrochemical and Solid-State Letters*, 6(9):C134–C136, 2003. ISSN 1099-0062.

- [14] Tan M. and Harb J. N. Additive behavior during copper electrodeposition in solutions containing cl-, peg, and sps. *Journal of The Electrochemical Society*, 150(6):C420–C425, 2003. ISSN 0013-4651.
- [15] Dow W-P. and Huang H-S. Roles of chloride ion in microvia filling by copper electrodeposition i. studies using sem and optical microscope. *Journal of The Electrochemical Society*, 152(2):C67–C76, 2005. ISSN 0013-4651.
- [16] Dow W-P., Yen M-Y., Lin W-B., and Ho S.W. Influence of molecular weight of polyethylene glycol on microvia filling by copper electroplating. *Journal of The Electrochemical Society*, 152(11):C769–C775, 2005. ISSN 0013-4651.
- [17] Cao Y., Taephaisitphongse P., Chalupa R., and West A. C. Three-additive model of superfilling of copper. *Journal of The Electrochemical Society*, 148(7):C466–C472, 2001. ISSN 0013-4651.
- [18] Kim S-K., Hwang S., Sung K.C., and Kim J.J. Leveling of superfilled damascene cu film using two-step electrodeposition. *Electrochemical Solid State Letters*, 9(2):C25–C28, 2006. ISSN 1099-0062.
- [19] Lin K-C., Shieh J-M., Chang S-C., Dai B-T., Chen C-F., and Feng M-S. Electroplating copper in sub-100 nm gaps by additives with low consumption and diffusion ability. *Journal of Vacuum Science and Technology B*, 20(3):940–945, 2002. ISSN 1071-1023.
- [20] Hayase M., Taketani M., Aizawa K., Hatsuzawa T., and Hayabusa K. Copper bottom-up deposition by breakdown of PEG-Cl inhibition. *Electrochemical and Solid-State Letters*, 5(10):C98–C101, 2002. ISSN 0013-4651.
- [21] Hayase M., Taketani M., Hatsuzawa T., and Hayabusa K. Preferential copper electrodeposition at submicrometer trenches by consumption of halide ion. *Electrochemical and Solid-State Letters*, 6(6):C92–C98, 2003. ISSN 0013-4651.
- [22] Kondo K., Yamakawa N., Tanaka Z., and Hayashi K. Copper damascene electrodeposition and additives. *Journal of Electroanalytical Chemistry*, 559:137–142, 2003. ISSN 0022-0728.
- [23] Kondo K., Yamakawa N., and Hayashi K. Number 358, 2000. ECS Meeting Abstracts of Toronto Meeting.
- [24] Moffat T. P., Wheeler D., Kim S.K., and Josell D. Curvature enhanced adsorbate coverage model for electrodeposition. *Journal of The Electrochemical Society*, 153(2):C127–C132, 2006. ISSN 0013-4651.
- [25] Dow W-P. and Cheng H-H. A novel copper electroplating formula for laser-drilled micro via and through hole filling. *Circuit World*, 30(3):33–36, 2004.
- [26] J. O. Dukovic. Feature-scale simulation of resist-patterned electrodeposition. *IBM Journal of Research and Development*, 37(2):125–142, 1993. ISSN 0018-8636.
- [27] Akolkar R. and Landau U. A time-dependent transport-kinetics model for additive interactions in copper interconnect metallization. *Journal of the Electrochemical Society*, 151(11):C702–C711, 2004. ISSN 0013-4651.

- [28] West A. C. Theory of filling high-aspect ratio trenches and vias in presence of additives. *Journal of The Electrochemical Society*, 147(1):227–232, 2000. ISSN 0013-4651.
- [29] Moffat T. P., Wheeler D., Huber W. H., and Josell D. Superconformal electrodeposition of copper. *Electrochemical and Solid-State Letters*, 4(4):C26–C29, 2001. ISSN 1099-0062.
- [30] Moffat T. P., Wheeler D., and Josell D. Electrodeposition of copper in the SPS-PEG-Cl additive system (I. kinetic measurements: Influence of SPS). *Journal of The Electrochemical Society*, 151(4):C262–C271, 2004. ISSN 0013-4651.
- [31] Kang M. and Gewirth A. A. Influence of additives on copper electrodeposition on physical vapor deposited (pvd) copper substrates. *Journal of The Electrochemical Society*, 150(6):C426–C434, 2003. ISSN 0013-4651.
- [32] Dow W-P., Huang H-S., Yen M-Y., and Huang H-C. Influence of convection-dependent adsorption of additives on microvia filling by copper electroplating. *Journal of The Electrochemical Society*, 152(6):C425–C434, 2005. ISSN 0013-4651.
- [33] Moffat T. P., Wheeler D., Edelstein M. D., and Josell D. Superconformal film growth: Mechanism and quantification. *IBM Journal of Research and Development*, 49(1):19–36, 2005. ISSN 0018-8646.
- [34] Josell D., Wheeler D., Huber W.H., Bonevich J.E., and Moffat T.P. A simple equation for predicting superconformal deposition in submicrometer trenches. *Journal of the Electrochemical Society*, 148(12):C767–C773, 2001. ISSN 0013-4651.
- [35] Wheeler D., Josell D., and Moffat T.P. Modeling superconformal electrodeposition using the level set method. *Journal of the Electrochemical Society*, 150(5):C302–C310, 2003. ISSN 0013-4651.
- [36] Zhang W., Brongersma S.H., Conard T., Wu W., Van Hove M., Vandervorst W., and Maexa K. Impurity incorporation during copper electrodeposition in the curvature-enhanced accelerator coverage regime. *Electrochemical and Solid-State Letters*, 8(7):C95–C97, 2005. ISSN 1099-0062.
- [37] Kim J. J., Kim S-K., and Kim Y. S. Catalytic behavior of 3-mercapto-1-propane sulfonic acid on cu electrodeposition and its effect on cu film properties for cmos device metallization. *Journal of Electroanalytical Chemistry*, 542:61–66, 2002. ISSN 0022-0778.
- [38] Taephaisitphongse P., Cao Y., and West A. C. Electrochemical and fill studies of a multicomponent additive package for copper deposition. *Journal of The Electrochemical Society*, 148(7):C492–C497, 2001. ISSN 0013-4651.
- [39] Bard A.J. and Faulkner L.R. John Wiley and Sons, 2001. ISBN 0-471-04372-9.
- [40] Geankoplis C.J. Prentice-Hall International, 2003. ISBN 0-13-101367-X.
- [41] Paunovic M. and Schlesinger M. John Wiley and Sons, 1998. ISBN 0-471-16820-3.
- [42] Georgiadou M., Veyret D., Sani R. L., and Alkire R. C. Simulation of shape evolution during electrodeposition of copper in the presence of additive. *Journal of The Electrochemical Society*, 148(1):C54–C58, 2001. ISSN 0013-4651.

- [43] West C., Mayer S., and Reid J. A superfilling model that predicts bump formation. *Electrochemical and Solid-State Letters*, 4(7):C50–C53, 2001. ISSN 1099-0062.
- [44] Dow W-P. and Huang H-S. Roles of chloride ion in microvia filling by copper electrodeposition ii. studies using epr and galvanostatic measurements. *Journal of The Electrochemical Society*, 152(2):C77–C88, 2005. ISSN 0013-4651.
- [45] Chang S-C., Shieh J-M., Lin K-C., Dai B-T., Wand T-C., Chen C-F., Fend M-S., Li Y-H., and Lu C-P. Wetting effects on gap filling submicron damascene by an electrolyte free of levelers. *Journal of Vacuum Science and Technology B*, 20(4):1311–1316, 2005. ISSN 1071-1023.
- [46] Kim S-K. and Kim J. J. Superfilling evolution in cu electrodeposition (dependence on aging time of the accelerator). *Electrochemical Solid State Letters*, 7(9):C98–C100, 2004. ISSN 1099-0062.
- [47] Moffat T. P., Baker B., Wheeler D., and Josell D. Accelerator aging effects during copper electrodeposition. *Electrochemical and Solid-State Letters*, 6(4):C59–C62, 2003. ISSN 0013-4651.
- [48] Pricer T.J., Kushner M.J., and Alkire R.C. Monte carlo simulation of the electrodeposition of copper (II. acid sulfate solution with blocking additive). *Journal of the Electrochemical Society*, 149(8):C406–C412, 2002. ISSN 0013-4651.
- [49] Comsol Incorporated. Comsol multiphysics modelling software, 2006.
- [50] Lide D.R. ed. in cheif. CRC Press, Taylor&Francis, 86 edition, 2005-2006.
- [51] Comsol Incorporated. *Cantilever beam modelling example*, 1999-2006.
- [52] Christian Stoker. *Developments of the Arbitrary Lagrangian-Eulerian Method in non-linear Solid Mechanics. Applications to Forming Processes*. PhD thesis, 1999. ISBN 90-36512646.

# Appendix A

## Via fill test sample images

Cross-section images of samples from via filling time-series tests. (Image series are in order of test age.)

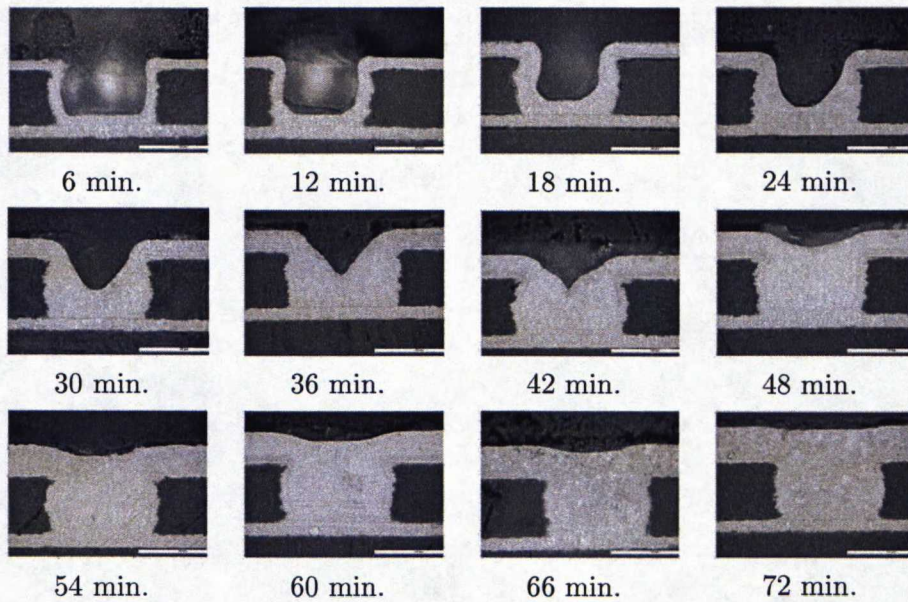


**Table A.1:** Microvia fill grade vs. time, 1st test batch, 1st series. Material courtesy of Aspocomp.

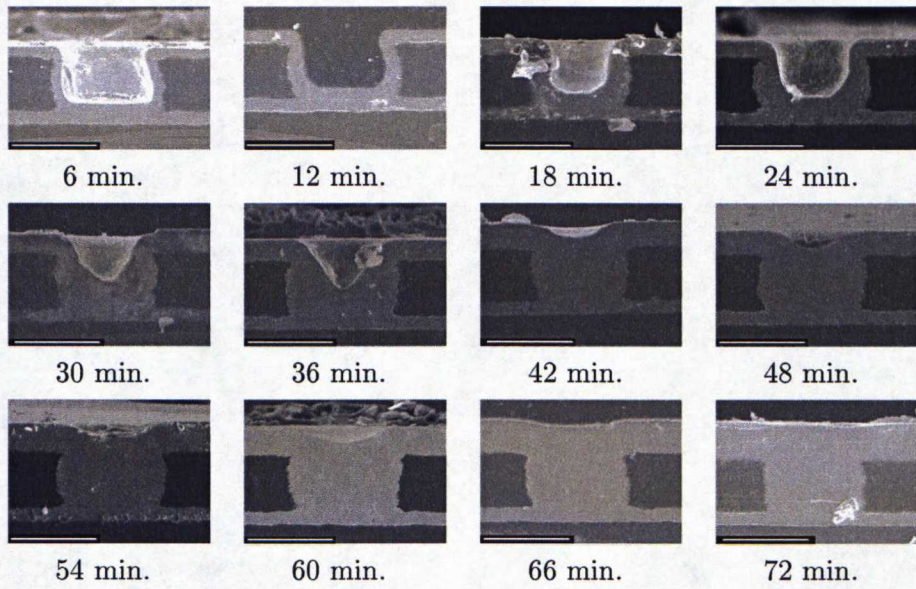


**Table A.2:** Microvia fill grade vs. time, 1st test batch, 2nd series. Material courtesy of Aspocomp.

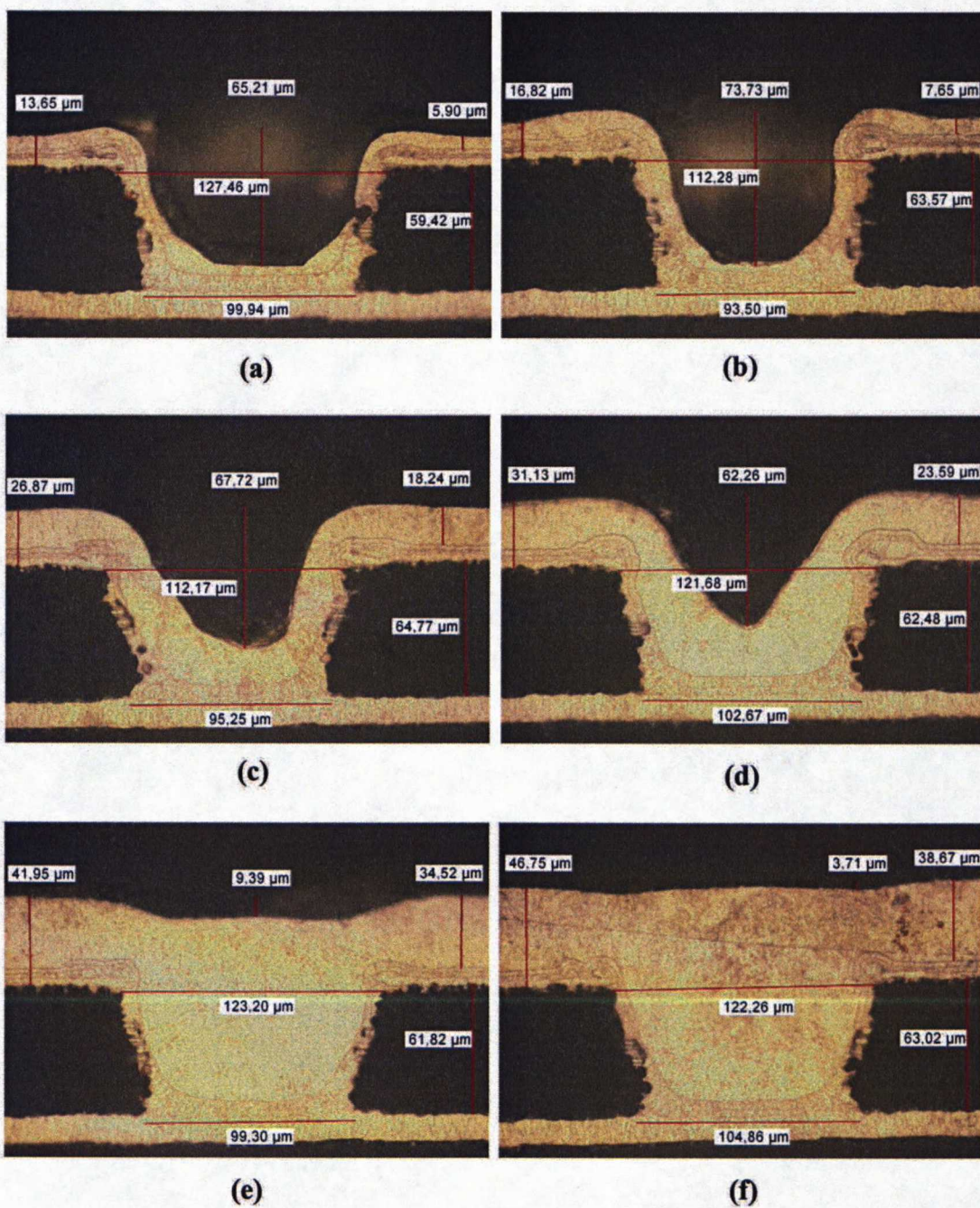


**Table A.3:** Microvia fill grade vs. time, 2nd test batch, 1st series, sample set n:o 1. Plating times are (a) 15min, (b) 30min, (c) 45min, (d) 60min, (e) 75min and (f) 90min. Material courtesy of Aspocomp.

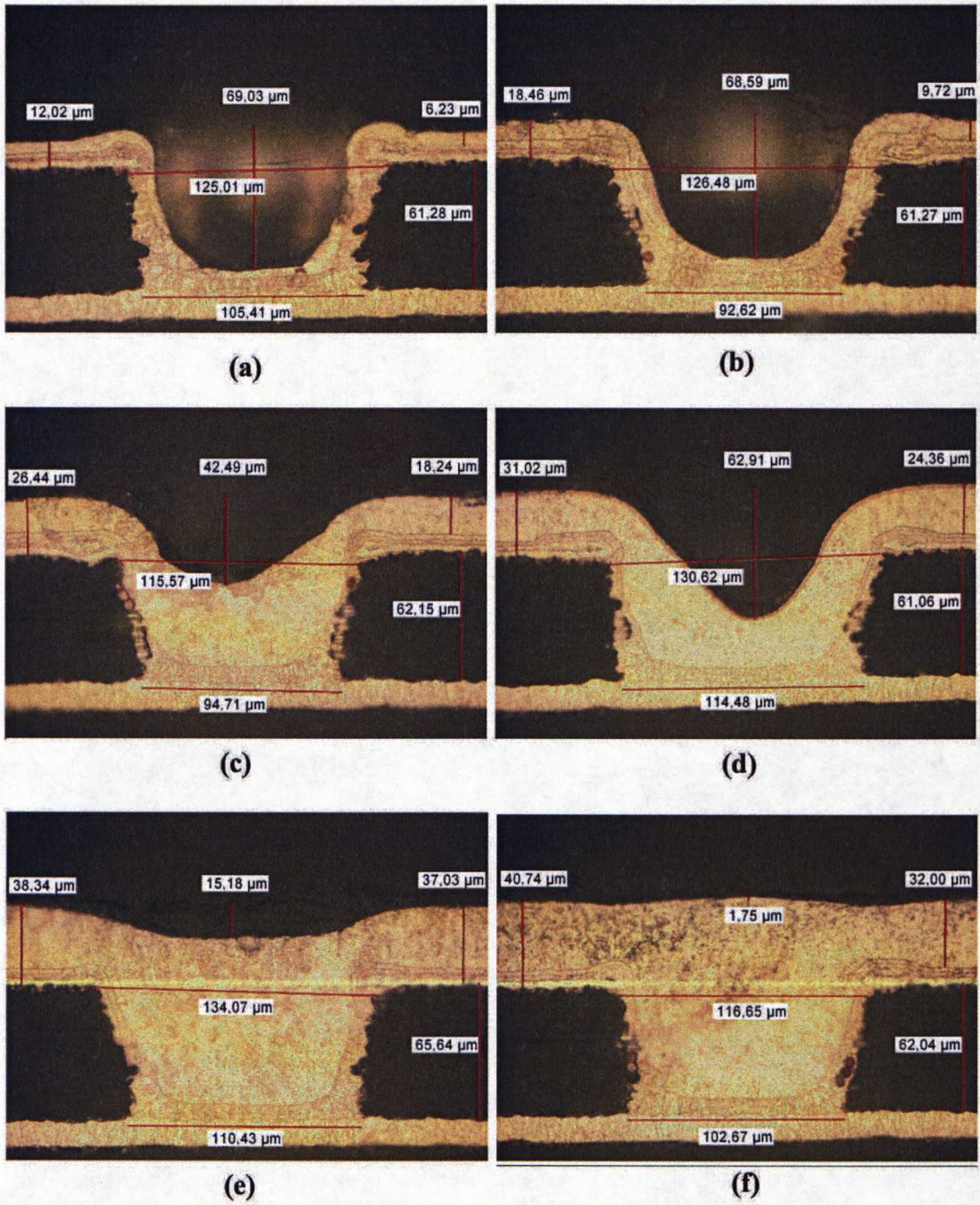


**Table A.4:** Microvia fill grade vs. time, 2nd test batch, 1st series, sample set n:o 2. Plating times are (a) 15min, (b) 30min, (c) 45min, (d) 60min, (e) 75min and (f) 90min. Material courtesy of Aspocomp.

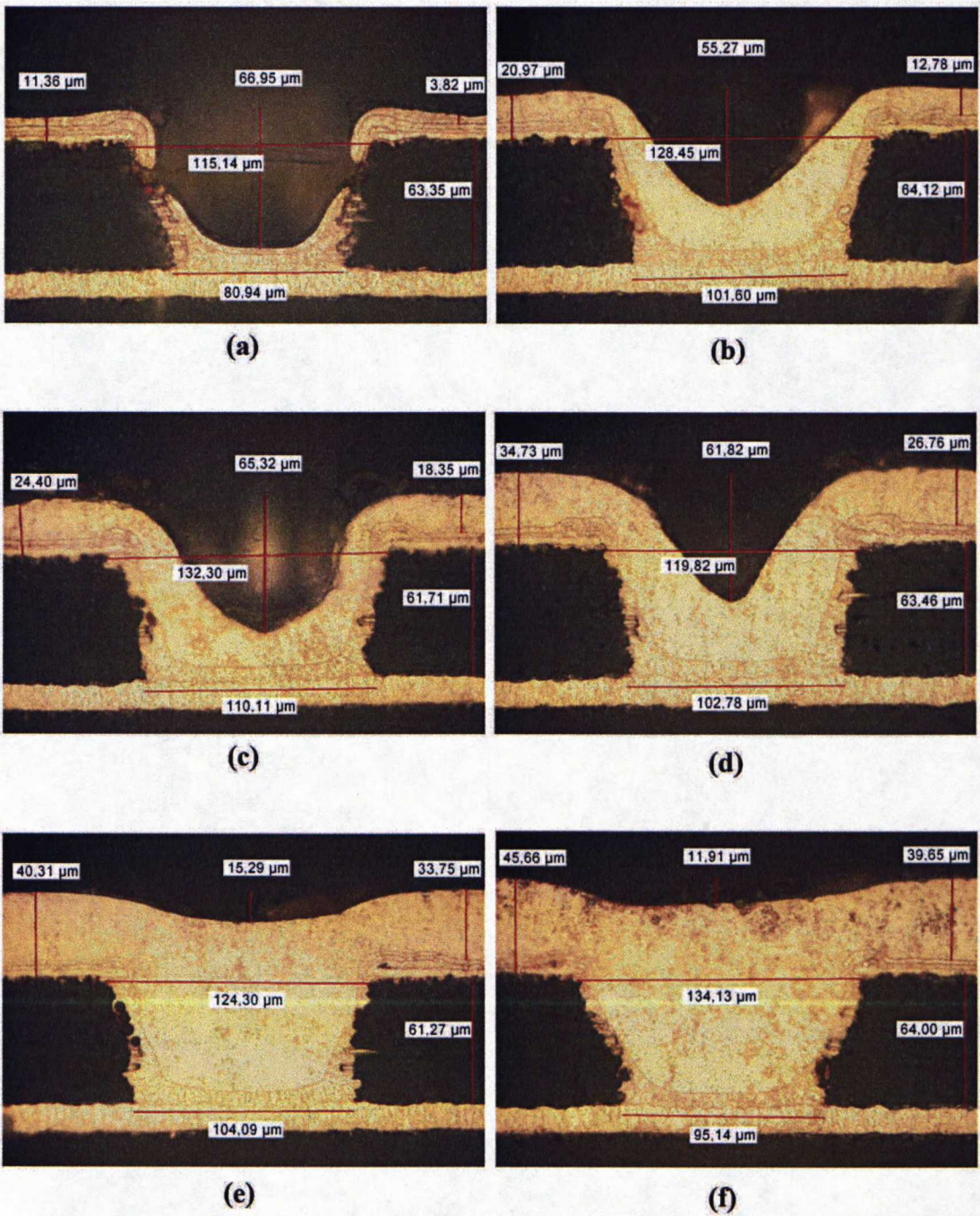


**Table A.5:** Microvia fill grade vs. time, 2nd test batch, 2nd series, sample set n:o 1. Plating times are (a) 15min, (b) 30min, (c) 45min, (d) 60min, (e) 75min and (f) 90min. Material courtesy of Aspocomp.

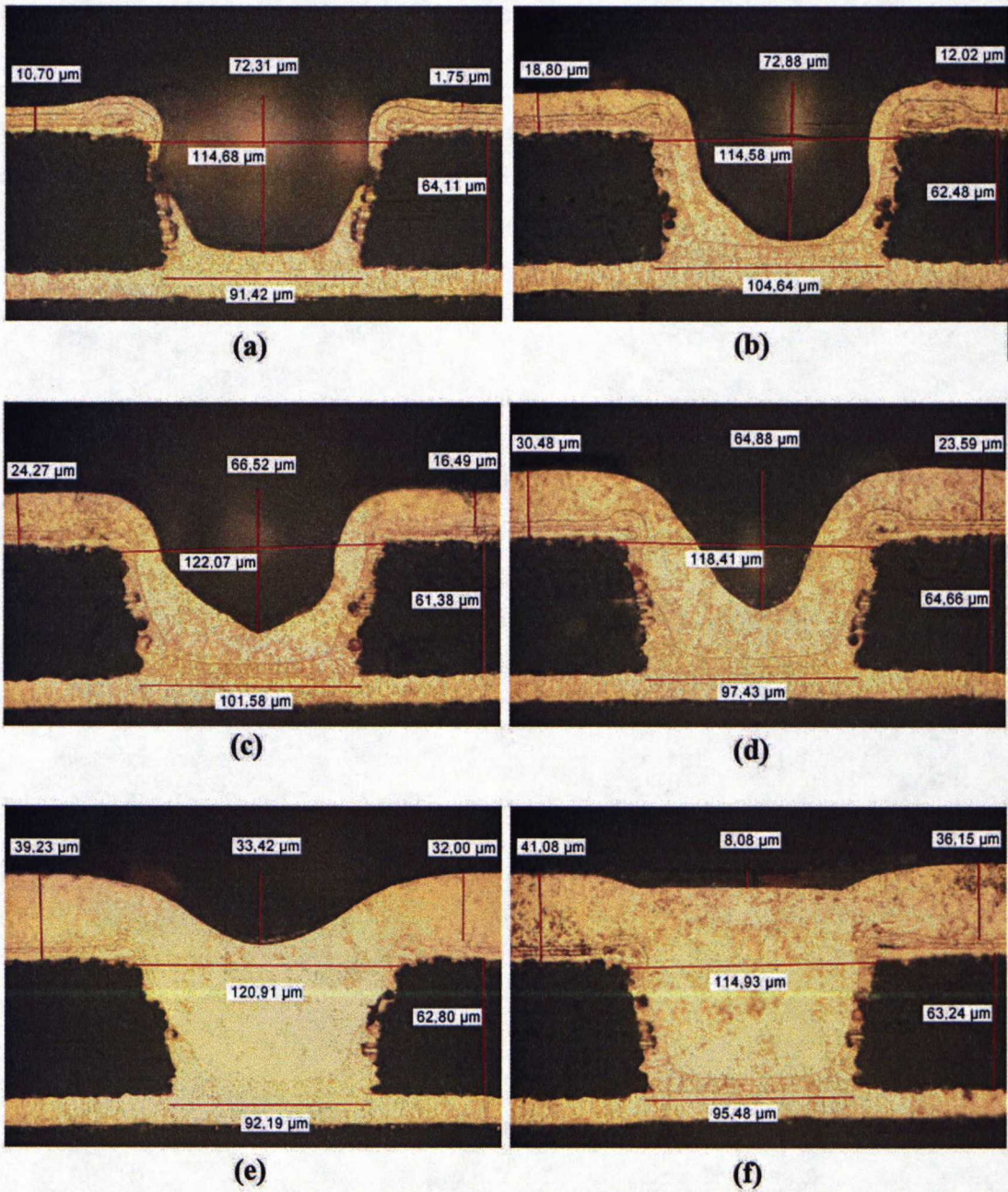


**Table A.6:** Microvia fill grade vs. time, 2nd test batch, 2nd series, sample set n:o 2. Plating times are (a) 15min, (b) 30min, (c) 45min, (d) 60min, (e) 75min and (f) 90min. Material courtesy of Aspocomp.

## Appendix B

# Via fill model screen-captured images

In the modelling environment screen-capture images, the blue color depicts the electrolyte diffusion layer and the original microvia as well as modelling domain geometry is shown as a black line. The moving microvia surface is where blue and white colors meet. Beneath the microvia surface there first is the deposited copper layer, until the original via geometry border, from where the substrate layer starts. Figure B.1 illustrates the model image interpretation.

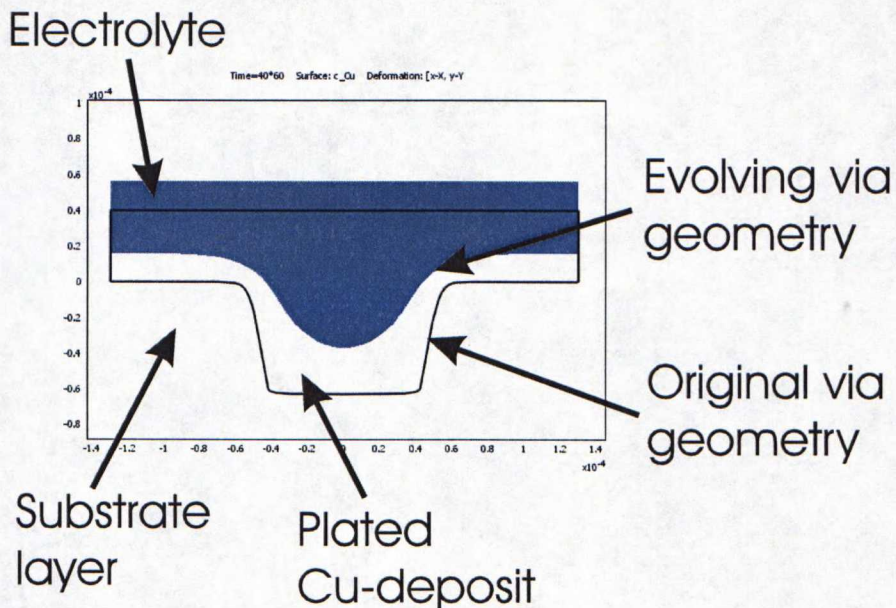
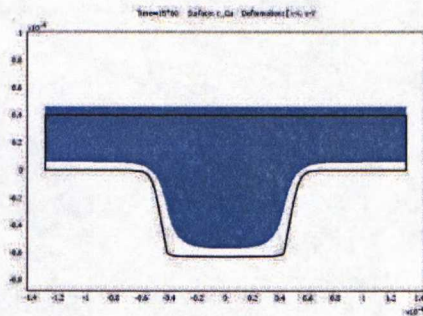
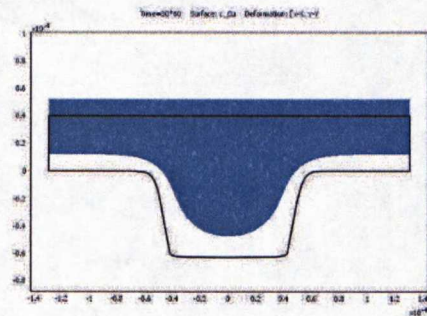


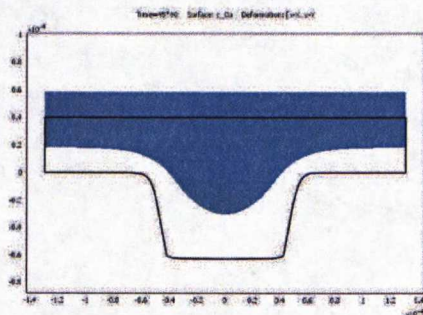
**Figure B.1:** Different parts of the model indicated.



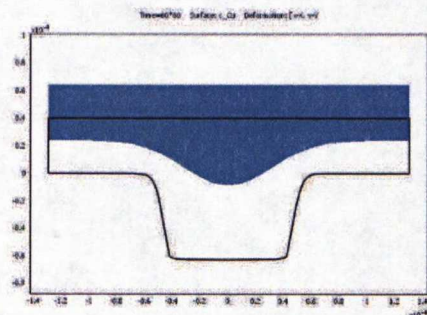
15 min.



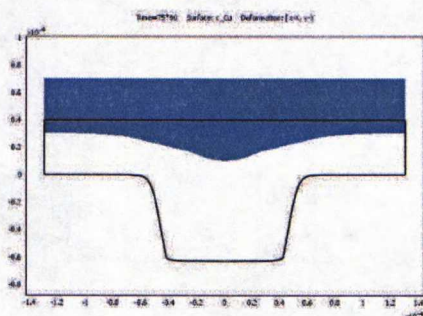
30 min.



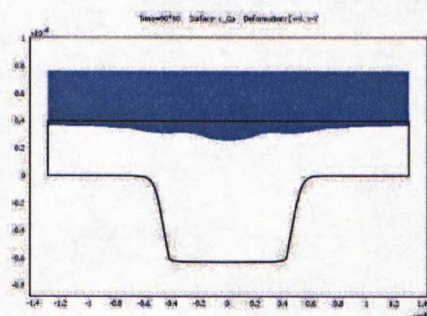
45 min.



60 min.



75 min.



90 min.

**Table B.1:** Modelled microvia fill grade vs. time. Model reference is the 1st test batch of the 2nd test series, as shown in teb. A.3.